UPGRADING OF PYROLYSIS BIO-OIL TO RENEWABLE FUELS BY

HYDRODEOXYGENATION

A Thesis

Presented in Partial Fulfillment of the Requirements for the

Degree of Master of Science

with a

Major in Natural Resources

in the

College of Graduate Studies

University of Idaho

by

Yinglei Han

December 2014

Major Professor: Armando G. McDonald, Ph.D.

Authorization to Submit Thesis

This thesis of Yinglei Han, submitted for the degree of Master of Science with a major in Natural Resources and titled " Upgrading of Pyrolysis Bio-oil to Renewable Fuels by Hydrodeoxygenation," has been reviewed in final form. Permission, as indicated by the signatures and dates below, is now granted to submit final copies to the College of Graduate Studies for approval.

Major Professor: _____ Date: _____

                                       Armando G. McDonald, Ph.D.

Committee
Members: _____ Date: _____

                                       David McIlroy, Ph.D.

_____ Date: _____

                                       Randall Brooks, Ph.D.

Department
Administrator: _____ Date: _____

                                       Anthony S. Davis, Ph.D.

Discipline's
College Dean: _____ Date: _____

                                       Kurt Pregitzer, Ph.D.

Final Approval and Acceptance

Dean of the College
of Graduate Studies: _____ Date: _____

                                       Jie Chen, Ph.D.

Abstract

Fast pyrolysis is a process can convert woody biomass to a crude bio-oil (pyrolysis oil) However, some of these compounds contribute to bio-oil shelf life instability and difficulty in refining. Catalytic hydrodeoxygenation (HDO) of the bio-oil can upgrade the bio-oil into transportation fuels. Therefore, nickel (Ni) and ruthenium (Ru) catalysts supporting on a novel nanomaterial, silica nanospring (NS) showed the best performance for HDO of phenol. In terms of bio-oil hydrotreatment, the bio-oil was fractionated by phase separation by addition of water to obtain a water-insoluble (WIS) and water-soluble (WS) fractions from the bio-oil. The WS of bio-oil can be upgraded into cycloalkanes of 30% wt. and alcohols of 18% wt. over $Ni(65\%)/SiO_2\text{-}Al_2O_3$ catalyst. The WIS of bio-oil had been effectively cracked in methanol over $Ni(65\%)/SiO_2\text{-}Al_2O_3$ catalyst. A further step of HDO on the cracked oil had successfully deoxygenated the phenolics into cycloalkanes.

Acknowledgements

My utmost gratitude goes to my academic advisor, Dr. Armando McDonald for his guidance, motivation, encouragement, and dedication in this study.

My thanks and appreciation goes to my thesis committee members, Drs. David McIlroy and Randy Brooks for their time and contributions to this research.

I would like to specifically thank Hui Li, Liqing Wei, Carl Morrow, Shaobo Liang and Jing Dai, for their expertise. I wish to thank all graduate students in Renewable Materials Program, especially our research group members for their friendly help and great support. Fouetio Kengne Blaise-Alexis's technical support and readiness to help made my work so much smother. I would like to thank all the faculty and staff in College of Natural Resources and National Institute for Advanced Transportation Technology (NIATT).

I wish to express my gratitude to NIATT for supporting this research. The project was supported from a NIATT award (DTRT12GUTC17) through the US Department of Transportation.

Finally, I would like to thank my wife (Saixiao Wang) for her support and encouragement throughout the journey of my academic career in life.

Table of Contents

List of Tables

List of Figures

Chapter 1: Introduction and Literature Review

1.1 Introduction

Human activity consumes considerable amounts of energy distributed between three types of activity: industrial, residential and transportation. With the explosive growth in the use of automobiles in the 20th century, the demand for transportation fuels in the world has increased tremendously during the last 30 years. However, the fuels used for present modes of transportation are almost exclusively from petroleum, of which the remaining reserves are being depleted rapidly. In addition to that, large consumption on such fuel mainly leads to the environmental problems ranging from poor air quality in large cities to regional pollution and the increase of concentration of greenhouse gases (GHG) in the atmosphere [1]. The urgency to find a more sustainable way forward for society has become clear with alarming trends in global energy demand, the finite nature of fossil fuel reserves, the need to decrease emissions of GHG to mitigate the devastating consequences of climate change and the damaging volatility of oil prices (in particular for the transport sector). Therefore, renewable resources besides petroleum are highly desirable for production of alternative fuels and chemicals.

To address this concern, researchers have started to develop a number of technologies for alternative fuel production [2-4]. Of these technologies in development are electric cars and the use of biofuels seem to be promising solutions. Liquid fuels derived from bio-based material can be defined as biofuels. Due to the properties of the feedstock, biofuels are renewable, and therefore contribute little to the production of GHG. Therefore, many technologies have been developed for biofuels production such as (1) ethanol

production from food crops like wheat, maize, corn and sugar cane via biological processes, (2) the production of biodiesel through trans-esterification of triglycerides from vegetable oils including palm, corn, soybean, rapeseed, and sunflower, (3) pyrolysis and upgrading, (4) gasification, and (5) butanol [5-14].

However, non-edible feedstock, including woody biomass, grasses, and even agricultural and forestry waste biomass, are becoming increasingly important nowadays for production of biofuels. Because of the inherent properties and vast availability of lignocellulosic biomass, it is considered a promising feedstock for non-food based biofuels production. Technologies that can depolymerize the recalcitrant nature of the lignocellulosic biomass into liquid fuels are thus highly preferred. Fast pyrolysis is a thermochemical technology that can convert biomass into liquid bio-oil, bio-char, and gaseous products [7, 15]. Among these three products, bio-oil is the most desirable one and its yield currently can be maximized up to 72% through fast pyrolysis process. This high yield is acquired for relatively short residence times (0.5-2 s), moderate temperatures (400-600°C), and rapid quenching at the end of the process [7]. As the byproducts of the process, the yield of gases and biochar depends on the biomass composition and rate and duration of heating during fast pyrolysis.

Nevertheless, the major components in pyrolysis bio-oil are the oxygenated compounds including saccharides, alcohols, ketones, aldehydes, carboxylic acids, phenolic compounds, lignin oligomers and water [15]. The compounds in bio-oil cause high viscosity, poor thermal and chemical stability, corrosion, and immiscibility with hydrocarbon fuels [7, 16]. Fortunately, these drawbacks can be overcome with catalytic hydrotreatment, which targets the removal of oxygen in the bio-oil. The treatment rejects oxygen as water by catalytic reaction with hydrogen under moderate temperature (200-400°C)[17]. For this

reason, this process is also considered as hydrodeoxygenation (HDO) of bio-oil even though hydrogenation (HYD) occurs inevitably under the same condition. In addition, active compounds polymerize under hydrotreatment conditions and have been also involved with coke formation during the process [18]. However, the HDO reaction occurs only on the surfaces of the applied catalysts. Therefore, it is feasible to develop effective catalysts that can deoxygenate and reduce active functional groups first before they undergo polymerization and thus impair the coke formation.

Therefore, the catalyst plays a very important role in catalytic HDO for bio-oil upgrading. Development of an effective catalyst for HDO is necessary and urgently required. A well-recognized method to evaluate the performance of specific catalyst is using bio-oil model compounds as the feedstock [19-22]. Guaiacol and phenol are the two being studied the most as bio-oil model compounds because they are both the major components of bio-oil. More importantly, the evaluation on the activity and selectivity of catalyst can be easily achieved by characterizing the conversion and degree of deoxygenation (DOD) of these compounds, respectively [19,21,23]. But it should be noted that pyrolysis bio-oil contains more than 300 compounds, which are either small molecules with different types of functional groups or oligomers with larger molecular weight. This complexity makes the catalytic HYD of bio-oil extremely difficult.

To upgrade the bio-oil, researchers developed several methods including esterification, catalytic reforming, and ketonization have been studied [24, 25]. Because of the different reactivity and interactions of more than 300 components in the bio-oil, it is rather difficult to improve its qualities to meet the requirement of transportation fuels by a single treatment. However, it should be noted that all the above mentioned methods cannot upgrade the bio-oil into oxygen-free hydrocarbons like gasoline and diesel. However, oxygen

present in the bio-oil contribute to its highly reactive nature and thus make the bio-oil unstable [26]. To address these problems, HDO is proposed and proven as an effective way to remove the oxygen atoms in bio-oil for hydrocarbon production [27].

1.2 Literature Review

1.2.1 Fuels and pyrolysis bio-oils production and upgrading

1.2.1.1 Conventional transportation fuels

Traditional transportation fuels are mainly gasoline, diesel, and jet fuels, which are all derived from petroleum oil distillation. Gasoline is a mixture of low-boiling hydrocarbons suitable for use in spark-ignited internal combustion engines [28]. Typical gasoline consists of hydrocarbons containing between 4 and 12 carbon atoms per molecule (C_4-C_{12}). It has an initial boiling point at atmospheric pressure of about 35°C and a final boiling point of about 200°C. Diesel fuel is a mixture of hydrocarbons typically contain between 8 and 21 carbon atoms per molecule (C_8-C_{21}). The boiling points for diesel fuels range from 200 to 325°C. Jet fuel is generally composed by hydrocarbons with carbon number ranging from C_5 to C_{14}, and the corresponding boiling points are between 150 to 275°C. In addition, kerosene is another generally used fuel which is similar to jet fuel. It contains hydrocarbons from C_6 to C_{16} and the boiling points for these hydrocarbons range from 150 to 300°C [29].

1.2.1.2 Biomass composition and its effect on pyrolysis products

Fast pyrolysis of lignocellulosic biomass is a promising route to produce liquid fuels. In fact, any form of biomass can be considered for pyrolysis, although most studies have

been carried out on wood [30, 31]. In view of major components, nearly all lignocellulosic biomass is composed of cellulose, hemicellulose and lignin while the composition varies from different biomass sources. Thus, the produced pyrolysis oil from different biomass may be different. Bertero et al. studied the pyrolysis bio-oil from different biomass feedstock including softwood, hardwood, and wheat shell (Table 1.1)[31]. Typically, there is more cellulose in hardwood but less lignin compared with softwood. Due to the differences in composition, the bio-oil yields from fast pyrolysis of different types of biomass are variable. Furthermore, chemical composition also varied from different biomass derived bio-oils.

Lignin in biomass is a complex polymer of aromatic alcohols which includes three types of aromatic nuclei, guaiacyl (G), syringyl (S) and p-hydroxyphenyl (H) units [32]. Their compositions are quite different in softwood and hardwood lignins. Softwood lignins consist almost entirely of G with small quantities of H, while G and S are mainly included in hardwood lignins. In addition, many grasses have mostly G, while some palms have mainly S [33]. Therefore, lignins from hardwoods have much higher amount of methoxy groups than those from softwoods and grass biomass, thus explaining the much higher concentration of phenolic ethers in bio-oil from hardwood [34].

Table 1.1 Pyrolysis oil production from different lignocellulosic biomass [31]

	Pine-sawdust (softwood)	Mesquite-sawdust (hardwood)	Wheat shell
Lignocellulosic material composition (%, dry basis)			
Cellulose	35	40-45	10-15
Hemicellulose	29	25-30	30
Lignin	28	11-28	4-8
Yields of the main pyrolysis products (wt.%)			
Bio-oil	50.3	38.7	38.0
Char	28.9	36.6	36.1
Gases	20.8	24.7	25.9
Chemical composition of produced bio-oil identified by GC-MS (%)			
Acids	18.71	16.99	18.91
Esters	8.29	7.62	8.62
Aldehydes and ketones	23.63	14.89	13.40
Furans	5.95	6.25	3.44
Alcohols and sugars	9.81	8.06	6.04
Ethers	0.80	1.22	1.38
Phenols	15.74	28.23	19.02
Hydrocarbons	0.80	2.15	2.42
Others oxygenates	2.38	3.34	2.05
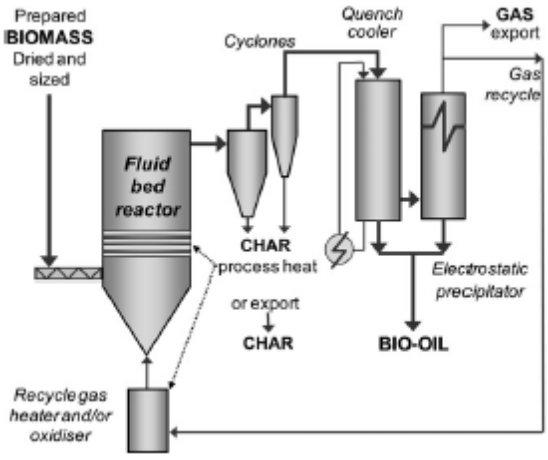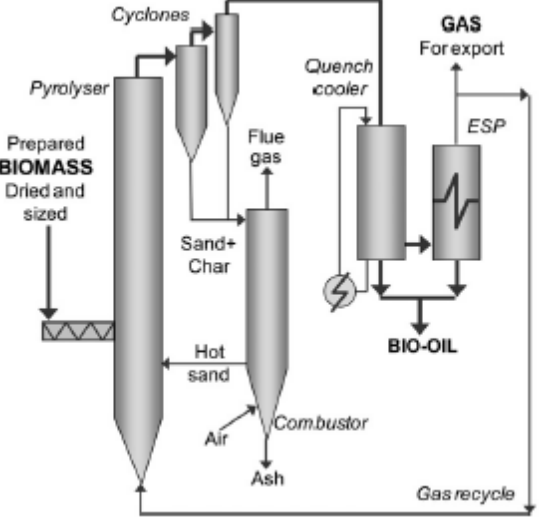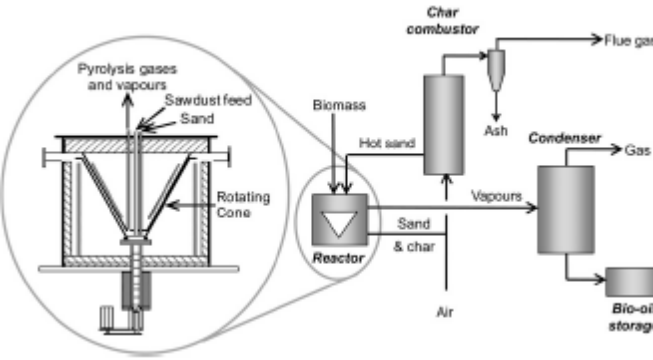
1.2.1.3 Bio-oil production and characteristics

Thermochemical processing of biomass uses heat to modify or even transform plant polymers into fuels, chemicals, or electric power [15]. One of the most mild thermochemical process is torrefaction, during which raw biomass is heated in an inert or nitrogen atmosphere with temperature in the range of 225 to 300°C [35]. Pyrolysis processes are

carried out in the absence of oxygen, at atmospheric pressure, and at temperatures ranging from 300 to 600°C. Charcoal is the main product of the traditional slow pyrolysis process, in which the biomass (usually wood) is heated slowly to temperatures between 300 and 400°C. Fast pyrolysis, on the other hand, involves very high heating rates to temperature around 500°C followed by rapid cooling and condensation of the vapors produced. This yields a maximum quantity of dark-brown liquid with heating value roughly equal to that of wood, which is approximately half the heating value of fossil fuel oil [15, 30]. With the continued increase of temperature to 800°C or higher, however, biomass will be gasified instead of pyrolyzed because the produced pyrolysis vapors will be quickly decomposed to gaseous products (H_2, CO and CO_2) [36]. Therefore, the great virtues for fast pyrolysis of biomass are the simplicity of generating bio-oil and the attractiveness of liquid products compared with either gasified or unprocessed biomass.

The state of the art development of pyrolysis can be compared to the situation of the petrochemical industry in 1936, when demonstration of fluidized catalytic cracker (FCC) at a scale of 2000 barrels per day occurred [15]. As a matter of fact, the heart of a fast pyrolysis process is the reactor. To maximize the total liquid oil yield, different reactor designs have been carried out for a number of years. The main types of fast pyrolysis reactor include 1) bubbling fluid bed pyrolyzer, 2) circulating fluid-bed pyrolyzer, 3) rotating cone pyrolyzer, 4) ablative pyrolyzer, and 5) auger pyrolyzer (Table 1.2) [7, 15, 37].

Table 1.2 Summary of types of pyrolysis reactors and characteristics [7, 15, 37].

Key features	Scheme of different pyrolyzers
1. Bubbling fluid bed pyrolyzer Advantages: 1) Good heat transfer; 2) High bio-oil yield (up to 75%); 3) Easy to scale up; Disadvantages: 1) Require small particle feed sizes; 2) Require large quantity of inert gas; 3) High operating cost	
2. Circulating fluid bed pyrolyzer Advantages: 1) High bio-oil yield (up to 75%); 2) Require medium feed particle size; Disadvantages: 1) Require large quantity of heat carrier; 2) High level complexity in operation 3) High operating cost	
3. Rotating cone pyrolysis Advantages: 1) Relatively simple construction and operation 2) Low heat carrier/sand requirement; Disadvantages: 1) Limited scale / capacity; 2) Require fine feed particles 3) Very difficult to scale up	

4. Ablative pyrolyzer

Advantages:

1) Good heat transfer;

2) Large particles can be used;

Disadvantages:

1) High level complexity in operation;

2) Hard to scale up;
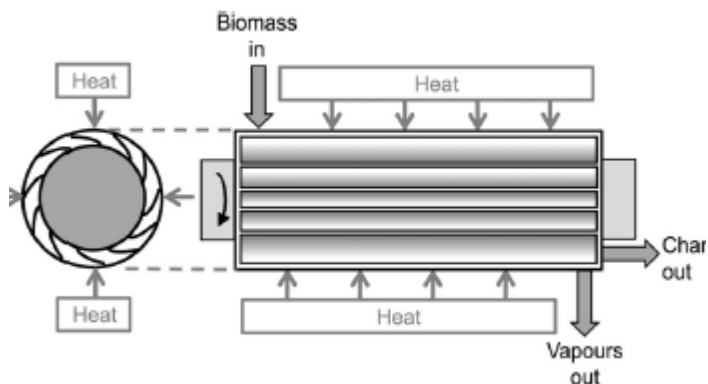
5. Auger pyrolyzer

Advantages:

1) Simple construction and easy to operate;

2) Low carrier gas needed;

Disadvantages:

1) Long residence time

2) Lower bio-oil yields
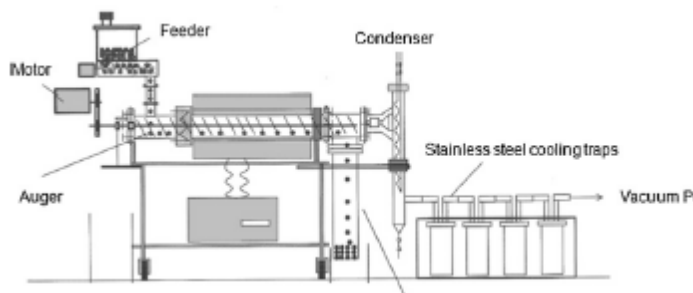
No matter what type of pyrolyzer is applied, the produced bio-oils are essentially similar. In fact, bio-oil is a very complex mixture of compounds derived from the depolymerization reactions of the main three components in biomass: cellulose, hemicellulose and lignin. It was reported that bio-oils contain approximately 35-40% of oxygen, 55-60% of carbon, an acidic pH, density close to 1.2 g/cm^3, and 15-60% water [38-41]. The composition of bio-oil can be associated to the composition with the original biomass (Table 1.3). The liquid phase obtained from cellulose and hemicellulose pyrolysis is mainly composed of aldehydes, ketones, furans, anhydro-sugars, sugars, acids, esters and small amount of hydrocarbons, ethers and alcohol [42, 43]. Phenolic compounds in bio-oil are derived from lignin pyrolysis [44]. Due to the different type of lignin between softwood

and hard, however, bio oils from softwood fast pyrolysis will only contain guaiacols while there will be syringols present in the bio-oil from hardwood fast pyrolysis [45].

In terms of thermal stability, lignin is proven to be more thermally resistant than cellulose and hemicellulose [46-48]. Under the fast pyrolysis conditions, complete depolymerization of lignin to monomeric phenolics is nearly impossible. The pyrolysis of lignin always produces certain amounts of small lignin fragments bearing more than two phenolic units but still being liquid in ambient temperature. Due to their molecular weight, these fragments are characterized as oligomers which are also called pyrolytic lignin or tar as described in the literature [44, 49-51]. Many studies have successfully characterized the pyrolytic lignin in bio-oil by FTIR, NMR and ESI-MS [51-53]. Research has shown that pyrolytic lignin oligomers have biphenyl, phenyl coumaran, diphenyl ethers, stilbene and resinol structures [51]. Moreover, it should be noted that these oligomers contain lower oxygen but higher carbon content than regular bio-oil. Therefore, it is a promising feedstock for hydrocarbon production.

Pyrolytic lignin oligomers can be solubilized in the phenolics-rich bio-oil. However, the oligomers can be easily separated from the bio-oil by adding enough cold water[31]. It is reported that water fractioning is a very efficient technique to obtain water soluble and insoluble phases of bio-oil for further upgrading [55-57]. The water soluble phase basically contains acids, aldehydes, ketones, alcohols, sugars and phenols [57]. For the water insoluble phase of bio-oil, pyrolytic lignin oligomers are the main component [50]. An interesting phenomenon is that the amount of these oligomers increases with aging time of the bio-oil even at room temperature [58]. This result clearly shows that pyrolytic lignin has a propensity to polymerize at mild conditions.

Table 1.3 Main pyrolysis products formed from carbohydrates and lignin [33, 39, 54]

Cellulose/Hemicellulose derived compounds	Group	Carbon numbers	Lignin derived compounds	Group	Carbon numbers
formic acid	acids	1	phenol	phenol	6
methanol	alcohol	1	guaiacol	phenol	7
acetic acid	acids	2	methyl-guaiacol	phenol	8
glyoxal	aldehyde	2	ethyl-phenol	phenol	8
glycoaldehyde	aldehyde	2	2,6-dimethoxyphenol	phenol	8
ethanol	alcohol	2	cresol (para-, ortha-, meta-)	phenol	7
hydroxyacetaldehyde	oxygenates	2	dimethyl-phenol	phenol	8
acetol	oxygenates	3	vinyl-guaiacol	phenol	9
furfural	furan	5	propyl-guaiacol	phenol	10
furfural alcohol	furan	5	isoeugenol	phenol	10
2-methyl-2-cyclopenten-1-one	ketone	6	vanillin	phenol	8
3-methyl-2-cyclopenten-1-one	ketone	6	syringol (hardwood)	phenol	8
4-hydroxy-4-methyl-2-pentanone	oxygenates	6	methyl-syringol(hardwood)	phenol	9
levoglucosan	sugar	6	ethyl-syringol(hardwood)	phenol	10
cellobiosan	sugar	12	synapylaldehyde (hardwood)	Phenol	11

1.2.2 Bio-oil upgrading for production of transportation fuels

Bio-oil can be upgraded to transportation fuels through several techniques. The principal of these techniques is to overcome the existed drawbacks of bio-oil in term of being utilized as liquid fuels. As illustrated elsewhere, bio-oil is an acidic, chemically unstable liquid with 10-50% water [31, 59, 60]. The bio-oil cannot be used directly as transportation fuels

due to its corrosiveness in engines and low energy density [61]. However, bio-oil is a liquid feedstock which can be chemically processed into different products.

Esterification is considered an effective option for stabilizing bio-oil [24]. Esterification converts the acids in bio-oil, in the presence of alcohol, to esters resulting in neutralizing its pH. Meantime, the bio-oil can also be stabilized partially due to the consumption of reactive functional groups during esterification. However, esterification cannot really upgrade bio-oil into "drop in" fuels because the upgraded bio-oil still contains water which is hard to remove. Apart from esterification, organic solvents addition, emulsification, ketonization of carboxylic acids and aldol condensation of aldehydes and ketones have also been reported as possible ways to improve the quality of the bio-oil [25, 62, 63]. Although there are still other stabilization methods available, the final products from all these approaches are still not distillable in the fuel range. In order to make bio-oil useful as transportation fuel, it requires chemical transformation to increase its energy density and reduce viscosity, reactivity through oxygen removal and molecular weight reduction. Therefore, deoxygenation of bio-oil becomes highly desirable. Significant efforts have already been put forth to develop efficient processes for deoxygenation of bio-oil [17, 64].

Catalytic hydrotreatment of bio-oil has been proven to be an efficient process to deoxygenate bio-oil. The main reactions occurred during hydrotreatment of bio-oil are HDO although partial hydrogenation (HYD) of unsaturated carbon double bonds is inevitable. This strategy has been widely proposed since early the 1980s [65], which currently has developed into three options 1) hydrotreating in batch reactor after condensation of bio-oil; 2) high pressure post-pyrolysis hydrotreating integrated with a hydropyrolysis reactor (*ex-situ*); and 3) catalytic fast pyrolysis of biomass with zeolite catalysts (*in-situ*).

1.2.2.1 Hydrotreatment in batch reactor

With respect of the former case (batch hydrotreating), a successful HDO of bio-oil will produce hydrocarbons (top organic phase) and an aqueous product phase (bottom layer). However, these HDO hydrocarbons can only be acquired under high temperature (>300°C) and H_2 pressure (20 MPa)[66]. As a result of the high oxygen content and presence of some highly reactive species the pyrolysis bio-oil has a high propensity for coke formation even under mild hydrotreating conditions. Early studies by Elliot et al. revealed that hydrotreating of pyrolysis oils at temperatures above 350°C resulted in plugging of the reactor system and catalyst encapsulation by coke-like material [67]. Many studies proposed that it is difficult for bio-oil simply translated to hydrocarbon fuel by directly catalytic HDO [68-71].

Thus, searching for other alternative methods such as employing a stabilization treatment before HDO of bio-oil to hydrocarbon fuel is needed. Elliot et al. first applied this stabilization method to treat bio-oil under mild condition [72]. Consequently, this concept started being used elsewhere. Xu et al. carried out a two-step catalytic HDO of bio-oil [73]. The first step in their study was aimed to overcome coke formation under 300°C and 10 MPa of H_2 pressure. Then a more severe condition (400°C, 13 MPa H_2) was applied on the stabilized bio-oil to acquire the hydrocarbon fuel. However, it should be noted that organic solvents (tetraline, decalin, diesel or diesel/isopropanol) were also added to the bio-oil to increase the hydrogen transferred in liquid phase during all their hydrotreatments. In this study, obviously, the cost of the two-step hydrotreatment of bio-oil was relatively high. Furthermore, the applied high hydrogen pressure makes the process hard to be scaled up. Therefore, HDO in the liquid phase under moderate conditions is an important goal in the future of bio-fuels production.

1.2.2.2 Hydropyrolysis

The second option of the hydrotreating is to conduct biomass pyrolysis under medium hydrogen pressure in a catalytic fluidized bed directly connected to a hydrotreating unit, which can further deoxygenate pyrolysis oil in vapor phase. This process is also called catalytic hydropyrolysis. The products from the catalytic hydropyrolysis are low-oxygen-containing hydrocarbon-rich liquid, which can be easily converted into pure hydrocarbons by simple hydrotreatment. Dayton et al. have demonstrated that biomass hydropyrolysis performed at 375-400°C and 2 MPa of H_2 pressure with catalysts can yield 16% of hydrocarbon-rich liquid that only contained 4.2% oxygen on a dry basis [74]. In addition, Meesuk et al. compared the products from catalytic and non-catalytic hydropyrolysis of rice husk at 500 °C [75]. The results indicated that bio-oil yield markedly reduced in the presence of Ni catalyst. But the catalytic hydropyrolytic oil contained more aromatic hydrocarbons than the ones from non-catalytic hydropyrolysis. The bio-oil with the lowest oxygen content (20.7 wt.%) and the highest heating value (30 MJ/kg) was obtained with a 75% volume fraction of the catalyst.

1.2.2.3 Catalytic fast pyrolysis

In addition, another similar upgrading process for pyrolysis oil is catalytic fast pyrolysis, which is the pyrolysis of biomass in the presence of a zeolite catalyst. This process is also called zeolite cracking which geared towards the elimination and substitution of oxygen and oxygen-containing functionalities although there is no hydrogen involved [13]. Carlson et al. reported that catalytic fast pyrolysis of pine wood sawdust with ZSM-5 based catalyst can directly produce aromatic hydrocarbons of 14% carbon in a fluidized bed reactor

at 600°C. Furthermore, olefins (primary ethylene and propylene) were also obtained with a carbon yield of 5.4% through this process [76]. Another study from Paasikallio et al. demonstrated that ZSM-5 catalyst can partially deoxygenate bio-oil from forest thinnings even at reaction temperatures of 400 to 500°C [77]. Meantime, they concluded that the catalyst was effective in eliminating carbohydrate-derived oxygenate molecules, which led to more aromatic hydrocarbons being produced.

The major difference between catalytic fast pyrolysis (*in-situ*) and hydropyrolysis (*ex-situ*) is the placement of the deoxygenation catalyst in the process, either external or internal with respect to the pyrolysis reactor. In *ex-situ* hydropyrolysis, dried biomass is rapidly heated to produce pyrolysis vapors, which are then sent into the deoxygenation reactor by using H_2 gas. In *in-situ* catalytic fast pyrolysis, dried biomass is rapidly heated in the presence of zeolite catalysts (often ZSM-5). The involved catalysts in this process are supposed to modify the depolymerization reactions of biomass which induces more hydrocarbon production [78].

In summary, catalytic hydrotreatment in a batch reactor can hold high pressure of H_2 gas and thus achieve high yield of hydrocarbons. However, the maximum temperature the batch reactor can reach is around 400°C (most run only at 300°C) which may limit many reactions needing high activation energy. Catalytic hydropyrolysis, on the other hand, can be carried out at temperatures up to 600°C while the pressure of H_2 in the hydropyrolysis reactor is typically low. Although hydropyrolysis may yield less hydrocarbons than the one generated from a batch reactor, it saves more energy than hydrotreatment in a batch reactor. This is due to not having the need to condense the pyrolysis vapors and re-heating of the batch reactor to hydrotreat the bio-oil in hydropyrolysis reactor. Zeolite cracking of biomass can directly produce low oxygen content aromatics or even oxygen free

hydrocarbons. However, it generally needs more zeolite involved during pyrolysis and coke is inevitably formed.

1.2.3 Reactions pathways during catalytic hydrotreatment

1.2.3.1 Hydrodeoxygenation (HDO)

During HDO, oxygen in the feedstock is converted to H_2O which is environmentally benign. The produced hydrocarbons will float to the top of the aqueous phase, which is easily separated after reaction. In the bio-oil, the oxygen content may approach 50% as reported [31]. Some of the oxygen-containing compounds in the bio-oil readily polymerize and as such are the cause of the fuel instability which may lead to poor performance during the fuel combustion. During hydrotreatment, such compounds may be cause of a rapid catalyst deactivation [27]. Due to the complex compositions of bio-oils, most of the HDO studies reported have been focused on using model compounds rather than the real bio-oils. Phenols have been received considerable attentions because of their low reactivity in HDO process.

The HDO of phenolic compounds is believed to occur via three parallel paths as shown in Figure 1.1. In the presence of H_2, direct cleavage or hydrogenolysis of the C-OH bond to yield benzene and water (HDO pathway) in the first pathway. The second route involves the saturation of the aromatic ring via hydrogenation (HYD), followed by dehydration to yield cyclohexane and water. Meanwhile, aromatic ring condensation reactions inevitably occurred as depicted in the third route shown in Figure. 1.1. Similar HDO mechanisms of phenol were proposed elsewhere and have been well-recognized nowadays [13, 78-80].
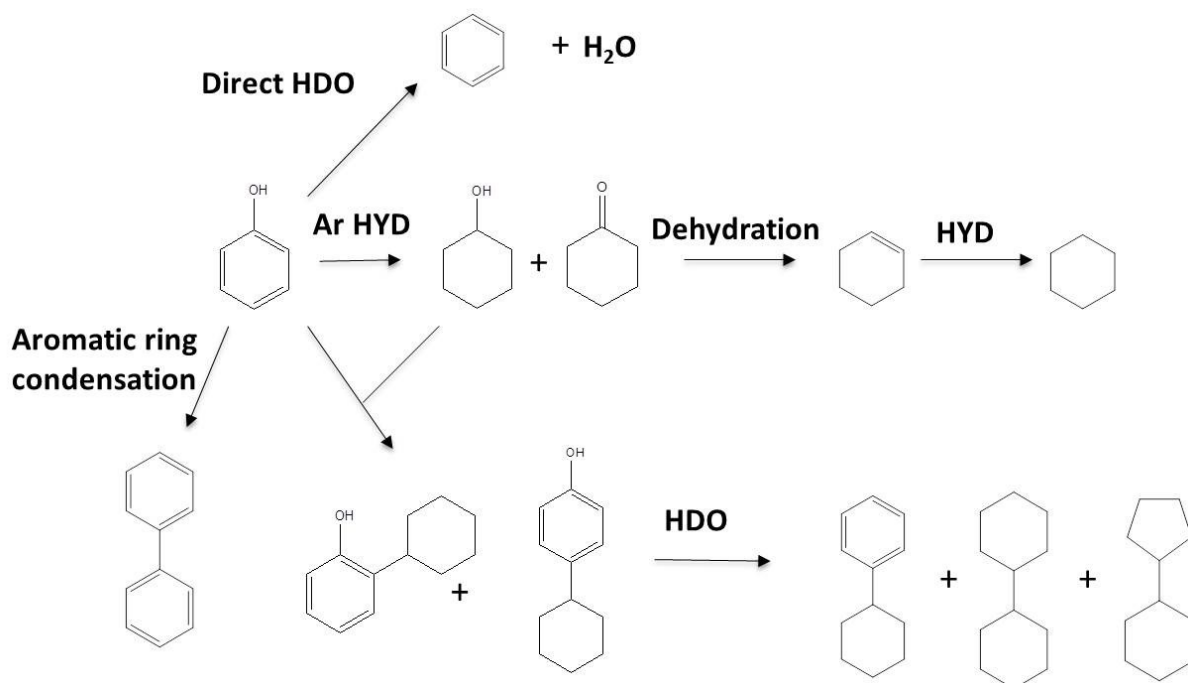
Figure 1.1 Proposed phenol HDO and HYD mechanisms to hydrocarbons

The H_2 consumption and severity of the operation required for achieving high HDO conversion depend on the content and type of the compounds in the feed. An active catalyst must be present to achieve desirable HDO conversions. Also a good HDO conversion is often achieved at temperature more than 300°C in term of most heterogeneous catalysts [81]. This is because the HDO of some oxygen containing compounds in bio-oil needs higher activation energy to be initialized even in the presence of a catalyst. However, oxygen containing compounds can readily polymerize even at the temperature around 150°C during hydrotreatment and the polymerization rate increased with the increasing reaction temperature, resulting in coke formation [73, 82].

In order to avoid the coke formation, a stabilization stage hydrotreatment on bio-oil was carried out first before the HDO in some studies [72, 73]. The hypothesis was that those very active oxygen-containing compounds (such as aldehydes) can be reduced to more

stable compounds beforehand and thus minimize their polymerization for coke formation. However, this process generally needs the catalyst to maintain their activity even at low temperature. In addition, the pyrolytic lignin oligomers in bio-oil are hard to deoxygenate using this multiple-stage hydrotreatment approach. Therefore, researchers are now starting to use these oligomers from the bio-oil for production of phenolics, which then can be further upgraded to aromatics or cycloalkanes [56, 83-85]. Huber et al. studied the ruthenium (Ru) based catalysts for the low temperature hydrotreatment on the aqueous phase of oak wood-derived pyrolysis oil. The authors suggest that separation of the pyrolysis oil into two phases prior to upgrading allows for better control of catalyst design and optimization [86].

1.2.3.2 Hydrocracking

In addition to HDO, another reaction that can occur during hydrotreatment is hydrocracking. Conventional hydrocracking processes are commonly applied in petroleum industry with zeolite based catalysts for isomerization or production of light hydrocarbons. This catalytic hydrocracking produces an excess of branched hydrocarbons largely because the rather rapid splitting reaction is accompanied by an equally rapid isomerization reaction as in catalytic cracking. Such a mechanism permits even normal paraffins to be split into products rich in iso-paraffins [87]. With respect to the bio-oil, catalytic hydrocracking is mostly introduced to depolymerize the tar or pyrolytic lignin oligomers for small molecules production, such as phenolics. The proposed mechanism for this hydrocracking involves the cleavage of β-O-4 and α-O-4 linkages in pyrolytic lignin, which are favored by the acidic zeolite catalysts [88, 89]. In the application of upgrading biomass pyrolysis oil or vapors, a

fundamental understanding of the factors that favor C-O bond cleavage and C-C bond formation is still needed.

Tang et al. demonstrated in their studies that pyrolytic lignin from rice husk pyrolysis oil can be hydrocracked at 260°C in supercritical ethanol under a H_2 atmosphere using a Ru-based catalyst [83]. Although there is no zeolite catalyst involved in their study, the pyrolytic lignin was still successfully cracked into small molecules including phenols, guaiacols, anisoles, esters, and light ketones. More recently, Ferrini et al. developed a novel routine to produce non-pyrolytic lignin bio-oil through catalytic hydrogen transfer reactions [90]. In this process, lignin was released by solvolysis from the plant cell wall as fragments having much lower molecular weight (M_w) than currently believed. In fact, this is another type of hydrocracking which occurred under cooking with propanol and nickel (Ni) catalysts instead of fast pyrolysis. The results also indicated that the produced lignin fragments are mainly phenolics, which only needs low-severity conditions to be further deoxygenated.

1.2.3.3 Decarboxylation and decarbonylation

In contrast with HDO and hydrocracking, decarboxylation and decarbonylation can take place even in the absence of H_2 gas. Decarboxylation is a chemical reaction that removes a carboxyl group and releases carbon dioxide (CO_2). Usually, decarboxylation refers to a reaction of carboxylic acids, removing a carbon atom from a carbon chain. With similar fashion, decarbonylation is also a transformation that involves the conversion of aldehydes to alkanes with the byproduct of carbon monoxide (CO), usually catalyzed by metal complexes. During hydrotreatment of bio-oil, decarboxylation and decarbonylation can also be considered as deoxygenating pathways. However, decarboxylation is also commonly applied

in triglycerides deoxygenation to produce alkanes [91]. Wang et al. investigated the effect of process parameters on catalytic decarboxylation of soybean oil. The results revealed that a complete conversion of the triglycerides was observed at 650 psi and 360-450°C with Ni-Mo/ZSM-5 catalysts [92].

1.2.4 Catalysts for hydrodeoxygenation of bio-oil

Under the fixed H_2 pressure and temperature, the reaction rate of HDO is mainly determined by the activity of catalyst involved. Therefore, it is important to study how to design good catalysts which can increase the conversion of feedstock and the selectivity of hydrocarbon products. Catalysts involved in studies on hydrotreatment of pyrolysis bio-oils are often solid which are considered as heterogeneous catalysts in terms of liquid feedstock. Heterogeneous catalysts are more preferred than homogeneous catalysts in the application of biomass pyrolysis oil hydrotreatment because solid catalysts can be easily separated from the liquid products and thus favor the reuse of catalysts.

In a homogeneous catalyzed reaction the determination of the kinetic factors for the process is usually straightforward. But a heterogeneous catalyzed process is more complex because the catalyst is not uniformly distributed throughout the reaction medium. Reactions mainly take place in a two phase system, either vapor/solid or liquid/solid. In such a system several steps are needed to complete the catalytic cycle: 1) transport of the reactants to the catalyst; 2) interaction of the reactants with the catalyst (adsorption); 3) reaction of adsorbed species to give the product; 4) desorption of the product from the catalyst; and 5) transport of the product away from the catalyst [93]. The phenol HDO mechanisms on solid catalysts surface is shown in Figure 1.2. Hydrogen gas is firs activated on the noble metal

surface. Oxygen from oxygen containing compounds that absorbed either on metal sites (Figure 1.2-A) or on catalyst support (Figure 1.2-B) can then react with the activated H species to form hydrocarbons and water. Vispute and Huber pointed out in their research that catalyst support should maintain enough acidic sites for the dehydration of oxygen compounds [86]. Furthermore, metal sites in the catalyst system are responsible for the hydrogenation reactions.
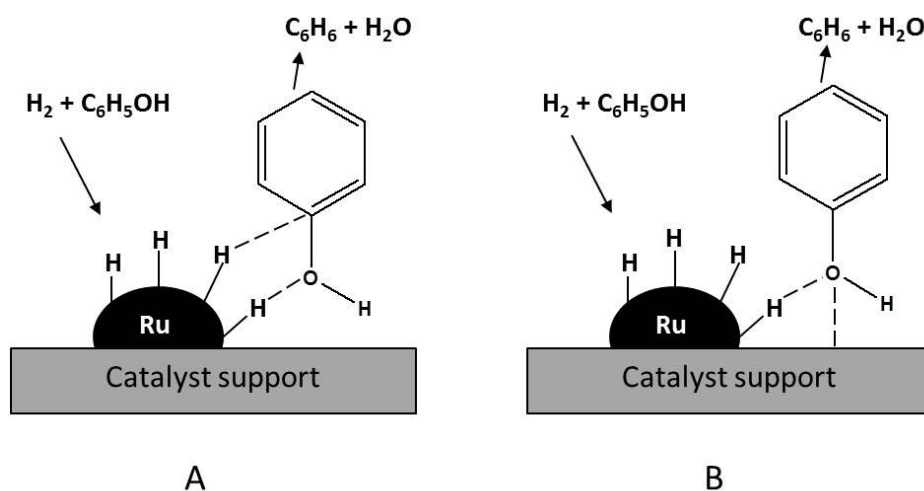
Figure 1.2 HDO reaction on oxide-supported noble metal catalyst (A) HDO at the noble metal, and (B) HDO at the metal-support interface [78, 81].

Solid catalysts for bio-oil HDO are generally composed by active metals and support. The active metals are found on the support surface. The most efficient catalysts usually have a large catalytically active surface area exposed to the reaction medium. One way of maximizing the active surface of a catalyst is using a very fine powder as support. However, heating powdered catalysts usually results in sintering or the agglomeration of the small particulates into larger, less efficient entities. In addition, metal loading is another critical parameter that can determine the catalyst's activity. Generally the more expensive precious metal catalysts have low metal loadings and are highly dispersed while catalysts containing

less expensive base metals have higher metal loadings, usually 20-40% or higher. The relationship between the catalyst loading and crystallite size or catalyst dispersion is dependent on many factors, of which one of the more important is the surface area of the support [93].

In this review, focus is placed on studies that made use of model compounds for comparisons of catalysts and the reaction networks they promote. Different metal based catalysts are separately discussed in term of the HDO of bio-oil model compounds. To achieve better conversion, organic hydrocarbons (tetradecane, n-hexadecane, decalin,) are often introduced as solvents to phenol and guaiacol HDOs. It is believed that the organic solvent can increase the hydrogen transfer in reaction medium. To better mimic bio-oil, HDO of phenol or guaiacol in aqueous solution is highly desirable but still challenging due to leaching and deactivation of many solid catalysts. All these issues are discussed in the literature review below.

1.2.4.1 Noble metal catalysts

Noble metal catalysts are readily available, which has facilitated deoxygenation studies with whole bio-oils, and these have been included in recent upgrading reviews [7, 13, 64, 79]. Noble metals are attractive because they are known to activate H_2 at mild conditions since H_2 is easily activated and split on the interface or surface to react with other reactants. In addition, noble metals (rhenium (Rh), Ru, platinum (Pt), and palladium (Pd)) are less susceptible to deactivation by water during hydrotreatment and thus secure catalyst stability.

Gutierrez et al. conducted a study of guaiacol HDO using zirconia supported noble metal (Rh, Pd and Pt) catalysts [94]. Their results showed that these catalysts were active for guaiacol aromatic ring hydrogenation (HYD) even at 100°C and 8 MPa of H_2 pressure. According to the product distributions, methyl transfer on the hydrocarbon ring was catalyzed by the noble metals but not by conventional $CoMo/Al_2O_3$ catalysts. The products from all reactions were nearly all hydrogenated oxygen-containing compounds at 100°C. They pointed out that deoxygenation of guaiacol over noble metals took place only at 300°C. These noble metals supported on zirconia were also employed for pyrolysis oil hydrotreatment in subsequent studies [70]. The yields of upgraded oils (7-11% oxygen) were between 37-47% based on the feedstock. Elkasabi et al. carried out a systematic HDO study with respect to hydrotreatment of pyrolysis bio-oil from various feedstock [17]. Bio-oil catalyzed with Pt/C showing the most promise for overall upgrading efficiency.

Furthermore, Vispute et al. used activated carbon supported Ru catalyst (Ru/C) to hydrogenate the aqueous phase of pyrolysis bio-oil at 125-175°C and 6.9 MPa (H_2 pressure) [86]. Under this condition, various oxygen containing functionalities in the bio-oil (including aldehydes; acids; sugars) were converted to their corresponding alcohols and light gases (mainly CH_4). These results proved that the noble metal catalysts can maintain the activity in aqueous solution. A study by Zhao et al. further investigated the HDO of phenol in aqueous solution over Pd/C catalyst in the presence of an acid at 200-250°C [85]. Although water was present, the yield of cyclohexane from phenol HDO approached 100%. As illustrated in their study, phenol did not undergo direct hydrogenolysis to benzene in water. However, the Pd as well as Pt-, Ru- and Rh-based catalysts efficiently favored phenol HYD to cyclohexanol. With an increase of reaction temperature to 200°C, cyclohexanol was quantitatively dehydrated to cyclohexene which was catalyzed by mineral acids. The HYD of cyclohexene to

cyclohexane proceeds at high rates catalyzed by Pd-based catalysts. This implied that the formation of cyclohexane from phenol requires bi-functional catalysis, i.e. the presence of both acidic catalyst and metal catalyst. More recently, Nan et al. carried out the hydrotreatment of pyrolysis oil over Ru- and Rh/C catalysts in the presence of polyethylene glycol as solvent. With Ru/C at 280°C and 6.9 MPa of H_2 pressure, 21% of hydrocarbons were obtained from the hydrotreatment [95]. Overall, noble metals combined with acid catalyst support are promising for HDO of bio-oil especially lignin-derived compounds. However, their high price is a limitation for these catalysts in large-scale utilization.

1.2.4.2 Transition metal catalysts

Inexpensive transition metals (mainly Ni, copper (Cu), iron (Fe), and molybdenum (Mo)) are also active for HDO [13, 20, 91]. However, these type of catalysts easily suffer from leaching and/or sintering during the reaction [96] even though there are still a number of studies that achieved good HDO conversion on phenolics with nickel based catalysts. Valle et al. studied the Ni modified HZSM-5 catalyst for converting bio-oil to hydrocarbons. They pointed out the major drawback in their hydrotreatment of bio-oil was the rapid catalyst deactivation caused by the deposition of coke that is thermal and catalytic origin. However, the co-feeding of methanol with bio-oil can effectively reduce coke deposition [97]. Consequently, a similar study on Ni/HZSM-5 modified with Cu and cobalt (Co) was also carried out by Huynh et al, which revealed the presence of Ni was essential for high activity of HDO of phenol in the presence of water [20]. However, modification with Cu deteriorated the catalyst performance significantly whereas the co-mixture with Co increased the activity and selectivity toward the target hydrocarbons. It should be noted that the transition metal

leaching or sintering often easily occurs when water is introduced as solvent. This is important because other studies on the similar Ni-Cu catalysts can achieve very different results if water is not involved. For example, Bykova et al. conducted a very similar study to that of Huynh et al. [71]. However, they used pure guaiacol without water in the feedstock. After HDO tests at 320°C and 17 MPa of H_2 pressure, NiCu/SiO_2-ZrO_2 showed good HDO conversion and selectivity to hydrocarbons. The negative effect on HDO from Cu in this study was not observed. This was because there was no water, as solvent, in the system and thus a different HDO mechanism over the Ni-Cu catalyst was revealed.

Meesuk et al. reported that bio-oils from hydropyrolysis, using Ni-loaded Loy Yang brown coal (Ni/LY) char, contained more aromatic hydrocarbons with slightly reduced oxygenated compounds and can be used as liquid fuel [75]. Additionally, Ardiyanti et al. investigated the bimetallic Ni-Cu catalysts on various supports [68]. They concluded that the NiCu/TiO_2 showed the highest activity on bio-oil hydrotreatment at 350°C and 20 MPa initial H_2 pressure although moderate Ni and Cu leaching was observed after the reaction. Ni based catalysts on different supports were employed for HDO of guaiacol and anisole in other studies, which all showed a high HDO activity for benzene and cyclohexane production with good yields [19, 98].

Besides incorporating Cu and Co into the Ni catalyst systems, phosphide and/or Mo based catalysts are also well studied for the HDO reactions. Metal phosphides have been extensively studied as catalysts for hydrodenitrogenation (HDN) and hydrodesulfurization (HDS), but only recently have their deoxygenation properties attracted scientific and technological attention [64]. Whiffen systematically investigated Ni_2P and MoP based catalysts for hydrodeoxygenation of pyrolysis oil and phenol [99]. Although successful HDO of pyrolysis oil over sulfide, oxide, and phosphide catalysts were all achieved, MoP and Ni_2P

were found to have the highest yield of oxygen free liquid and lowest coke yield. Yang et al. studied Ni_2P/SBA-15 catalyst for HDO of methyl oleate, which produced n-heptadecane at a high yield [100]. Moreover, Rensel and Hicks et al. reported a synthesized bimetallic FeMoP catalyst with remarkable selectivity to the HDO of aryl ethers and phenol [101]. Even under a low H_2 pressure (2.1 MPa), a near complete conversion (>99%) of benzene was produced over this catalyst at 400°C.

1.2.4.3 Support effects on catalysts

There are a number of physical characteristics of supports that are important for proper performance of the supported catalyst. These are hardness, density, pore volume, pore size, pore distribution, particle size and particle shape [93]. The surface area is directly related to pore size, distribution and volume. Support particles must be sufficiently hard to withstand the abrasion associated with the type of process. Therefore, metal catalysts used in industry are typically supported on a carrier for achieving better metal dispersion and thus higher reaction activity [102]. For this reason, materials with large surface area are highly desirable to be a good support. Al_2O_3, SiO_2, and SiO_2-Al_2O_3 as well as zeolites, especially the HZSM-5 have been extensively studied as Ni catalyst supports [103]. As a shape-selective zeolite, HZSM-5 has intermediate pore sizes and good thermal ability. Only small molecules are allowed to diffuse into the micropores. Although this microporous material is very effective for aromatic hydrocarbon production, coke is easily formed on it in terms of bio-oil HDO. One important reason is there are many high molecular weight oligomers present in bio-oil and thus easily block the micropores of HZSM-5 [104-106]. Amorphous SiO_2 or Al_2O_3

are therefore preferred but efforts should be made to increase their surface area and selectivity.

Yang et al. studied hydrodeoxygenation of anisole over a series of Ni containing catalysts based on different carriers including SBA-15, Al-SBA-15, γ-Al_2O_3, microporous carbon, TiO_2 and CeO_2 [19]. It was proposed in this study that acidity of the supports was very important because strong acid sites may contribute the hydrogenolysis of anisole, while metallic sites can further hydrogenate intermediate compounds to yield cyclohexane. Zhang et al. reported that Ni supported on mixed oxides (Al_2O_3-SiO_2, Al_2O_3-TiO_2, TiO_2-SiO_2 and TiO_2-ZrO_2) also showed high activity on HDO of guaiacol with good cyclohexane selectivity at 300°C and 4 MPa H_2 pressure [98]. However, these catalysts performed poorly when water was used as solvent, which was explained by the impaired adsorption on the acid sites of catalyst between water and guaiacol. Most recently, Neumann et al. elucidated the mechanisms of different zeolite type catalyst (HZSM-5, H-beta, and HY) during catalytic fast pyrolysis of lignin model compounds [107]. With respect to the dominant linkage of β-O-4 in lignin, the zeolite H-Beta gave the best benzene production in all cases while the least amount of coke was produced with HZSM-5. The characterization of these catalysts revealed that intact lignin model compounds were unable to enter the micropores of the zeolites and thus coke easily formed at the pore openings. In addition, Wang et al. evaluated the support effects of NiMo based catalysts during HDO of soybean oil [108]. Their results indicated that zeolite-supported catalysts had a strong cracking activity, producing more gaseous and gasoline products. On the other hand, meso-porous γ-Al_2O_3, and Al-SBA-15 supported catalysts led to higher production of green diesel (C_{15}-C_{18}), which was due to their high surface area, large porosity and regular channel structure.

Supports that limit chemisorption of large reactants (leading to blockage of catalyst sites) should be employed. Silica nanosprings are a novel synthesized material which has 100% chemical accessible surface [109]. The first publication on the synthesis of boron carbide nanosprings reported a yield of less than 10% [110], and similar yields were reported for SiO_2 [111]. A later study from Wang et al. illustrated that the silica-based nanosprings can be synthesized with yield higher than 90% [112]. As a novel nanomaterial, the inherent chemical and physical properties of nanosprings are still under-investigated [113-115]. However, a very attractive application for nanosprings is for use as catalyst support. Sai et al. coated silica nanosprings with noble metal nanoparticles using chemical vapor deposition method [116]. More recently, Luo et al. reported that the silica nanosprings can also be successfully coated with Co by thermal assisted reduction process, which was conducted on a quartz frit [117]. It should be noted that nanosprings can grow from a single or multiple nanowire(s) [112]. The diameter of the synthesized nanosprings thus is around 200 nm with a pitch close to 150 nm and an overall length of between 10 and 200 μm. All these characters make the nanosprings a promising catalyst support for HDO reactions.

1.2.4.4 Catalyst stability and deactivation

The stability of metal catalysts under hydrotreatment conditions (i.e., high temperature, high partial pressures of H_2 and steam, and low pH) has not been well investigated. Ruddy et al. pointed out that surface oxidation of transition metal materials is likely to be the cause of catalyst deactivation and may lead to changes in product selectivity [78]. Zhao and Lercher investigated the detailed kinetics of phenol HDO in liquid aqueous medium over Ni supported on HZSM-5 with and without 19.3% Υ-Al_2O_3 binder [118]. Catalyst

stability tests indicated that Ni leaching was almost negligible from Ni/Al$_2$O$_3$-HZSM-5 after 90 h. The HZSM-5 support was stable, but the Al$_2$O$_3$-HZSM-5 support lost 7% in weight. The catalytic activity gradually decreased when the catalyst was recovered and reused, mainly due to Ni particle sintering. The results agreed well with the theory Augustine proposed [93]. The mechanism of the metal sintering is shown in Figure 1.3.
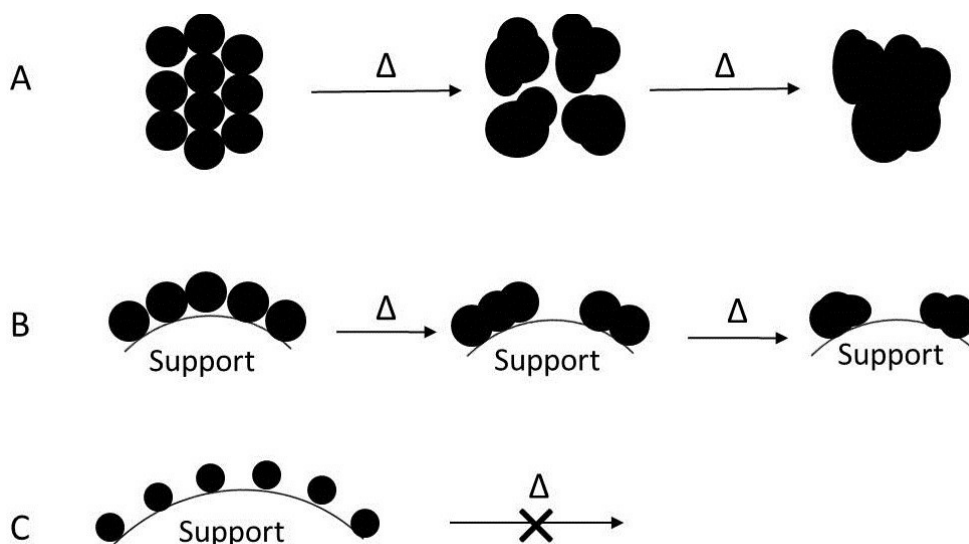
Figure 1.3 Effect of catalyst load and the presence of a support on the sintering of a catalyst. A) unsupported powdered catalyst; B) high loading supported catalyst; C) low load supported catalyst [93].

In addition to the metal sintering, other deactivation mechanisms of solid catalysts were also proposed. Ramasamy et al. studied HZSM-5 catalyst deactivation using aqueous feed mixtures containing ethanol, acetic acid, ethyl acetate, and acetaldehyde in a fixed bed reactor at 360°C and 2 MPa of H$_2$ [104]. Experimental results showed that the presence of acetaldehyde generated high molecular weight aromatic compounds which deactivate the catalyst through a pore-blocking mechanism. Acetic acid deactivated the catalyst through an

active site poisoning mechanism. Although different mechanisms have been proposed, a way to attenuate catalyst deactivation is still rare. Gayubo et al. suggested that co-feeding methanol with bio-oil can attenuate HZSM-5 catalyst deactivation by minimizing the pore blocking of catalyst support [103]. However, efficient methods to overcome the metal sintering or active site poisoning are still highly desirable. In the future, more attention will likely be given to technologies that prevent catalyst deactivation in order to increase the lifetime of catalysts.

1.3 Research objectives

The main objective of the following study is to develop effective catalysts for bio-oil hydrodeoxygenation (HDO). There are two obstacles needing to be overcome: 1) how to increase the catalyst activity and selectivity to hydrocarbons; and 2) how to effectively conduct bio-oil HDO without coke formation. In terms of increasing catalyst activity, a novel material, silica nanosprings, will be initially introduced as catalyst support for phenol HDO. The hypothesis is that catalysts perform well on phenol HDO and can also have good performance on bio-oil HDO. To better simulate pyrolysis bio-oil, water will be used as solvent during phenol HDO. The activity of developed catalysts under this condition will be also evaluated as well as to test if silica nanosprings can improve catalyst performance compared to conventional silica gel and alumina supports. In addition, both transition and noble metals will be used for the catalyst synthesis. The corresponding activity of these two types of catalysts will be also compared.

Nevertheless, the only research conducted on catalyst activity has not been enough to further bio-oil HDO because since is very difficult to conduct HDO of bio-oil due to coke

formation during hydrotreatment. Therefore, another parallel study was carried out on developing a suitable process for bio-oil HDO. Due to the complexity of bio-oil, it is reasonable to separate it into several homogenous parts. A feasible separation routine is to remove the pyrolytic lignin oligomers from bio-oil by adding water. Since the oligomers are completely insoluble in water, it is easy to get two phases 1) water soluble phase (WS) and 2) water insoluble phase (WIS) of bio-oil. Theoretically, each phase should undergo specific hydrotreatment due to their different properties. For hydrotreatment of WS of bio-oil, a similar HDO can be conducted on it as the one carried out for phenol HDO. On the other hand, WIS of bio-oil needs to first be treated for HDO because it is a viscous liquid and will form coke if direct HDO is carried out on it. Hydrocracking may be an effective process to transform these oligomers into small molecules. Therefore, the hydrocracking on WIS was conducted and results will be discussed. A subsequent HDO will be followed to test if hydrocarbons can be produced from the cracked bio-oil.

1.4 References

1.   Rafael Luque, J.C.a.J.C., *Handbook of biofuels production: processes and technologies*. Woodhead Publishing Series. 2011: Woodhead. 659.

2.   Gunawan, R., et al., *Upgrading of bio-oil into advanced biofuels and chemicals. Part I. Transformation of GC-detectable light species during the hydrotreatment of bio-oil using Pd/C catalyst.* Fuel, 2013. **111**: p. 709-717.

3.   Junming, X., et al., *Bio-oil upgrading by means of ethyl ester production in reactive distillation to remove water and to improve storage and fuel characteristics.* Biomass and Bioenergy, 2008. **32**(11): p. 1056-1061.

4.   Ma, L., et al., *A review of thermal–chemical conversion of lignocellulosic biomass in China.* Biotechnology Advances, 2012. **30**(4): p. 859-873.

5.   Alvira, P., et al., *Pretreatment technologies for an efficient bioethanol production process based on enzymatic hydrolysis: A review.* Bioresource Technology, 2010. **101**(13): p. 4851-4861.

6.   Fangrui Ma, M.A.H., *Biodiesel production: a review.* Bioresource Technology, 1999. **70**: p. 1-15.

7.   Bridgwater, A.V., *Review of fast pyrolysis of biomass and product upgrading.* Biomass and Bioenergy, 2012. **38**: p. 68-94.

8.   Kumar, A., D.D. Jones, and M.A. Hanna, *Thermochemical Biomass Gasification: A Review of the Current Status of the Technology.* Energies, 2009. **2**(3): p. 556-581.

9.   Dürre, P., *Biobutanol: An attractive biofuel.* Biotechnology Journal, 2007. **2**(12): p. 1525-1534.

10.   Patil, P.D., et al., *Optimization of direct conversion of wet algae to biodiesel under supercritical methanol conditions.* Bioresource Technology, 2011. **102**(1): p. 118-122.

11.   Smith, P.C., et al., *Improving the low-temperature properties of biodiesel: Methods and consequences.* Renewable Energy, 2010. **35**(6): p. 1145-1151.

12.   Al Maksoud, W., et al., *Direct thermocatalytic transformation of pine wood into low oxygenated biofuel.* Green Chemistry, 2014. **16**(6): p. 3031.

13.   Dickerson, T. and J. Soria, *Catalytic Fast Pyrolysis: A Review.* Energies, 2013. **6**(1): p. 514-538.

14.   Kuo, P.-C., W. Wu, and W.-H. Chen, *Gasification performances of raw and torrefied biomass in a downdraft fixed bed gasifier using thermodynamic analysis.* Fuel, 2014. **117**: p. 1231-1241.

15.   Brown, R.C., ed. *Thermochemical Processing of Biomass: Conversion into Fuels, Chemicals, and Power.* ed. C.V. Stevens. 2011, John Wiley & Sons.

16.   Alcala, A. and A.V. Bridgwater, *Upgrading fast pyrolysis liquids: Blends of biodiesel and pyrolysis oil.* Fuel, 2013. **109**: p. 417-426.

17.   Elkasabi, Y., et al., *Hydrodeoxygenation of fast-pyrolysis bio-oils from various feedstocks using carbon-supported catalysts.* Fuel Processing Technology, 2014. **123**: p. 11-18.

18.   Zhang, H., et al., *Characterization of Coke Deposition in the Catalytic Fast Pyrolysis of Biomass Derivates.* Energy & Fuels, 2014. **28**(1): p. 52-57.

19.   Yang, Y., et al., *Effect of metal–support interaction on the selective hydrodeoxygenation of anisole to aromatics over Ni-based catalysts.* Applied Catalysis B: Environmental, 2014. **145**: p. 91-100.

20.   Huynh, T.M., et al., *Hydrodeoxygenation of Phenol as a Model Compound for Bio-oil on Non-noble Bimetallic Nickel-based Catalysts.* ChemCatChem, 2014: p. n/a-n/a.

21.   Leng, S., et al., *NiFe/γ-Al2O3: A universal catalyst for the hydrodeoxygenation of bio-oil and its model compounds.* Catalysis Communications, 2013. **41**: p. 34-37.

22.   Mortensen, P.M., et al., *Screening of Catalysts for Hydrodeoxygenation of Phenol as a Model Compound for Bio-oil.* ACS Catalysis, 2013. **3**(8): p. 1774-1785.

23.   Zhao, H.Y., et al., *Hydrodeoxygenation of guaiacol as model compound for pyrolysis oil on transition metal phosphide hydroprocessing catalysts.* Applied Catalysis A: General, 2011. **391**(1-2): p. 305-310.

24.   Zhe Tang, Q.L., Ying Zhang, Xifeng Zhu, and Qingxiang Guo, *One Step Bio-Oil Upgrading through Hydrotreatment, Esterification, and Cracking.* Industrial & Engineering Chemistry Research, 2009(48): p. 6923-6929.

25.   Pham, T.N., et al., *Ketonization of Carboxylic Acids: Mechanisms, Catalysts, and Implications for Biomass Conversion.* ACS Catalysis, 2013. **3**(11): p. 2456-2473.

26.   Pham, T.N., D. Shi, and D.E. Resasco, *Evaluating strategies for catalytic upgrading of pyrolysis oil in liquid phase.* Applied Catalysis B: Environmental, 2014. **145**: p. 10-23.

27.   Furimsky, E., *Review:Catalytic hydrodeoxygenation.* Applied Catalysis A: General, 2000(199): p. 147-190.

28.   Registry, A.f.T.S.a.D., *Total petroleum hydrocarbons.* 1999. p. 17-37.

29.   D.Collins, C., *Implementing Phytoremediation of Petroleum Hydrocarbons.* Phytoremediation Methods in Biotechnology 2007. **23**: p. 99-108.

30.   Pan, S., et al., *Compositional Characterization and Pyrolysis of Loblolly Pine and Douglas-fir Bark.* BioEnergy Research, 2012. **6**(1): p. 24-34.

31. Bertero, M., G. de la Puente, and U. Sedran, *Fuels from bio-oils: Bio-oil production from different residual sources, characterization and thermal conditioning.* Fuel, 2012. **95**: p. 263-271.

32. Boerjan, W., J. Ralph, and M. Baucher, *Ligninbiosynthesis.* Annual Review of Plant Biology, 2003. **54**(1): p. 519-546.

33. Ken-ichi Kuroda, T.O., and Takahiro Ueno, *Characterization of Sago Palm (Metroxylon sagu) Lignin by Analytical Pyrolysis.* Journal of Agricultural and Food Chemistry, 2001. **49**: p. 1840-1847.

34. Faravelli, T., et al., *Detailed kinetic modeling of the thermal degradation of lignins.* Biomass and Bioenergy, 2010. **34**(3): p. 290-301.

35. Chen, W.-H. and P.-C. Kuo, *A study on torrefaction of various biomass materials and its impact on lignocellulosic structure simulated by a thermogravimetry.* Energy, 2010. **35**(6): p. 2580-2586.

36. Brewer, C.E., et al., *Characterization of biochar from fast pyrolysis and gasification systems.* Environmental Progress & Sustainable Energy, 2009. **28**(3): p. 386-396.

37. Liaw, S.-S., et al., *Effect of pyrolysis temperature on the yield and properties of bio-oils obtained from the auger pyrolysis of Douglas Fir wood.* Journal of Analytical and Applied Pyrolysis, 2012. **93**: p. 52-62.

38. A.V.Bridgwater, S.C.a., *Overview of Applications of Biomass Fast Pyrolysis Oil.* Energy& Fuels, 2004(18): p. 590-598.

39. Mullen, C.A. and A.A. Boateng, *Chemical Composition of Bio-oils Produced by Fast Pyrolysis of Two Energy Crops†.* Energy & Fuels, 2008. **22**(3): p. 2104-2109.

40.   Kim, K.H., et al., *Comparison of physicochemical features of biooils and biochars produced from various woody biomasses by fast pyrolysis.* Renewable Energy, 2013. **50**: p. 188-195.

41.   Bertero, M., G. de la Puente, and U. Sedran, *Effect of Pyrolysis Temperature and Thermal Conditioning on the Coke-Forming Potential of Bio-oils.* Energy & Fuels, 2011. **25**(3): p. 1267-1275.

42.   Garcìa-Pérez, M., et al., *Vacuum pyrolysis of softwood and hardwood biomass.* Journal of Analytical and Applied Pyrolysis, 2007. **78**(1): p. 104-116.

43.   Wei, X., et al., *Characterization of the water-insoluble pyrolytic cellulose from cellulose pyrolysis oil.* Journal of Analytical and Applied Pyrolysis, 2012. **97**: p. 49-54.

44.   b.Scholze, D.M., *Characterization of the water insoluble fraction from fast pyrolysis liquids(pyrolytic lignin). Part 1. PY-GC/MS, FTIR, and functional groups.* Journal of Analytical and Applied Pyrolysis, 2001(60): p. 41-54.

45.   Mullen, C.A. and A.A. Boateng, *Characterization of water insoluble solids isolated from various biomass fast pyrolysis oils.* Journal of Analytical and Applied Pyrolysis, 2011. **90**(2): p. 197-203.

46.   Poletto, M., A.J. Zattera, and R.M.C. Santana, *Thermal decomposition of wood: Kinetics and degradation mechanisms.* Bioresource Technology, 2012. **126**: p. 7-12.

47.   Kim, U.-J., S.H. Eom, and M. Wada, *Thermal decomposition of native cellulose: Influence on crystallite size.* Polymer Degradation and Stability, 2010. **95**(5): p. 778-781.

48.   Yang, H., et al., *Characteristics of hemicellulose, cellulose and lignin pyrolysis.* Fuel, 2007. **86**(12-13): p. 1781-1788.

49.   B.Scholze, C.H., D. Meier, *Characterization of the water insoluble fraction from fast pyrolysis liquids(pyrolytic lignin) Part 2.GPC, carbonyl groups, and ^{13}C-NMR.* Journal of Analytical and Applied Pyrolysis, 2001(58-59): p. 387-400.

50.   Bayerbach, R., et al., *Characterization of the water-insoluble fraction from fast pyrolysis liquids (pyrolytic lignin).* Journal of Analytical and Applied Pyrolysis, 2006. **77**(2): p. 95-101.

51.   Bayerbach, R. and D. Meier, *Characterization of the water-insoluble fraction from fast pyrolysis liquids (pyrolytic lignin). Part IV: Structure elucidation of oligomeric molecules.* Journal of Analytical and Applied Pyrolysis, 2009. **85**(1-2): p. 98-107.

52.   Zhou, S., et al., *Effect of sulfuric acid addition on the yield and composition of lignin derived oligomers obtained by the auger and fast pyrolysis of Douglas-fir wood.* Fuel, 2013. **103**: p. 512-523.

53.   Ben, H. and A.J. Ragauskas, *NMR Characterization of Pyrolysis Oils from Kraft Lignin.* Energy & Fuels, 2011. **25**(5): p. 2322-2332.

54.   Venkatakrishnan, V.K., et al., *High-pressure fast-pyrolysis, fast-hydropyrolysis and catalytic hydrodeoxygenation of cellulose: production of liquid fuel from biomass.* Green Chemistry, 2014. **16**(2): p. 792.

55.   Karagoz, S., et al., *Comparative studies of oil compositions produced from sawdust, rice husk, lignin and cellulose by hydrothermal treatment.* Fuel, 2005. **84**(7-8): p. 875-884.

56.   Fele Žilnik, L. and A. Jazbinšek, *Recovery of renewable phenolic fraction from pyrolysis oil.* Separation and Purification Technology, 2012. **86**: p. 157-170.

57. Xu, J., et al., *Rice husk bio-oil upgrading by means of phase separation and the production of esters from the water phase, and novolac resins from the insoluble phase.* Biomass and Bioenergy, 2010. **34**(7): p. 1059-1063.

58. Ortega, J.V., et al., *Physical and chemical characteristics of aging pyrolysis oils produced from hardwood and softwood feedstocks.* Journal of Analytical and Applied Pyrolysis, 2011. **91**(1): p. 190-198.

59. Oasmaa, A., D.C. Elliott, and J. Korhonen, *Acidity of Biomass Fast Pyrolysis Bio-oils.* Energy & Fuels, 2010. **24**(12): p. 6548-6554.

60. Samanya, J., et al., *Characteristics of the upper phase of bio-oil obtained from co-pyrolysis of sewage sludge with wood, rapeseed and straw.* Journal of Analytical and Applied Pyrolysis, 2012. **94**: p. 120-125.

61. Mullen, C.A., et al., *Bio-oil and bio-char production from corn cobs and stover by fast pyrolysis.* Biomass and Bioenergy, 2010. **34**(1): p. 67-74.

62. Liu, Y., et al., *Thermochemical liquefaction of rice husk for bio-oil production in mixed solvent (ethanol–water).* Fuel Processing Technology, 2013. **112**: p. 93-99.

63. Wang, S., et al., *Separation of bio-oil by molecular distillation.* Fuel Processing Technology, 2009. **90**(5): p. 738-745.

64. Bu, Q., et al., *A review of catalytic hydrodeoxygenation of lignin-derived phenols from biomass pyrolysis.* Bioresource Technology, 2012. **124**: p. 470-477.

65. Choudhary, T.V. and C.B. Phillips, *Renewable fuels via catalytic hydrodeoxygenation.* Applied Catalysis A: General, 2011. **397**(1-2): p. 1-12.

66. Jelle Wildschut, F.H.M., Robbie H. Venderbosch, and Hero J. Heeres, *Hydrotreatment of Fast Pyrolysis Oil Using Heterogeneous Noble-Metal Catalysts.pdf.* Industrial & Engineering Chemistry Research, 2009. **48**: p. 10324-10334.

67.   Elliott, D.C., et al., *Catalytic Hydroprocessing of Fast Pyrolysis Bio-oil from Pine Sawdust.* Energy & Fuels, 2012. **26**(6): p. 3891-3896.

68.   Ardiyanti, A.R., et al., *Catalytic hydrotreatment of fast pyrolysis oil using bimetallic Ni–Cu catalysts on various supports.* Applied Catalysis A: General, 2012. **449**: p. 121-130.

69.   Ardiyanti, A.R., et al., *Catalytic hydrotreatment of fast-pyrolysis oil using non-sulfided bimetallic Ni-Cu catalysts on a δ-Al2O3 support.* Applied Catalysis B: Environmental, 2012. **117-118**: p. 105-117.

70.   Ardiyanti, A.R., et al., *Hydrotreatment of wood-based pyrolysis oil using zirconia-supported mono- and bimetallic (Pt, Pd, Rh) catalysts.* Applied Catalysis A: General, 2011. **407**(1-2): p. 56-66.

71.   Bykova, M.V., et al., *Stabilized Ni-based catalysts for bio-oil hydrotreatment: Reactivity studies using guaiacol.* Catalysis Today, 2014. **220-222**: p. 21-31.

72.   DC. Elliot, S.-J.L., and T.R. Hart, *Stabilization of Fast Pyrolysis Oil: Post Processing*. 2012, PNNL.

73.   Xu, X., et al., *Two-step catalytic hydrodeoxygenation of fast pyrolysis oil to hydrocarbon liquid fuels.* Chemosphere, 2013. **93**(4): p. 652-660.

74.   Dayton, D.C., et al., *Biomass Hydropyrolysis in a Pressurized Fluidized Bed Reactor.* Energy & Fuels, 2013. **27**(7): p. 3778-3785.

75.   Meesuk, S., et al., *Study of Catalytic Hydropyrolysis of Rice Husk under Nickel-Loaded Brown Coal Char.* Energy & Fuels, 2011. **25**(11): p. 5438-5443.

76.   Carlson, T.R., et al., *Production of green aromatics and olefins by catalytic fast pyrolysis of wood sawdust.* Energy & Environmental Science, 2011. **4**(1): p. 145.

77.   Paasikallio, V., et al., *Catalytic Pyrolysis of Forest Thinnings with ZSM-5 Catalysts: Effect of Reaction Temperature on Bio-oil Physical Properties and Chemical Composition.* Energy & Fuels, 2013. **27**(12): p. 7587-7601.

78.   Ruddy, D.A., et al., *Recent advances in heterogeneous catalysts for bio-oil upgrading via "ex situ catalytic fast pyrolysis": catalyst development through the study of model compounds.* Green Chemistry, 2014. **16**(2): p. 454.

79.   Jacobson, K., K.C. Maheria, and A. Kumar Dalai, *Bio-oil valorization: A review.* Renewable and Sustainable Energy Reviews, 2013. **23**: p. 91-106.

80.   Wang, H., J. Male, and Y. Wang, *Recent Advances in Hydrotreating of Pyrolysis Bio-Oil and Its Oxygen-Containing Model Compounds.* ACS Catalysis, 2013. **3**(5): p. 1047-1070.

81.   He, Z. and X. Wang, *Hydrodeoxygenation of model compounds and catalytic systems for pyrolysis bio-oils upgrading.* Catalysis for Sustainable Energy, 2012. **1**.

82.   Saidi, M., et al., *Upgrading of lignin-derived bio-oils by catalytic hydrodeoxygenation.* Energy & Environmental Science, 2014. **7**(1): p. 103.

83.   Zhe Tang, Y.Z., and Qingxiang Guo, *Catalytic Hydrocracking of Pyrolytic Lignin to Liquid Fuel in Supercritical Ethanol.* Industrial & Engineering Chemistry Research, 2010. **46**: p. 6.

84.   Bi, P., et al., *Production of aromatics through current-enhanced catalytic conversion of bio-oil tar.* Bioresource Technology, 2013. **136**: p. 222-229.

85.   Zhao, C., et al., *Highly Selective Catalytic Conversion of Phenolic Bio-Oil to Alkanes.* Angewandte Chemie International Edition, 2009. **48**(22): p. 3987-3990.

86.   Vispute, T.P. and G.W. Huber, *Production of hydrogen, alkanes and polyols by aqueous phase processing of wood-derived pyrolysis oils.* Green Chemistry, 2009. **11**(9): p. 1433.

87.   Yuan, Y.-n., T.-j. Wang, and Q.-x. Li, *Production of Low-carbon Light Olefins from Catalytic Cracking of Crude Bio-oil.* Chinese Journal of Chemical Physics, 2013. **26**(2): p. 237.

88.   Graça, I., et al., *Catalytic cracking of mixtures of model bio-oil compounds and gasoil.* Applied Catalysis B: Environmental, 2009. **90**(3-4): p. 556-563.

89.   Wang, S., et al., *Biogasoline Production from the Co-cracking of the Distilled Fraction of Bio-oil and Ethanol.* Energy & Fuels, 2014. **28**(1): p. 115-122.

90.   Ferrini, P. and R. Rinaldi, *Catalytic Biorefining of Plant Biomass to Non-Pyrolytic Lignin Bio-Oil and Carbohydrates through Hydrogen Transfer Reactions.* Angewandte Chemie International Edition, 2014. **53**(33): p. 8634-8639.

91.   Santillan-Jimenez, E., et al., *Catalytic deoxygenation of triglycerides and fatty acids to hydrocarbons over carbon-supported nickel.* Fuel, 2013. **103**: p. 1010-1017.

92.   Wang, H., et al., *Hydrocarbon Fuels Production from Hydrocracking of Soybean Oil Using Transition Metal Carbides and Nitrides Supported on ZSM-5.* Industrial & Engineering Chemistry Research, 2012. **51**(30): p. 10066-10073.

93.   Augustine, R.L., ed. *Heterogeneous Catalysis for the Synthetic Chemist*. 1996, Marcel Dekker, INC: New York.

94.   Gutierrez, A., et al., *Hydrodeoxygenation of guaiacol on noble metal catalysts.* Catalysis Today, 2009. **147**(3-4): p. 239-246.

95.   Nan, W., et al., *Catalytic Upgrading of Switchgrass-Derived Pyrolysis Oil Using Supported Ruthenium and Rhodium Catalysts.* Energy & Fuels, 2014. **28**(7): p. 4588-4595.

96.   Bui, L., et al., *Domino Reaction Catalyzed by Zeolites with Brønsted and Lewis Acid Sites for the Production of γ-Valerolactone from Furfural.* Angewandte Chemie International Edition, 2013. **52**(31): p. 8022-8025.

97.   Valle, B., et al., *Selective Production of Aromatics by Crude Bio-oil Valorization with a Nickel-Modified HZSM-5 Zeolite Catalyst.* Energy & Fuels, 2010. **24**(3): p. 2060-2070.

98.   Zhang, X., et al., *Catalytic Upgrading of Bio-oil over Ni-Based Catalysts Supported on Mixed Oxides.* Energy & Fuels, 2014. **28**(4): p. 2562-2570.

99.   Whiffen, V., *A Study of Metal Phosphides for the Hydrodeoxygenation of Phenols and Pyrolysis Oil.*, in *Chemical and Biological Engineering*. 2013, The University of British Columbia: Vancouver. p. 268.

100.   Yang, Y., et al., *Synthesis of Nickel Phosphide Nanorods as Catalyst for the Hydrotreating of Methyl Oleate.* Topics in Catalysis, 2012. **55**(14-15): p. 991-998.

101.   Rensel, D.J., et al., *Highly selective bimetallic FeMoP catalyst for C–O bond cleavage of aryl ethers.* Journal of Catalysis, 2013. **305**: p. 256-263.

102.   Wang, X., *Valorization of lignin and bio-oil by catalytic hydrogenation with Ni catalyst.pdf*, in *Max Planck Institute*. 2013, Max Planck Institute Mülheim. p. 221.

103.   Gayubo, A.G., et al., *Hydrothermal stability of HZSM-5 catalysts modified with Ni for the transformation of bioethanol into hydrocarbons.* Fuel, 2010. **89**(11): p. 3365-3372.

104.   Ramasamy, K.K., et al., *Conversion of biomass-derived small oxygenates over HZSM-5 and its deactivation mechanism.* Green Chemistry, 2014. **16**(2): p. 748.

105. Zhao, C., et al., *Understanding the impact of aluminum oxide binder on Ni/HZSM-5 for phenol hydrodeoxygenation.* Applied Catalysis B: Environmental, 2013. **132-133**: p. 282-292.

106. Singh, S.K. and J.D. Ekhe, *Towards effective lignin conversion: HZSM-5 catalyzed one-pot solvolytic depolymerization/hydrodeoxygenation of lignin into value added compounds.* RSC Advances, 2014. **4**(53): p. 27971.

107. Neumann, G.T., et al., *Correlating lignin structure to aromatic products in the catalytic fast pyrolysis of lignin model compounds containing β–O–4 linkages.* Catal. Sci. Technol., 2014. **4**(11): p. 3953-3963.

108. Wang, H., et al., *Support effects on hydrotreating of soybean oil over NiMo carbide catalyst.* Fuel, 2013. **111**: p. 81-87.

109. Schilke, K.F., et al., *A novel enzymatic microreactor with Aspergillus oryzae β-galactosidase immobilized on silicon dioxide nanosprings.* Biotechnology Progress, 2010. **26**(6): p. 1597-1605.

110. McIlroy, D.N., et al., *Nanosprings.* Applied Physics Letters, 2001. **79**(10): p. 1540.

111. Hai-Feng Zhang, C.-M.W., Edgar.C. Buck, and Lai-Sheng Wang, *Synthesis, Characterization, and Manipulation of Helical SiO₂ Nanosprings.* Nano Letters, 2003. **3**(5): p. 577-580.

112. Wang, L., et al., *High yield synthesis and lithography of silica-based nanospring mats.* Nanotechnology, 2006. **17**(11): p. S298-S303.

113. da Fonseca, A. and D. Galvão, *Mechanical Properties of Nanosprings.* Physical Review Letters, 2004. **92**(17).

114. Liu, L., et al., *Wet-Chemical Synthesis of Palladium Nanosprings.* Nano Letters, 2011. **11**(9): p. 3979-3982.

115. Fouetio Kengne, B.-A., et al., *Self-Assembled Monolayers of Thiols Adsorbed on Au/ZnO-Functionalized Silica Nanosprings: Photoelectron Spectroscopy-Analysis and Detection of Vaporized Explosives.* ACS Applied Materials & Interfaces, 2014. **6**(16): p. 13355-13366.

116. V.V.R.Sai, D.G., Ishwar Niraula, Jamie M.F.Jabal, Giancarlo Corti, D.N. McIlroy, D.Eric Aston, Josh.R. Branen, and Patrick J. Hrdlicka., *Silica Nanosprings Coated with Noble Metal Nanoparticles-Highly Active SERS Substrates.* Journal of Physics and Chemistry.C, 2011. **115**: p. 453-459.

117. Luo, G., et al., *A novel nano fischer-tropsch catalyst for the production of hydrocarbons.* Environmental Progress & Sustainable Energy, 2014. **33**(3): p. 693-698.

118. Zhao, C., et al., *Comparison of kinetics, activity and stability of Ni/HZSM-5 and Ni/Al2O3-HZSM-5 for phenol hydrodeoxygenation.* Journal of Catalysis, 2012. **296**: p. 12-23.

Chapter 2: Hydrodeoxygenation of Phenol over Silica Nanosprings based Ni and Ru Catalysts

2.1 Abstract

Nickel (Ni) and ruthenium (Ru) catalysts for hydrodeoxygenation (HDO) of phenol, model compounds for biomass pyrolysis bio-oil, were supported on a novel nanomaterial, silica nanospring (NS). The nanocatalysts were characterized by TEM and XRD and showed the NSs had a helical and mesoporous structure. The Ni and Ru decorated NSs showed good metal dispersity at the NS surface. Catalytic HDO conversion of phenol using NSs were compared to conventional alumina (Al_2O_3) and silica (SiO_2) catalyst supports. Ni-alumina (Ni-Al_2O_3) was easily deactivated in the presence of water while the Ni-NS catalysts performed the best regardless of whether HDO was carried out in the presence of water. An increase in Ni loading (up to 50%) increased the Ni-NS activity while the high loading resulted in a detrimental effect on the activity of silica gel based catalysts. Ru based catalysts showed better activity and conversion on phenol HDO performed than Ni based catalysts, even in the presence of water. There was no obvious increase of phenol conversion observed when Ru loading increased from 5 to 20%. The Ru-NS catalyst showed good stability for HDO of phenol even after five time use.

2.2 Introduction

Fast pyrolysis of lignocellulosic biomass is considered a feasible and efficient process to convert biomass into a crude bio-oil (pyrolysis oil). However, bio-oil from fast pyrolysis

contains a large amount of oxygen, distributed in hundreds of oxygenated compounds [1]. These compounds lead to many negative properties, such as low heating value, high corrosiveness, high viscosity, and instability. In order to make drop-in transportation fuels from bio-oil, HDO is a necessary step to remove these oxygen with hydrogen under pressure in the presence of suitable catalyst. HDO of bio-oil has been extensively studied and well documented during the past decades [2]. Phenol has been used as a model compound to represent lignin derived components in pyrolysis bio-oil. Phenol and its derivatives are the least active compounds in HDO but the most studied substrates over different catalysts [3-6].

The key for bio-oil HDO is the catalyst. Solid catalysts are preferred for this process because these heterogeneous catalysts can be easily separated from the substrate after reaction. As reported in the literature, Ru is an active metal for use in HDO catalysts of bio-oil or its model compounds [7-9]. In contrast to Ru, Ni based catalyst show great potential for industrial application due to its low cost and high activity towards hydrogenation (HYD) and hydrogenolysis of several chemical functional groups [10, 11]. However, pure Ni shows a relatively low surface area and poor stability. Therefore, Ni catalysts used in industry are usually supported on a carrier or support for achieving better metal dispersion and thus higher reaction activity [12]. For this reason, materials with large surface area are highly desirable as a good support. Alumina, silica, and SiO_2-Al_2O_3 as well as zeolites (such as HZSM-5) have been extensively studied as Ni catalyst supports [13]. As a shape-selective zeolite, HZSM-5 has intermediate pore sizes and good thermal ability. Only small molecules are allowed to diffuse into the micropores. Although this microporous material is very effective for aromatic hydrocarbon production, coke is easily formed on it in terms of bio-oil HDO. One important reason is that there are many high molecular weight oligomers present

in the bio-oil and thus easily block the micropores of HZSM-5. Thus, amorphous silica or alumina is preferred but effort should be made to increase their surface area and selectivity.

Silica nanosprings (NS) with large surface-to-volume ratios are one of the most promising silica based catalyst supports. Amorphous NS can be consistently synthesized via plasma enhanced chemical vapor deposition by McIlroy et al [14]. The formation of the amorphous silica NSs is explained in terms of the contact angle anisotropy model [15]. It should be noted that silica NSs are grown on a substrate such as aluminum foil, stainless steel, glass and quartz. Luo et al. successfully synthesized SiO_2 NS on quartz frits which were decorated with cobalt (Co) by wetness impregnation method for Fischer-Tropsch synthesis of C_1-C_{18} hydrocarbons from synthesis gas [16]. However, a catalyst in liquid phase HDO generally needs a high surface area. Therefore, free standing NSs can be obtained by removing the NS mat through mechanical action and then decorated with the desired active catalytic metal [14].

A considerable number of phenol HDO studies have been reported in the literature [3-5, 17-21]. Phenol HDO has been carried out in either stirred batch reactors or in fixed bed tubular reactors [22]. In some of these studies a phenol solution in different organic solvents (tetradecane, n-hexadecane, decalin, and propanol) were used to investigate oxygen-removal capability of catalyst [23]. Solvents such as alkanes or alcohols can act as effective hydrogen donors since it has excellent solubility for H_2 in a supercritical state [24]. However, this will increase the reaction cost. A more challenging way to carry out phenol HDO reaction is using water as a solvent. Although the water-phenol mixture can better simulate the bio-oil better, some Ni based catalysts are easily deactivated in water due to partial Ni leaching from the catalyst into water [25].

Nevertheless, water has been already successfully employed as solvent for phenol HDO by using Ni catalysts [21, 26]. But water involved in the system may affect the catalytic behaviors on phenol. Therefore, one of the aims of this study is to investigate how water influences the selectivity of product from phenol HDO catalyzed by Ni catalysts. According to previous research, it was found that the activity of Ni catalyst on HDO was obviously enhanced by increasing reaction temperature from 200 to 300°C. Herein, all the phenol HDO reactions were carried out at 300°C and no coke formed as previously shown. Bio-oil HDO was subsequently carried out using the catalysts showing good performance on phenol HDO.

This research focused on the potential of silica NSs as a support of Ni or Ru for model compound and bio-oil HDO. The activities of catalysts were tested on phenol under desirable temperature and H_2 pressure in this study. For comparison purposes, conventional silica and alumina gels with different particle size were also introduced as the supports of Ni. Other catalyst properties including metal loading and catalyst deactivation were also investigated in this research.

2.3 Materials and Methods

2.3.1. Catalyst preparation

All the catalysts used in this study were prepared by using the wetness impregnation method [20]. $NiCl_2·6H_2O$ and $RuCl_3·6H_2O$ were used as Ni and Ru precursors, respectively. The applied catalyst supports were silica gel (40-63 μm (#1) and 210-500 μm (#2), Fisher Chemical), alumina (Υ-Al_2O_3, 74-177 μm, Fisher Chemical) and silica nanosprings (NS). Chemical vapor deposition (CVD) method was applied for synthesizing NSs onto an aluminum foil substrate using flow furnace technique [14]. After the NS mats were formed,

they were easily peeled off from the foil to give free standing NSs. The desire amounts of precursors were dissolved in water (100 mg/mL for 20% Ni, 400 mg/mL for 50% Ni, 15 mg/mL for 5% Ru) in a flask (10 mL) and then the silica and alumina gel support (1 g) were introduced to the solution and the mixture was ultrasonicated for 4 h at room temperature. For NSs (200 mg), the metal precursors were dissolved in ethanol (10 mL, HPLC grade, > 99.9%, 25 mg/mL for 20% Ni, 100 mg/mL for 50% Ni, 3 mg/mL for 5% Ru, 6.4 mg/mL for 10% Ru, 14.3 mg/mL for 20% Ru) due the NSs hydrophobicity and again the mixture ultrasonicated. To note, ultrasonication is a critical step to disperse the NSs. The solvent was then evaporated at room temperature and the samples were dried overnight at 104°C. The dried catalysts were ground in a mortar and pestle and then calcined in air for 4h (450°C for Ni catalysts and 350°C for Ru catalysts). The calcined catalyst materials were reduced in a tubular quartz reactor (10 mm Ø × 300 mm) by heating from room temperature to desired temperature (400°C for Ni catalysts and 300°C for Ru catalysts) under a H_2 flow (60 mL/min). This reduction step was maintained for 4 h. After cooling to room temperature, the reduced sample was transferred to the reactor for HDO.

2.3.2. Catalyst characterization

The X-ray powder diffraction (XRD) pattern were obtained using a Siemens D5000 powder diffractometer with Cu/Kα radiation (λ=1.54 Å). The diffractograms were recorded from 2ϴ = 2° to 80° with 0.01° step using a 1 s acquisition time per step. The average particle size of metal oxides were calculated according to Scherrer's equation (d= K λ/βcos ϴ), where K is the shape factor (K=1), λ is the wavelength of X-ray, β is the line broadening at half the maximum intensity (FWHM) in radians, and ϴ is the Bragg angle. The

morphologies of the catalysts were characterized by transmission electron microscopy (TEM, Jeol JEM-2010 TEM, 200kV). Sample specimens for TEM tests were prepared by dispersion of catalysts in ethanol (2 mg/mL) and the suspension dropped onto a copper grid. Several micrographs were recorded for each sample to determine the particle size distribution of the metals and their oxides. The H_2-temperature programmed reduction (H_2-TPR) was performed to investigate the reducibility of the catalyst as well as determine the optimum temperature to reduce the metal oxide completely. The H_2-TPR spectra of the catalysts were recorded using a Micromeritics AutoChem II 2920 Chemisorption Analyzer, equipped with a thermal conductivity detector (TCD). Sample (50 mg) was loaded in a U-shape quartz reactor and first purged in a flow of He (50 mL min^{-1}) at 250°C for 1 h to remove water, cooled to 50°C, then a 10% H_2 in Ar (50 mL min^{-1}) was purged and heated to 800°C at 10°C min^{-1}.

2.3.3. Catalyst activity measurement

In a typical test, phenol (5 g, 53 mmol), water (15 g), and a catalyst (0.05-0.20 g) are loaded into a stirred Parr Instruments reactor model 4561 (300 mL, Figure 2.1). For Ni catalysts, a series of phenol (5 g) HDO were carried out without water as solvent. The amount of Ni catalysts applied were all 0.20 g which made the catalyst phenol (C/F) ratio equal to 1:25. For Ru catalyst, all the phenol (5 g) HDO experiments were carried out with adding water (15 g) as solvent. The amount of Ru catalyst was 0.20 g giving a C/F = 1:25. An additional series of phenol HDO over Ru catalysts were performed under the same conditions as above using a decreased amount of catalyst (0.05 g) giving a C/F = 1:100. The phenol, water and catalysts were loaded into the reactor which was flushed with H_2 five times to remove air. Then, the reactor was pressurized with H_2 to 3 MPa (400 psi) and

heated (6°C /min) to 300°C. The start time was recorded when the required temperature was reached, and the stirring speed was set to 500 rpm. After the completion of the reaction (6 or 12 h), the reactor was cooled to room temperature. The liquid products which separated into an organic and aqueous phases were analyzed with GC-MS.

Figure 2.1 Parr reactor setup and the applied parameters during hydrotreatment of phenol

2.3.4. Product characterization by GC-MS

GC-MS (FOCUS-ISQ, ThermoScientific) was used to characterize the volatile components in the bio-oil fractions (1.0 mg of bio-oil sample was solubilized in 1 mL of CH_2Cl_2 containing anthrancene (0.05 mg mL^{-1}) as internal standard), where the separation was achieved using a RTx-5MS capillary column (30 m × 0.25 mm Ø, Restek) using a temperature program of 40°C (hold for 2 min) to 250°C (10 min) at 5°C min^{-1}. Compounds were identified using known standards, mass spectral library matching (National Institute of Standards and Technology (NIST) 2008), and by their mass spectra. The HDO reaction over each catalyst was carried out twice and the corresponding calculated values were the average for both reactions. Conversion and selectivity (degree of deoxygenation, DOD) were calculated on the basis of the number of carbon moles defined as follows.

$$\text{Conversion} = \left(1 - \frac{\text{Moles of residual phenol}}{\text{Moles of initial phenol}}\right) \times 100\%$$

$$\text{DOD} = \left(1 - \frac{\text{Oxygen content in the final organic compounds}}{\text{Total oxygen content in the initial phenol}}\right) \times 100\%$$

2.4 Results and discussion

### 2.4.1. Catalyst characterization

2.4.1.1. TEM analysis

Figure 2.2 shows some representative TEM micrographs of the Ni(20% loading)-silica gel (210-500 μm), Ni(20% loading)-NS, Ru(5% loading)-silica gel (210-500 μm), and Ru(5%)-NS catalysts. Figure 2.2 shows the micrographs of the various catalysts. The NS structure still maintained its helical shape after the wetness impregnation method (Figure 2.2 b and d). The silica gel supports showed globular structure after calcination (Figure 2.2 a and c). This result revealed the good thermal stability of silica NSs after calcination. Due to the higher density of Ni and Ru relative to silica they appear as dark dots on the TEM micrographs. Nanosprings were supposed to be macro-porous materials since most pores formed by the helical structure were more than 12 nm in size. However, it can be clearly seen from Figure 2.2 d that there were many nano-scale channels on the surface of the NS, where most small metal particles were located. The diameters of these channels were < 12 nm and can thus be considered as mesoporous structures.

To analyze metal dispersity on these catalysts, particle size was manually determined for the active metal (Ni, and Ru) in the catalysts from the TEM images (Figure 2.3). For the Ni-silica gel and Ni-NS, the average sizes of metal particles were 15.2 ± 0.5 nm and 13.7 ±

0.5 nm, respectively (Table 2.1). The Ni particle size distributions gave a wide range of particle sizes: 5 to 27 nm for NS and 7 to 31 nm for silica gel. Conversely, the average size of metal particles for Ru-silica gel and Ru-NS were 5.9 ± 0.2 nm and 2.3 ± 0.01 nm, respectively. The Ru particle size distributions gave a wide range of particle sizes: 1 to 5 nm for NS and 1 to 31 nm for silica gel. These results demonstrated that Ru particles dispersed better than Ni particles on both supports (silica gel and NSs) and the smaller average particle size was always observed on the surface of NS.

(a) Ni(20%)-silica gel

(b) Ni(20%)-NS

(c) Ru(5%)-silica gel
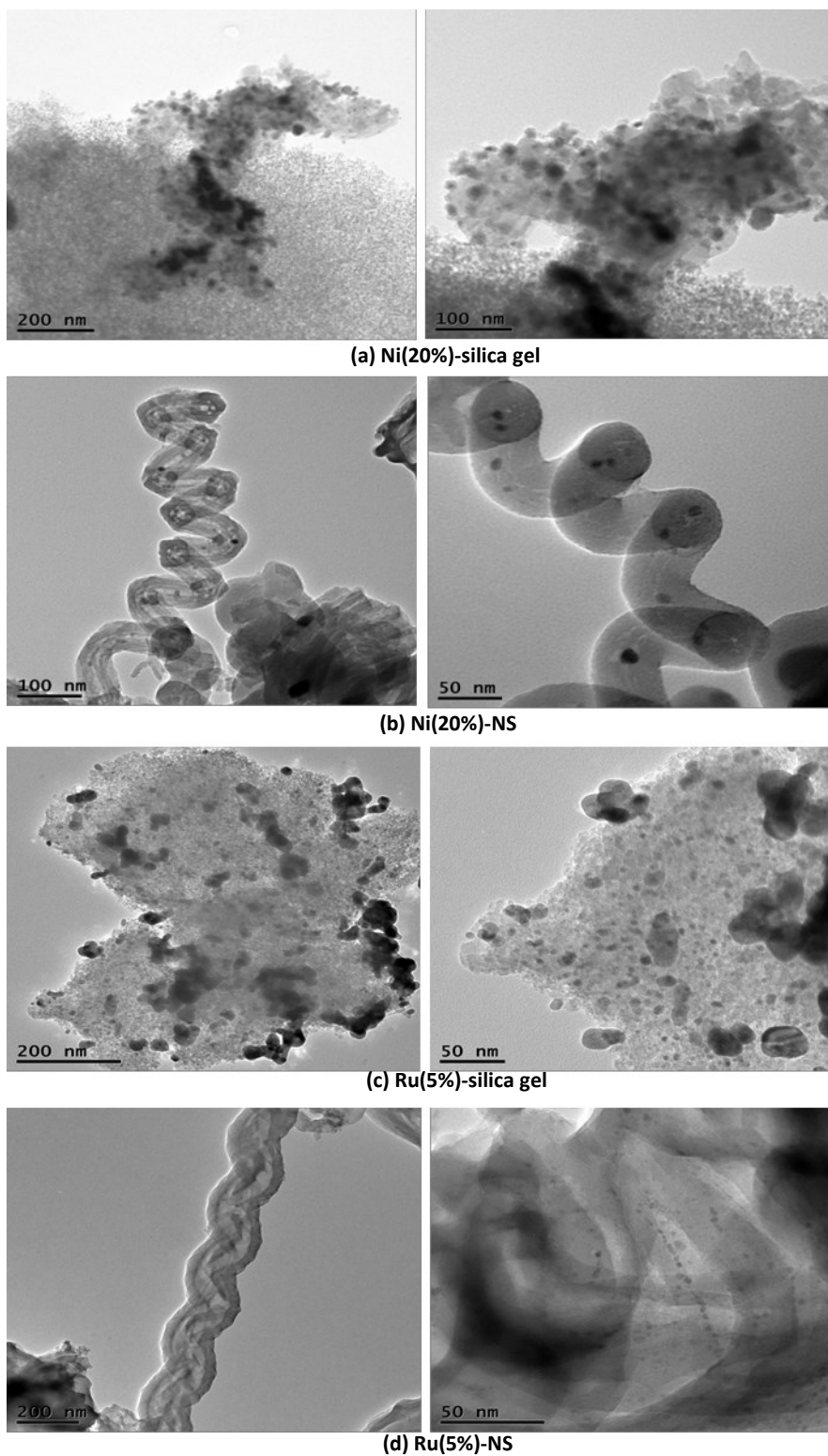
(d) Ru(5%)-NS

Figure 2.2 TEM micrographs of Ni and Ru on various catalyst supports: (a) Ni(20%)-silica gel (210-500 μm), (b) Ni(20%)-NS, (c) Ru(5%)-silica gel (210-500 μm), and (d) Ru(5%)-NS
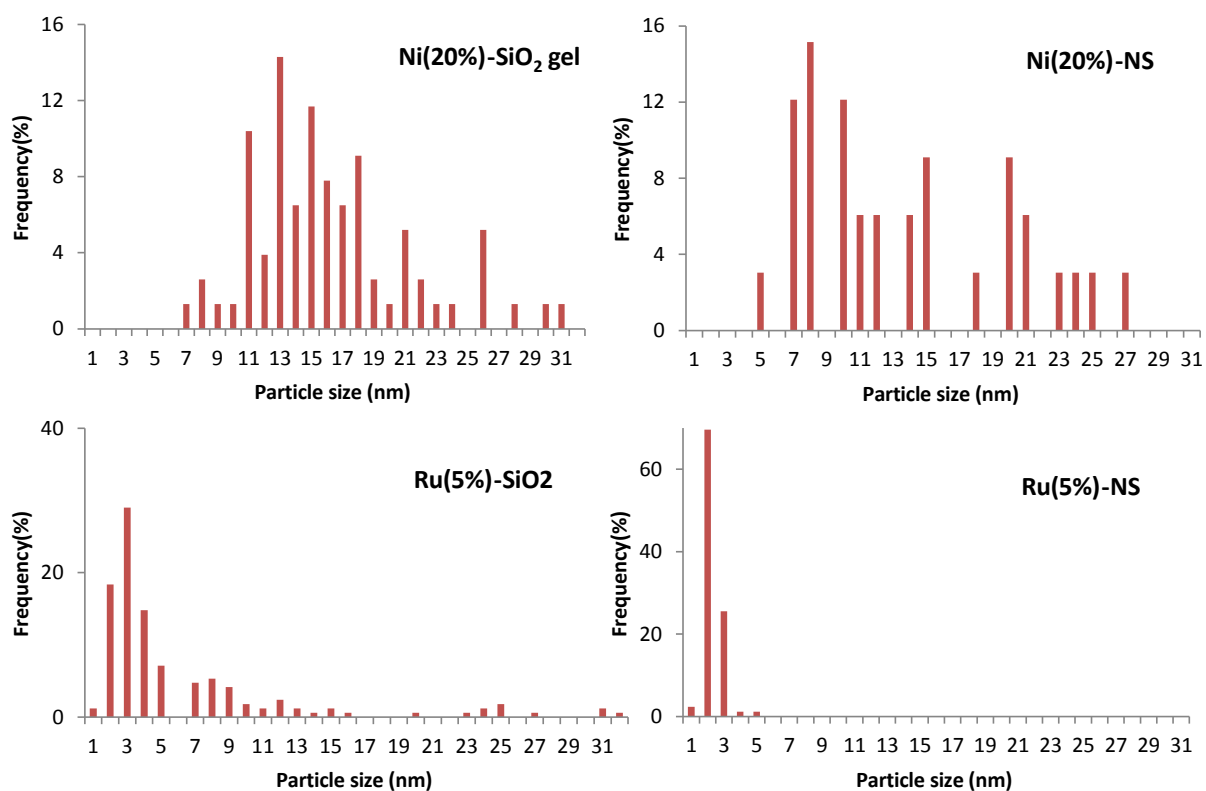
Figure 2.3 Particle size distribution of Ni and Ru nanoparticles on the various catalyst supports: (a) Ni(20%)-silica gel (210-500 µm), (b) Ni(20%)-NS, (c) Ru(5%)-silica gel (210-500 µm), and (d) Ru(5%)-NS.

2.4.1.2. XRD

X-ray diffractograms of the Ru and Ni catalysts are shown in Figure 2.4. Both Ni-NS and Ni-silica gel shows the characteristic peaks of Ni at 44.6°, 51.9° and 76.5° (2θ), that are associated to the (111), (200), and (220) planes, respectively [5, 27]. For both Ru catalysts, diffraction signals due to (100) and (002) planes became visible, which correspond to crystallites of the face-centered cubic phase of this metal reported in other studies [28, 29].

In addition, the broad peak at approximately 22° for both catalysts is due to amorphous silica, as is usually found for these meso-structured materials [27]. These results further confirmed the existence of mesoporous structures on NSs.

The peaks of (111) from Ni and (002) from Ru were used to calculate the corresponding nanoparticle crystal size by the Scherrer equation (Table 2.1). The particle size for Ni-silica gel and Ni-NS were 8.0 and 7.2 nm, respectively. Although the calculated values were lower than the ones from TEM, the particle size on NS was still smaller than those on silica gel as evidenced by XRD measurements. A similar result was also observed between the Ru-silica gel and Ru-NS, whose metal particle size were 3.8 and 2.0 nm, respectively. These results were shown to be in closer agreement with those obtained by TEM.
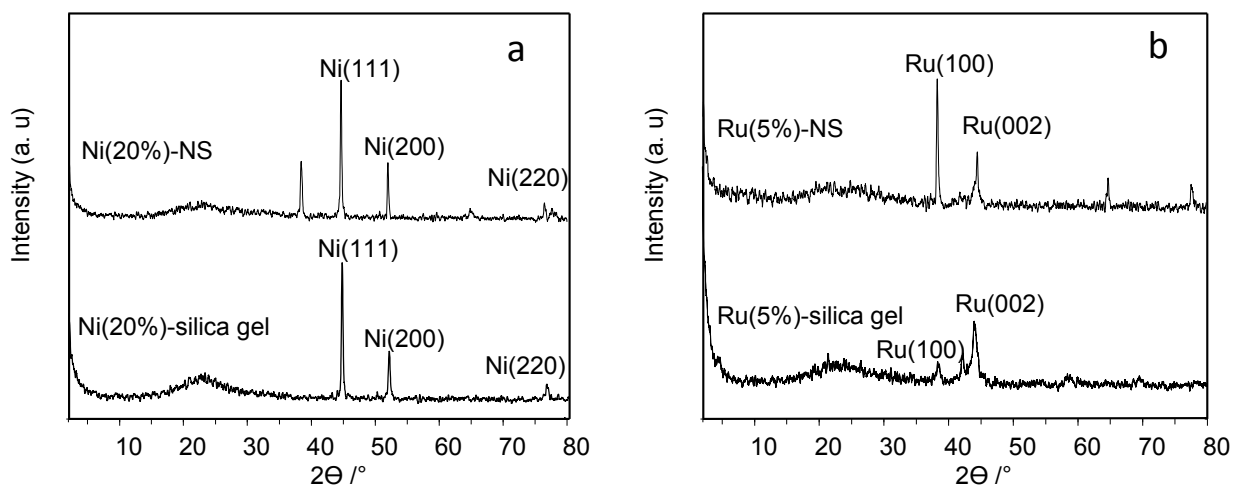
Figure 2.4 XRD diffractograms of (a) the Ni(20%)-silica gel (210-500 µm) and Ni(20%)-NS catalysts and (b) Ru(5%)-silica gel (210-500 µm) and Ru(5%)-NS catalysts.

Table 2.1 Calculated average particle sizes of Ni and Ru catalysts

|	Ni(20%)-silica gel (210-500 μm)	Ni(20%)-NS	Ru(5%)-silica gel (210-500 μm)	Ru(5%)-NS
Metal particle size (TEM)	15.2 ± 0.5 nm	13.7 ± 0.5 nm	5.9 ± 0.2 nm	2.3 ± 0.01 nm
Metal particle size (XRD)	8.0 nm	7.2 nm	3.8 nm	2.0 nm

2.4.1.3 H_2-TPR

Figure 2.5 shows the H_2-TPR profiles for Ni-NS and Ru-NS catalysts. The H_2-TPR analysis of the two catalysts was performed to determine the temperature when the metals (Ni or Ru) are fully reduced. With the reduction temperature increasing, the maximum absorption peak can be observed at around 400°C for Ni-NS (Figure 2.5). This result implies that 400°C is an appropriate temperature to activate Ni-NS catalyst. This temperature is in agreement with those determined by other studies [18]. However, multiple peaks appeared on the H_2-TPR profile of Ru-NS catalyst. This is mainly due to the reduction from RuO_x to Ru. The most significant peak for Ru-NS catalyst was the one at around 400°C, which represented the best temperature to activate Ru-NS during reduction.
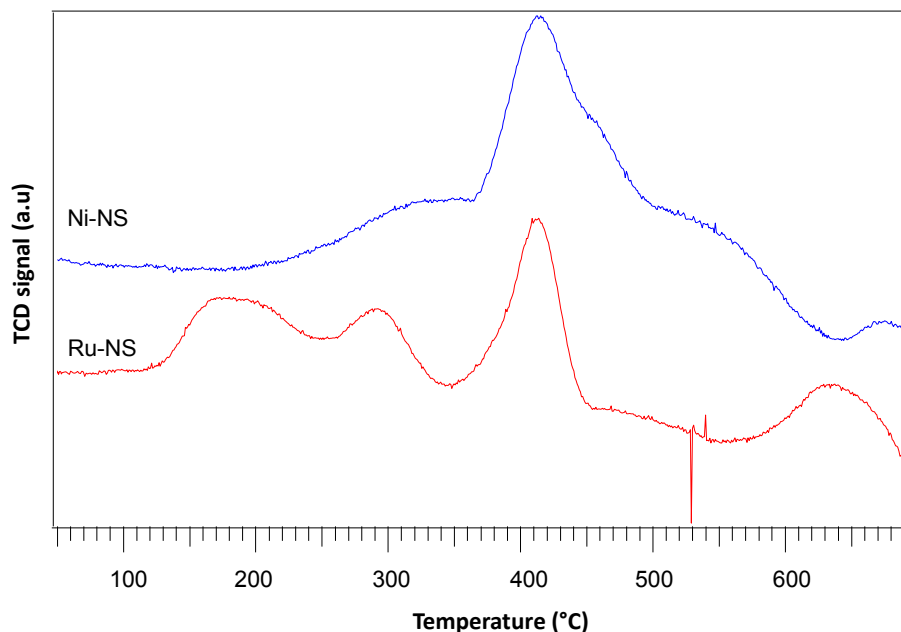
Figure 2.5 H$_2$-TPR profiles for Ni-NS and Ru-NS catalysts

2.4.2. Catalyst performance evaluation by HDO of phenol

2.4.2.1. Phenol HDO products characterization

The liquid products from HDO of phenol were characterized by GC-MS. Figure 2.6 shows GC-MS chromatogram of products from HDO of phenol over Ni(20%)-NS and Ru(5%)-NS catalysts. Since the good performance of these two catalysts, the products mainly contain hydrocarbons with only minor phenols (Ni-NS) or no phenols (Ru-NS) at all. Ru-NS catalyst maintains a better capability of deoxygenation on cyclohexyl-phenol than Ni-NS does. The identified compounds from all the reactions are shown in Table 2.2. Cyclohexane, cyclohexene, cyclohexanol and cyclohexanone are products derived from a series of reactions: 1) phenol aromatic hydrogenation forming cyclohexanol and cyclohexanone; and 2) then the dehydration of cyclohexanol to cyclohexene following the double bonds

hydrogenation to cyclohexane. Furthermore, benzene was also produced from phenol by direct dehydration (direct HDO). Generally, the hydrogenation series reactions and the direct HDO occur in parallel during phenol HDO. However, benzene underwent a further hydrogenation to cyclohexane. These proposed HDO mechanisms have been well recognized in other related studies [3-5, 17].
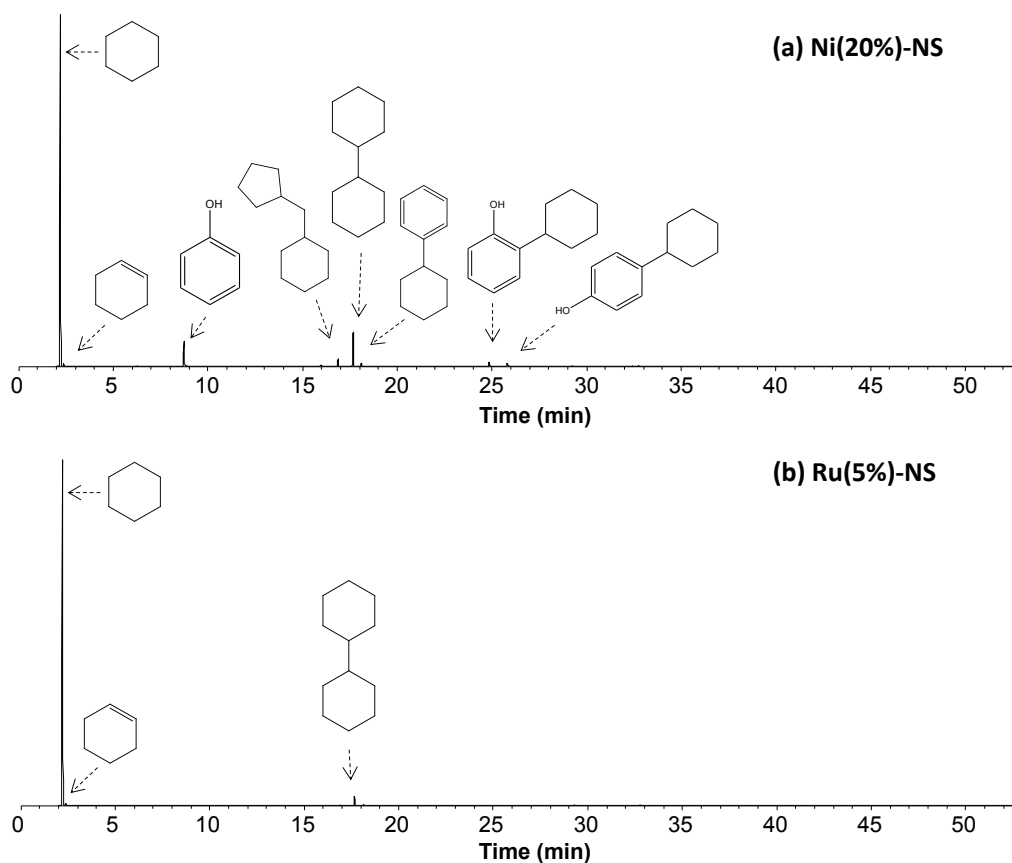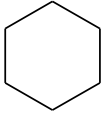
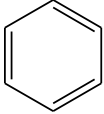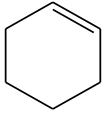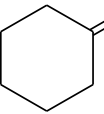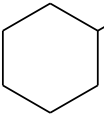**Figure 2.6** GC-MS chromatogram of products from HDO of phenol in water over (a) Ni(20%)-NS and (b) Ru(5%)-NS catalysts

Besides the desired products from HDO of phenol, bicyclohexyl, cyclohexyl-benzene, cyclohexyl-cyclohexanone, cyclohexyl-phenol were also detected in the organic phase. A
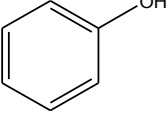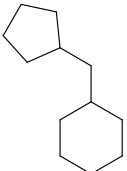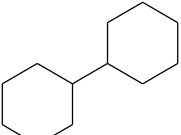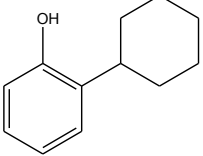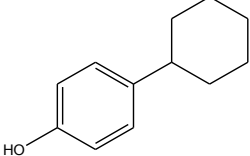
possible reaction routine for these products is the condensation between phenol and cyclohexanol via active ortho and para sites on the aromatic ring of phenol. Additional hydrogenation and dehydration occurred with some of the catalysts, since bicyclohexyl, cyclopentyl-cyclohexane and cyclohexyl-benzene were observed in some reactions products. Furthermore, aromatic ring condensation also occurred due to the existence of biphenyl. These products were also observed in guaiacol HDO catalyzed by Ni catalysts as reported [25].

Table 2.2 Compounds structures in liquid products identified from all HDO of phenol at 300˚C and initial H_2 pressure of 400 psi.

cyclohexane	benzene	cyclohexene	cyclohexanone	cyclohexanol
phenol	cyclopentylmethyl-cyclohexane	bicyclohexyl	o-cyclohexyl-phenol	p-cyclohexyl-phenol

2.4.2.2. Catalyst activity and selectivity evaluation results

Although the identified compounds from liquid products over all catalysts were similar, the amount of each compound varied from catalyst to catalyst. To understand the effect of support, 20% of Ni supported on silica gel (1# 40-63 μm and 2# 210-500 μm), γ-alumina, and NSs, were prepared. Table 2.3 shows the conversion and product distribution in HDO of pure phenol over the synthesized Ni catalysts. The yield for each product was calculated on the basis of the number of carbon moles. As shown in Table 2.3, conversion and DOD of phenol over each Ni catalyst was almost complete which implied a successful HDO of phenol. It is well recognized that the reaction rate over a catalyst is typically determined by the surface area of the catalyst which is controlled by the support material [20]. Since the surface area varied for each applied support for Ni catalyst, it is expected to see different phenol conversions for the different Ni catalysts [4]. However, a similar phenol conversion over each Ni catalyst revealed their similarity and corresponding activities. A reasonable explanation for this is that Ni played a more important role than the support did under the reaction conditions employed.

In terms of product selectivity, cyclohexane, cyclohexene and bicyclohexyl were detected in all reactions in which cyclohexane was predominant with >70 % selectivity. This indicated that phenol mainly underwent hydrogenation of the aromatic ring to form cyclohexanol, which was consequently dehydrated into cyclohexene. Similar results were also achieved by other studies [3]. Over the highly active Ni catalyst, cyclohexene was easily hydrogenated into stable cyclohexane. On the other hand, aromatic condensation and corresponding deoxygenation reactions also occurred as evidenced by the presence of cyclohexyl-phenol and bicyclohexyl in the products. It should be noted that the HDO of phenol over Ni- Al_2O_3 yielded the most cyclohexyl-phenol (5.0%) and bicyclohexyl (15.2%)

compared to the other catalysts. This result is probably due to the strong acidity of Al_2O_3, which makes aromatic condensation more convenient. Besides, Ni-NS catalyst produced the most liquid hydrocarbons (95.8 %) including cyclohexane (gasoline range) and bicyclohexyl (diesel range). Mortensen et al. conducted a study on HDO of phenol over a series of Ni based catalysts under a similar condition [4]. Their results indicated that yields of cyclohexane were only 38 and 45 mol% over Ni(5%)-silica gel and Ni(5%)-alumina, respectively. Although other Ni catalysts including $Ni-ZrO_2$ and $Ni-V_2O_5-SiO_2$ gave a better cyclohexane yield (80%) and there was still cyclohexanol left (10%). These results implied that a complete deoxygenation was hardly achieved over the Ni catalysts.

Table 2.3 HDO of pure phenol over Ni (20 wt.%) catalysts with C/F=1:25 at 300 °C

catalyst	Ni(20%)-silica gel-1# 40-63 μm	Ni(20%)-silica gel-2# 210-500 μm	Ni(20%)-Al$_2$O$_3$ 74-177 μm	Ni(20%)-NS
Conversion %	98.5	100	99.1	100
Products distributions, %				
cyclohexane	84.5	86.9	72.6	84.9
cyclohexene	0.3	0.2	0.6	0.4
cyclohexanol	0.1	-	0.1	-
cyclohexanone	0.3	-	0.3	-
bicyclohexyl	6.3	4.9	15.2	10.9
cyclohexyl-phenol	-	-	5.0	-
DOD, %	98.1	100	93.7	100

[a] Reaction conditions: 0.2g of catalyst, 5 g of phenol, P(H$_2$)=3MPa, stirring speed=500 r/min, time =6 h.

Even though all four Ni catalysts showed better activity and selectivity for pure phenol HDO, their performances on phenol HDO in water solution are still unknown. This is important because water is also a major component in bio-oil. To better simulate actual bio-oil, evaluation on catalyst performance in water was necessary. Therefore, a similar series of phenol HDO with desirable amounts of water were carried out over the previously mentioned four Ni catalysts. The conversion, products distributions and DOD for all the reactions are listed in Table 2.4. When compared with Table 2.3, all the phenol conversion shown in Table 2.4 obviously decreased especially for Ni-alumina catalysts. This revealed that the addition of large amount of water further lowers the activity of all applied Ni catalysts. Furthermore, alumina was shown not to be a good support for Ni when large amounts of water are present in the reaction. This poor performance of Ni-alumina was also observed by Zhang et al. in their research [30]. Neumann et al. explained that Al atoms are easily leached from alumina under a steam treatment [31]. Moreover, little differences in conversion were observed between these silica supported Ni catalysts. Surprisingly, silica gel with larger particle size (210-500 μm) performed better than the smaller particle sized silica gel Ni catalyst. This was likely due to the better Ni particle dispersity achieved on the larger particle silica gel. However, Ni-NS showed the best conversion and selectivity toward hydrocarbons. These results indicate that Ni can still maintain good activity on silica NSs surface even in water. Additionally, sintering and support deactivation is likely not to occur on the Ni-NS catalyst.

In contrast with the results from pure phenol HDO, the products from phenol HDO in water contained more oxygenated compounds, together with unreacted phenol. The levels of cyclohexanol, cyclohexanone, and cyclohexyl-phenol after phenol HDO in water made the DOD for all reactions decrease. These results indicate that the selectivity towards

hydrocarbons for all Ni catalysts was weakened by addition of water. Meantime, condensation reactions of phenol still took place even in aqueous solution as evidenced by the presence of cyclohexyl-phenol, but the subsequent deoxygenation of cyclohexyl-phenol was seriously impaired as only trace amounts of bicyclohexyl was detected. In term of both conversion and hydrocarbon selectivity, Ni-NS consistently showed the best performance even in the presence of water. These results clearly show that the SiO_2 NSs was a good catalyst support for bio-oil HDO. Zhao et al. also evaluated the performance of Ni catalysts (RANEY Ni) by conducting phenol HDO in water solution at 300°C [21]. As they reported, the phenol conversion was 100% and the yield of cyclohexane was up to 93%. However, the catalyst and phenol weight ratio (C/F) in their study was 1:3 while the one in this study is 1:25. These results revealed that increasing the amount of Ni in the reaction is a promising way to increase the phenol conversion and DOD.

In this experiment, the metal loading of Ni catalyst was studied on silica gel and NSs. High Ni loading (50%) catalysts were prepared and their performance evaluated by phenol HDO in both the absence and presence of water with results shown in Figure. 2.4. The conversion and DOD of phenol over Ni-silica gel (210-500 μm) decreased even with an increase in Ni loading from 20 to 50%. As reported from other studies, an increase in metal loading does not necessarily correlate with an increased activity of the catalyst [7, 32]. For example, Zhang et al. used 6, 10 and 14% Ni supported on HZSM-5 for phenol HDO and the highest phenol conversion was achieved with 10% Ni-HZSM-5 [30]. In fact, there is a balance between metal loading and specific support surface area. If an excess of metal is loaded on supports, the metal will agglomerate or even crystallize more easily, and thus makes the metal non-functional. In this study, silica gel with lower surface area cannot carry much Ni particles and thus Ni crystallization occurred. For this reason, Ni (50%)-silica gel

only gave about 60% conversion and <20% DOD even in the absence of water. Therefore, 20% Ni loading seems to be better for silica gel particles although its performance in water solution was not as good as compared to other catalysts.

Table 2.4 HDO of phenol in aqueous solution over Ni (20%) catalysts with C/F =1:25

Catalyst and support	Ni(20%)-silica gel-1# 40-63 μm	Ni(20%)-silica gel-2# 210-500 μm	Ni(20%)-Al$_2$O$_3$ 74-177 μm	Ni(20%)-NS
Conversion %	77.1	85.0	56.3	86.5
Products distributions, %				
cyclohexane	67.6	64.3	17.3	69.1
cyclohexene	6.3	10.2	12.5	6.9
cyclohexanol	0.6	0.3	1.3	1.1
cyclohexanone	1.3	4.0	19.0	2.6
bicyclohexyl	0.7	0.9	-	0.5
cyclohexyl-phenol	1.4	5.4	6.0	1.9
DOD,%	73.8	75.3	30.0	80.9

[a] Reaction conditions: 0.2 g of catalyst, 5 g of phenol, 15 g of H$_2$O, P(H$_2$)=3MPa, stirring speed=500 r/min, time =6 h.

The Ni-NS catalysts at Ni loading of 20 and 50% were compared (Figure 2.7). There were no differences between performance of Ni(20%)-NS and Ni(50%)-NS for pure phenol HDO, which gave about 100% conversion and DOD. When water was added to the reaction, differences in performance between these two catalyst loadings were observed. Under this condition, the phenol conversion and DOD with Ni(20%)-NS decreased to 86.5% and 80.9%, respectively as compared with complete (100%) conversion and DOD with Ni(50%)-NS. These results revealed that the applied NSs can uptake as much as 50% Ni particles without

Ni crystallization occurring. This may be attributable to more active sites that can be placed on the NS surface and thus can maximize the catalyst activity. This trend of increased conversion by increasing Ni loading has also been observed by Huynh et al. [3]. As they reported, the supported Ni catalysts with loading of 4, 12 and 21% showed phenol conversions of 14, 82 and 98% at 250 °C, respectively. With the last catalyst, selectivity towards deoxygenated products in their study reached 98% DOD, which was close to the one achieved using the Ni(50%)-NS catalyst.
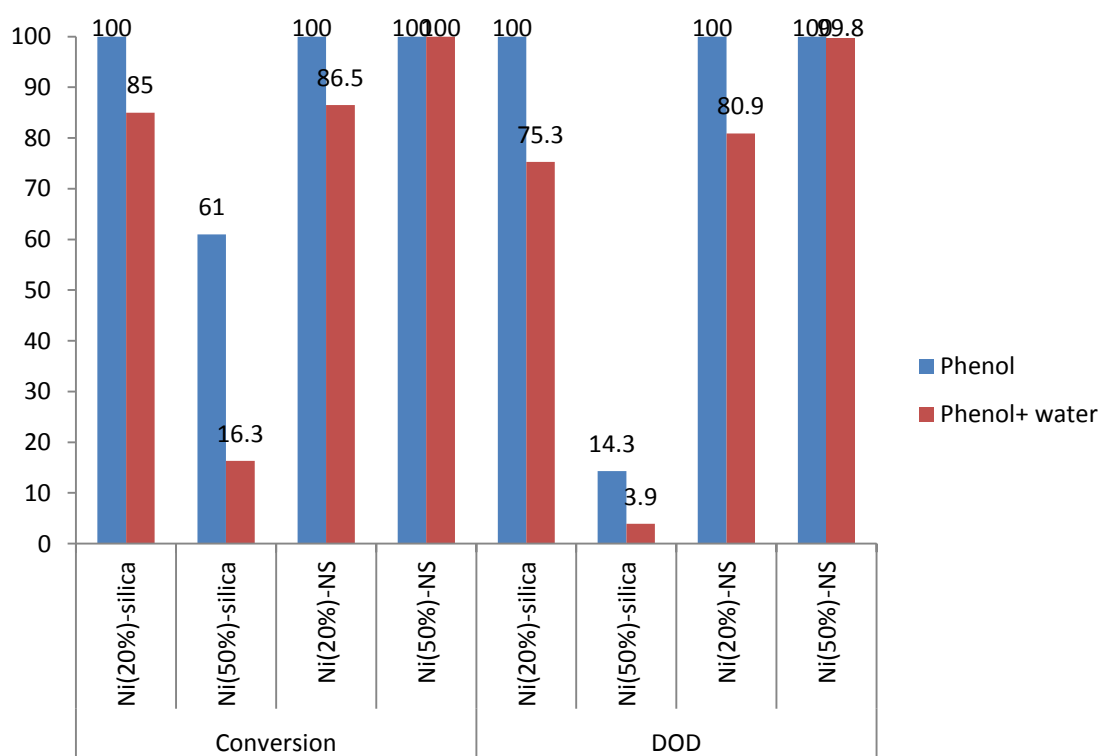
Figure 2.7 HDO of phenol on various Ni catalysts with high Ni loading with and without the addition of water

Another series of phenol HDO reactions over Ru catalysts was also carried out in the presence of water. There was no reaction over Ru catalysts conducted in pure phenol because all Ru catalysts performed well enough for phenol HDO in an aqueous environment.

The phenol conversion, DOD and product distribution over Ru catalysts are given in Table 2.5. For comparative purposes, this series of phenol HDO over Ru catalysts were carried out under the same condition as the Ni catalysts (Table. 2.4). As can be clearly seen, the phenol conversions over all the Ru catalysts nearly reached 100% with the DODs of more than 90% even though the Ru loading was only 5%. This may be attributable to a balance of acid and metal sites on the surface of these Ru catalysts. Therefore, only minor differences in the support effect on these Ru catalysts were observed due to the high activity of Ru itself. However, Ru-NS still performed the best of all the catalysts in term of the conversion and DOD. Additionally, it should be noted that γ-alumina appears to be a better support for Ru catalyst because a conversion of 99% and DOD of 97% was obtained. As compared with the poor performance of Ni-γ-alumina catalyst, Ru may also leach out from γ-alumina surfaces but the free-attached Ru can still maintain its activity during the reactions. On the other hand, these results also revealed that the phenol HDO activity was determined more by the metal itself rather than the support. The Ru catalysts were more active than the Ni catalysts which can attack the benzene ring and thus promote the final steps toward cyclohexane formation at a higher rate. The high activity of noble metal catalysts were also observed in other studies [8, 21, 33]. Wildschut et al. reported that Ru(5%)/C was a good catalyst for the hydrogenation of fast pyrolysis oil at 350°C and 20 MPa H_2 pressure [33]. Moreover, Ru catalysts were also reported to efficiently reduce ketones to alcohols even under mild conditions (4 MPa H_2 at 90°C) [9].

The product distribution using the Ru catalysts were similar to those obtained using the Ni catalysts. Cyclohexane was the major product with yields of >80%. Other products including cyclohexene, cyclohexanol, cyclohexanone, and bicyclohexyl were also detected which implied the HDO routine for phenol over Ru catalysts was similar to Ni. However, only

trace amount of intermediate products including cyclohexanol and cyclohexanone were observed, and cyclohexyl-phenol was not detected in the Ru based reactions. These results indicate the superior capability of Ru catalysts for deoxygenation reaction even in the presence of water. Ru activity was further improved using the NS support since no oxygenated intermediates were detected with the Ru-NS catalysts. More importantly, the highest cyclohexane yield was also obtained with the Ru-NS catalyst when compared with other Ru catalysts.

Table 2.5 HDO of phenol in aqueous solution over Ru (5%) catalysts with C/F =1:25

catalyst	Ru(5%)-silica gel-1# 40-63 μm	Ru(5%)-silica gel-2# 210-500 μm	Ru(5%)-Al_2O_3 74-177 μm	Ru(5%)-NS
Conversion %	96.8	96.3	98.7	100
Products distributions, %				
cyclohexane	83.6	80.5	86.6	91.5
cyclohexene	3.3	3.7	3.2	0.5
cyclohexanol	2.7	2.9	0.9	-
cyclohexanone	0.7	1.8	0.5	-
bicyclohexyl	0.8	0.7	1.7	2.9
DOD, %	93.3	91.5	97.2	100

[a] Reaction conditions: 0.2 g of catalyst, 5 g of phenol, 15 g of H_2O, P(H_2)=3MPa, stirring speed=500 r/min, time =6 h.

To gain more insight into the support effect of the Ru catalysts, another series of phenol HDO with less amount of Ru catalyst (C/F=1:100) was conducted under the same conditions. The corresponding conversion, DOD and product distribution are shown in Table 2.6. Under these conditions, the support effect on Ru catalysts was more obvious. As compared with Table 2.5, a noticeable change is that the conversion of phenol on Ru-Y-

alumina decreased to 69% when using a C/F of 1:100. A possible explanation could be the formation of Ru agglomerates on the ɣ-alumina support thus decreasing the catalyst's activity. Unlike Ru-alumina, all of the silica based Ru catalysts performed well enough even at low catalyst loadings. Again, Ru-silica gel (210-500 μm) still outperformed the Ru-silica gel (40-63 μm) catalyst. Yet again, the Ru-NS catalyst was the best performing catalyst preparation in the presence of water.

Although the phenol HDO routine has been clarified based on the previous results, the product distribution over Ru catalysts under this condition (C/F=1:100) can further show the support effect on Ru catalysts. Not surprisingly, cyclohexane was still the major product but cyclohexene yields over all Ru catalysts slightly increased, especially for Ru-alumina. Cyclohexene is considered an intermediate for cyclohexane and is derived from cyclohexanol dehydration. Lower cyclohexane yields and more cyclohexene residual indicated the hydrogenation over the Ru-Al_2O_3 was impaired while the dehydration was not. Since Al_2O_3 is reported as a good dehydration catalyst for alcohol, this result implied that Al_2O_3 still maintains its activity but Ru may partially deactivate during reactions. With respect to the silica based catalysts, Ru-NS yielded the most cyclohexane (91.1%) with no large difference observed when the C/F switched from 1:25 to 1:100. This perfect performance for Ru-NS indicates it is a very promising catalyst for pyrolysis bio-oil HDO.

Table 2.6 HDO of phenol in aqueous solution over Ru (5%) catalysts with a C/F = 1:100

catalyst	Ru(5%)-silica gel-1# 40-63 µm	Ru(5%)-silica gel-2# 210-500 µm	Ru(5%)-Al$_2$O$_3$ 74-177 µm	Ru(5%)-NS
Conversion %	92.5	98.5	69.2	100
Products distributions, %				
cyclohexane	80.6	85.7	46.7	91.1
cyclohexene	5.5	4.7	13.3	1.9
cyclohexanol	2.2	1.1	1.8	0.1
cyclohexanone	1.5	0.7	3.8	0.3
bicyclohexyl	0.7	1.4	0.3	1.2
cyclohexyl-phenol	-	-	1.3	-
DOD, %	89.9	96.7	62.3	99.6

[a] Reaction conditions: 0.05 g of catalyst, 5 g of phenol,15 g of H$_2$O, P(H$_2$)=3MPa, stirring speed=500 r/min, time =6 h.

To understand the Ru loading effect on catalyst performance, catalysts with different Ru loading were prepared on the silica gel (210-500 µm) and NSs using the same procedure as for the Ni catalysts. In terms of conversion and DOD, low Ru loading (5%) catalysts were compared with the higher Ru loading (10 and 20%) with two C/F ratios, as shown in Figure 2.8. A slight increase in the conversion and DOD were observed when the Ru loading on silica gel increased from 5 to 20%. All the Ru-NS catalysts with different metal loadings showed a high activity and hydrocarbon selectivity as evidenced by complete phenol conversion and DODs. These results suggest that no real gain in performance was obtained from the Ru-NS catalysts at a loading >5%. The 5% Ru-NS was pink-grey in color and the original NS were pink. At Ru loadings >10% the catalyst was grey and turned black at 20%.

The Ru-silica gel catalysts were black at 5% Ru. In terms of the Ru application on phenol HDO, there are only limited studies currently while several studies had only focused on the performance of Ru catalysts for pyrolysis oil hydrotreatment [8, 33-35].
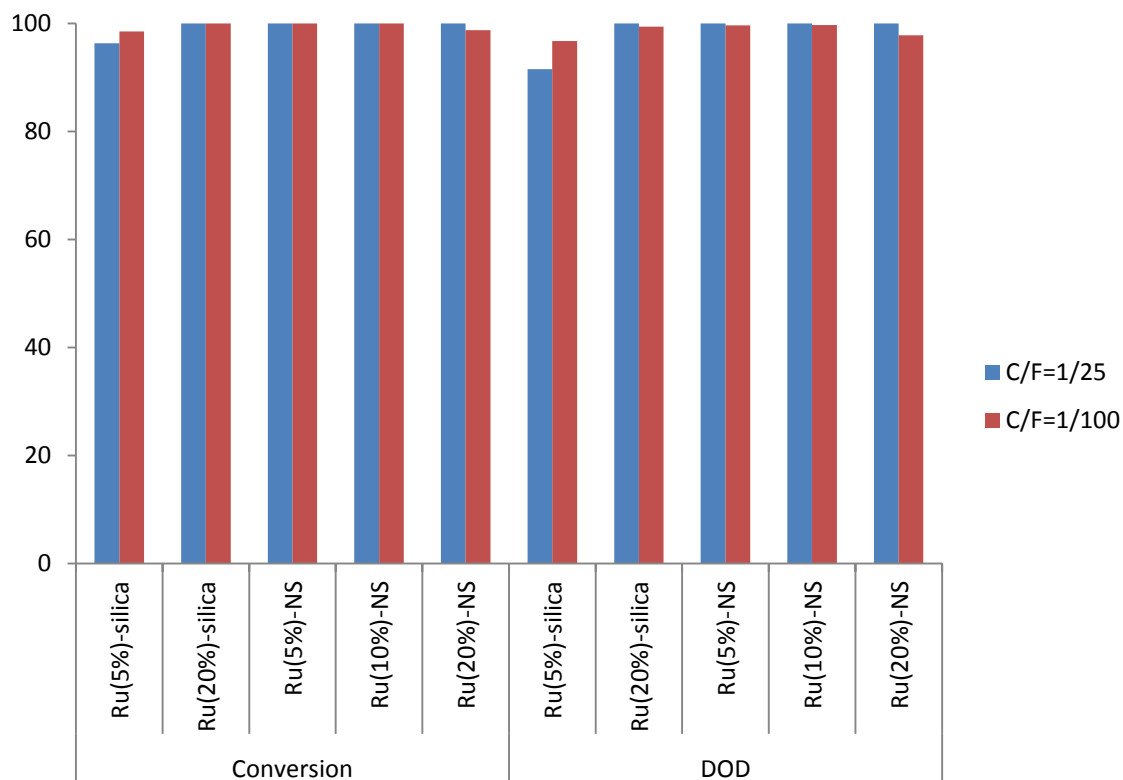
Figure 2.8 HDO of phenol over Ru catalysts with high Ru loading

2.4.2.3. Catalyst stability

The stability of the Ru-NS catalyst for phenol HDO in water was performed using the Ru(20%)-NS with a C/F of 1:100. Once the reaction was complete, the used catalyst was recovered for four subsequent phenol HDO treatments. The phenol conversion, DOD, and cyclohexane yield for each reaction are given in Table. 2.7. In this case, the conversion and DOD were about 100% even after 5 treatments. The cyclohexane yield for each treatment

was >94 % with no decreased activity. These results clearly show that the Ru-NS can maintain good activity during catalytic treatments

Table 2.7 Conversion of phenol by HDO using Ru(20%)-NS catalyst after 5 treatments

Ru(20%)-NS	1# run	2# run	3# run	4# run	5# run
Conversion %	100	99.9	100	99.2	99.9
cyclohexane	94.1	95.0	95.9	95.6	95.2
DOD, %	98.9	99.9	99.0	99.3	99.7

[a] Reaction conditions: 0.05 g of catalyst, 5 g of phenol, 15 g of H_2O,
$P(H_2)$=3MPa, stirring speed=500 r/min, time =6 h.

In summary, the Ni based catalysts can deoxygenate the phenol to hydrocarbons including cyclohexane, cyclohexene, and bicyclohexyl although several oxygenated intermediates were also identified after the reactions. The highest phenol conversion and DOD was obtained by the Ni(20%)-NS catalyst. When the same reactions were carried out in water solution, the phenol conversion and DOD over all Ni catalysts decreased especially for Ni(20%)-alumina. In this case, the Ni(20%)-NS still performed the best since the highest conversions (86.5%) and DOD (80.9%) were obtained. With an increase of Ni loading from 20 to 50%, the performance of Ni-silica gel catalyst actually decreased due to the crystallization of Ni particles. However, the Ni(50%)-NS performed better than the Ni(20%)-NS catalyst and thus indicated the high surface area of the NSs for Ni deposition. In contrast with the Ni catalyst, all the Ru based catalysts performed better even though the same supports were applied. In addition, no obvious support effects were observed among Ru catalyst except for the deactivation of Ru-alumina during phenol HDO in water. These results revealed that the catalyst activity was more affected by the active metals (Ru and Ni) versus the support and the Ru particles were more active than Ni particle in terms of phenol HDO.

Nevertheless, Ru(5%)-NS still performed the best of all the catalysts using phenol at a 1:100 ratio. The conversion and DOD obtained over Ru(5%)-NS under this condition were 100% and 99.1%, respectively. A subsequent experiment using a higher Ru loading (20%) did show a higher phenol conversion using a silica gel support, but this effect was not observed when using NSs as a support under similar reaction conditions since 100 conversion was observed for all Ru-NS catalysts (5, 10, 20%). Additionally, a series of recycling the catalyst showed good stability of the Ru(20%)-NS catalyst. In brief, the SiO_2 NSs were the best performing support for both Ni and Ru catalysts for phenol HDO in the presence of water.

2.5. Conclusions

In this work, a series of Ni and Ru-based catalysts on different supports were prepared and tested for the hydrodeoxygenation (HDO) of phenol. All the catalysts maintained a broad range of physicochemical properties as evidenced by TEM and XRD. Besides the helical structure, mesoporous channels were also observed from silica NSs based catalysts. The best metal dispersity was achieved on the surface of silica NSs which thus performed better than other supports (alumina and silica gels) in term of phenol conversion and DOD. The products from the HDO of phenol were mainly cyclohexane, cyclohexene and bicyclohexyl although several oxygenated intermediates were also identified after the reactions. For all the Ni catalysts, silica based catalysts performed better than alumina based especially in the presence of water. The Ni(20%)-NS was the best performing Ni catalyst based on it having the highest conversion and DOD. Of the Ru based catalysts the Ru-NS were the best performing giving nearly complete phenol conversion and DOD. The Ru-NS

showed good catalytic ability (stability) after 5 several treatments. These results clearly show that these NS were excellent supports for HDO reactions especially with Ru.

2.6. References

1.   Marsman, J.H., et al., *Identification of components in fast pyrolysis oil and upgraded products by comprehensive two-dimensional gas chromatography and flame ionisation detection.* Journal of Chromatography A, 2007. **1150**(1-2): p. 21-27.

2.   Bu, Q., et al., *A review of catalytic hydrodeoxygenation of lignin-derived phenols from biomass pyrolysis.* Bioresource Technology, 2012. **124**: p. 470-477.

3.   Huynh, T.M., et al., *Hydrodeoxygenation of Phenol as a Model Compound for Bio-oil on Non-noble Bimetallic Nickel-based Catalysts.* ChemCatChem, 2014: p. n/a-n/a.

4.   Mortensen, P.M., et al., *Screening of Catalysts for Hydrodeoxygenation of Phenol as a Model Compound for Bio-oil.* ACS Catalysis, 2013. **3**(8): p. 1774-1785.

5.   Wang, W., et al., *Effect of La on Ni–W–B Amorphous Catalysts in Hydrodeoxygenation of Phenol.* Industrial & Engineering Chemistry Research, 2011. **50**(19): p. 10936-10942.

6.   Yan, N., et al., *Hydrodeoxygenation of Lignin-Derived Phenols into Alkanes by Using Nanoparticle Catalysts Combined with Brønsted Acidic Ionic Liquids.* Angewandte Chemie International Edition, 2010. **49**(32): p. 5549-5553.

7.   Jelle Wildschut, F.H.M., Robbie H. Venderbosch, and Hero J. Heeres, *Hydrotreatment of Fast Pyrolysis Oil Using Heterogeneous Noble-Metal Catalysts.pdf.* Industrial & Engineering Chemistry Research, 2009. **48**: p. 10324-10334.

8.   Nan, W., et al., *Catalytic Upgrading of Switchgrass-Derived Pyrolysis Oil Using Supported Ruthenium and Rhodium Catalysts.* Energy & Fuels, 2014. **28**(7): p. 4588-4595.

9.   Mahfud, F.H., F. Ghijsen, and H.J. Heeres, *Hydrogenation of fast pyrolyis oil and model compounds in a two-phase aqueous organic system using homogeneous*

ruthenium catalysts. Journal of Molecular Catalysis A: Chemical, 2007. **264**(1-2): p. 227-236.

10.   Valle, B., et al., *Selective Production of Aromatics by Crude Bio-oil Valorization with a Nickel-Modified HZSM-5 Zeolite Catalyst.* Energy & Fuels, 2010. **24**(3): p. 2060-2070.

11.   Badawi, M., et al., *Promoting effect of cobalt and nickel on the activity of hydrotreating catalysts in hydrogenation and isomerization of olefins.* Journal of Molecular Catalysis A: Chemical, 2008. **293**(1-2): p. 53-58.

12.   Wang, X., *Valorization of lignin and bio-oil by catalytic hydrogenation with Ni catalyst*, in *Max Planck Institute*. 2013, Max Planck Institute Mülheim. p. 221.

13.   Gayubo, A.G., et al., *Hydrothermal stability of HZSM-5 catalysts modified with Ni for the transformation of bioethanol into hydrocarbons.* Fuel, 2010. **89**(11): p. 3365-3372.

14.   Wang, L., et al., *High yield synthesis and lithography of silica-based nanospring mats.* Nanotechnology, 2006. **17**(11): p. S298-S303.

15.   Daqing Zhang, A.A., Hongmei Han, Hasan Mahmood, and David N, McIlroy, *Silicon Carbide Nanosprings.* Nano Letters, 2003. **3**(7): p. 983-987.

16.   Luo, G., et al., *A novel nano fischer-tropsch catalyst for the production of hydrocarbons.* Environmental Progress & Sustainable Energy, 2014. **33**(3): p. 693-698.

17.   Whiffen, V., *A Study of Metal Phosphides for the Hydrodeoxygenation of Phenols and Pyrolysis Oil.*, in *Chemical and Biological Engineering*. 2013, The University of British Columbia: Vancouver. p. 268.

18.   Zhao, C., et al., *Understanding the impact of aluminum oxide binder on Ni/HZSM-5 for phenol hydrodeoxygenation.* Applied Catalysis B: Environmental, 2013. **132-133**: p. 282-292.

19.   Wang, X. and R. Rinaldi, *A Route for Lignin and Bio-Oil Conversion: Dehydroxylation of Phenols into Arenes by Catalytic Tandem Reactions.* Angewandte Chemie International Edition, 2013. **52**(44): p. 11499-11503.

20.   Zhao, C., et al., *Comparison of kinetics, activity and stability of Ni/HZSM-5 and Ni/Al2O3-HZSM-5 for phenol hydrodeoxygenation.* Journal of Catalysis, 2012. **296**: p. 12-23.

21.   Zhao, C., et al., *Hydrodeoxygenation of bio-derived phenols to hydrocarbons using RANEY® Ni and Nafion/SiO2 catalysts.* Chemical Communications, 2010. **46**(3): p. 412.

22.   Popov, A., *Bio-oils Hydrodeoxygenation- Adsorption of Phenolic Molecules on Oxidic Catalyst.* Journal of Physics and Chemistry.C, 2010. **114**: p. 10.

23.   Wang, X. and R. Rinaldi, *Exploiting H-transfer reactions with RANEY® Ni for upgrade of phenolic and aromatic biorefinery feeds under unusual, low-severity conditions.* Energy & Environmental Science, 2012. **5**(8): p. 8244.

24.   Zhang, X., et al., *Catalytic Upgrading of Bio-oil over Ni-Based Catalysts Supported on Mixed Oxides.* Energy & Fuels, 2014. **28**(4): p. 2562-2570.

25.   Bykova, M.V., et al., *Ni-based sol–gel catalysts as promising systems for crude bio-oil upgrading: Guaiacol hydrodeoxygenation study.* Applied Catalysis B: Environmental, 2012. **113-114**: p. 296-307.

26.   Bykova, M.V., et al., *Stabilized Ni-based catalysts for bio-oil hydrotreatment: Reactivity studies using guaiacol.* Catalysis Today, 2014. **220-222**: p. 21-31.

27.   Yang, Y., et al., *Effect of metal–support interaction on the selective hydrodeoxygenation of anisole to aromatics over Ni-based catalysts.* Applied Catalysis B: Environmental, 2014. **145**: p. 91-100.

28.   Marcel .M .T, M.B., Olandir. V.C, Almir. O.N, Marcelo.L, Estevam. V. S., *Preparation of PtRu-Carbon Hybrids by Hydrothermal Carbonization Process.* Materials Research, 2007. **10**(2): p. 171-175.

29.   Lai, Y.-H., et al., *Deposition of Ru and RuO2 thin films employing dicarbonyl bis-diketonate ruthenium complexes as CVD source reagents.* Journal of Materials Chemistry, 2003. **13**(8): p. 1999.

30.   Zhang, X., et al., *Hydrotreatment of bio-oil over Ni-based catalyst.* Bioresource Technology, 2013. **127**: p. 306-311.

31.   Neumann, G.T., et al., *Correlating lignin structure to aromatic products in the catalytic fast pyrolysis of lignin model compounds containing β–O–4 linkages.* Catal. Sci. Technol., 2014. **4**(11): p. 3953-3963.

32.   Ardiyanti, A.R., et al., *Catalytic hydrotreatment of fast pyrolysis oil using bimetallic Ni–Cu catalysts on various supports.* Applied Catalysis A: General, 2012. **449**: p. 121-130.

33.   Wildschut, J., et al., *Insights in the hydrotreatment of fast pyrolysis oil using a ruthenium on carbon catalyst.* Energy & Environmental Science, 2010. **3**(7): p. 962.

34.   Li, Z., et al., *A mild approach for bio-oil stabilization and upgrading: electrocatalytic hydrogenation using ruthenium supported on activated carbon cloth.* Green Chemistry, 2014. **16**(2): p. 844.

35.   Laskar, D.D., et al., *Noble-metal catalyzed hydrodeoxygenation of biomass-derived lignin to aromatic hydrocarbons.* Green Chemistry, 2014. **16**(2): p. 897.

Chapter 3: Hydrodeoxygenation of Pyrolysis Bio-oil for Hydrocarbons Production

3.1 Abstract

Hydrodeoxygenation (HDO) is a promising process to upgrade pyrolysis bio-oil into transportation fuels. However, coke is easily formed during hydrotreating condition and thus impedes the HDO of bio-oil. The objective of this study was to develop an effective routine for HDO of Douglas-fir (*Pseudotsuga menzeseii*) pyrolysis bio-oil. The bio-oil was fully characterized by GC-MS, HPLC, and ESI-MS. The bio-oil was fractionated using phase separation by addition of water to obtain a water-insoluble (WIS) and water-soluble (WS) fractions from the bio-oil. These two separate fractions were investigated for their suitability for hydrotreatment. The $Ni(65\%)/SiO_2-Al_2O_3$ catalyst was used for hydrocracking and HDO treatments. Results indicated that the WS of bio-oil can be upgraded into cycloalkanes (30%) and alcohols (18%) over a $Ni(65\%)/SiO_2-Al_2O_3$ catalyst at 300°C. The WIS of bio-oil was effectively cracked in methanol over a $Ni(65\%)/SiO_2-Al_2O_3$ catalyst, which was shown by ESI-MS. A further step of HDO on the cracked oil had successfully deoxygenated the phenolics into cycloalkanes.

3.2 Introduction

Due to increasing fossil fuel prices, continuing depletion of the reserves of nonrenewable petroleum, and greenhouse gas (GHG) emissions, the development of alternative liquid fuels from renewable biomass sources are very important [1]. Fast pyrolysis

is a thermochemical technology that can convert biomass into liquid bio-oil, biochar, and gaseous products. Among these three products, bio-oil is the most desirable and its yield can currently be maximized up to 72% through fast pyrolysis [2]. This high yield is acquired for relatively short residence times (0.5-2 s), moderate temperatures (400-600°C), and rapid quenching at the end of the process [3]. As byproducts of the process, the yield of bio-oil, gases and biochar depends on the biomass composition, particle size, and rate and duration of heating during fast pyrolysis [4]. Nevertheless, the major components in pyrolysis bio-oil are the oxygenated compounds including anhydro-saccharides, furans, alcohols, ketones, aldehydes, carboxylic acids, phenolic monomers, lignin/phenolic oligomers and water [5]. The compounds present in the bio-oil contribute to its high viscosity, poor thermal and chemical stability, corrosion, and immiscibility with hydrocarbon fuels. Fortunately, these drawbacks can be overcome with catalytic hydrotreatment and hydrogenation, which targets removal of oxygen in the bio-oil. Furthermore, this treatment eliminates oxygen as water by catalytic reaction with hydrogen under moderate temperature (200-400°C). For this reason, this process is also considered as hydrodeoxygenation (HDO) of the bio-oil [6].

Active compounds can polymerize under hydrotreatment conditions and are likely to contribute to coke formation during the process [7]. As reported in related studies, the oligomers derived from lignin decomposition (also known as pyrolytic lignin or lignin oligomers) are the active component contributing to coke formation during hydrotreatment of bio-oil [8]. In order to avoid coke formation, a stabilization hydrotreatment stage on bio-oil is carried before the main HDO treatment [9, 10]. The hypothesis was that those extremely active oxygen-containing compounds (such as aldehydes) can be reduced to more stable compounds beforehand and thus minimize their potential to polymerize to form coke. However, this process generally requires catalysts to maintain their activity even at low

temperatures. In addition, pyrolytic lignin oligomers in bio-oil are difficult to deoxygenate even when using multiple-stages hydrotreatments. As a result, research has focused on depolymerizing pyrolytic lignin oligomers in the bio-oil to phenolic monomers, which then can be further upgraded to aromatics or cycloalkanes [11-14]. Huber et al. studied the ruthenium (Ru) based catalysts for the low temperature hydrotreatment on the aqueous phase of oak wood bio-oil [15]. The authors suggest that separation of the bio-oil into two phases prior to upgrading allows for better control on catalyst design and optimization.

In terms of bio-oil, catalytic hydrocracking is applied to depolymerize the tar or pyrolytic lignin oligomers into smaller molecular fragments, such as phenolics. The proposed mechanism for this hydrocracking involves the cleavage of β-O-4 and α-O-4 linkages in pyrolytic lignin, which are favored using an acidic zeolite catalyst [16, 17]. In the application of upgrading pyrolysis bio-oil or vapors, a fundamental understanding of the factors that favor C-O bond cleavage and C-C bond formation is still needed. Tang et al. demonstrated in their studies that pyrolytic lignin from rice husk bio-oil can be hydrocracked at 260°C in supercritical ethanol under a hydrogen atmosphere using a Ru catalyst [11]. Although there was no zeolite catalyst involved, the pyrolytic lignin was still successfully cracked into small fragments including phenols, guaiacols, anisoles, esters, and light ketones. More recently, Ferrini et al. had developed a novel routine to produce non-pyrolytic lignin bio-oil through catalytic hydrogen transfer reactions. In this process, lignin was extracted from the plant cell wall by solvolysis as fragments having much lower molecular weight (M_w) than currently believed. In fact, this was another type of hydrocracking which occurred under cooking with propanol together with a Ni catalyst instead of fast pyrolysis. The results also indicated that the produced lignin fragments were mainly phenolics, which only required a low-severity treatment for deoxygenation [18].

The objective of this study was to develop an effective method for HDO of pyrolysis bio-oil. The bio-oil was fully characterized (see Figure 3.1) and fractionated by phase separation by addition of water to obtain a water-insoluble (WIS) and water-soluble (WS) fractions from the bio-oil. Subsequently, the two separate fractions were investigated for their suitability for hydrotreatment. A $Ni(65\%)/SiO_2$-Al_2O_3 catalyst was used for hydrocracking and HDO treatments. The hydrocarbons products were characterized and discussed in term of the potential application as transportation fuels.

3.3. Materials and Methods

3.3.1. Bio-oil production and fractionation

The pyrolysis bio-oil was produced by conventional pyrolysis of Douglas-fir sawdust (20 kg h^{-1}, <5 mm) in a 100 mm diameter auger pyrolyzer (mobile in-house modified ½ ton d^{-1} Advanced BioRefinery Inc (ABRI) pyrolysis unit) at 450-500˚C. The synthesis-gas generated was used to heat the reactor. The pyrolysis vapors were trapped using a series of five tube-shell condensers. The bio-oil was collected over a 2 hour operational period once the pyrolysis was at steady state, and then combined, thoroughly mixed, and stored in a freezer at -20˚C. Yield of bio-oil was 50% based on original wood dry weight basis. Bio-oil (20g, batches) was fractionated by dispersing the bio-oil in water (40 ml), sonicating for 30 min, and then centrifuged at 3000 rpm for 60 min. Once separation was achieved, gravimetric yields of the top aqueous water soluble (WS) layer and bottom water insoluble (WIS) layer were 79.1± 0.8% and 21.9 ± 0.5%, respectively. The WS and WIS fractions were characterized, as described below.
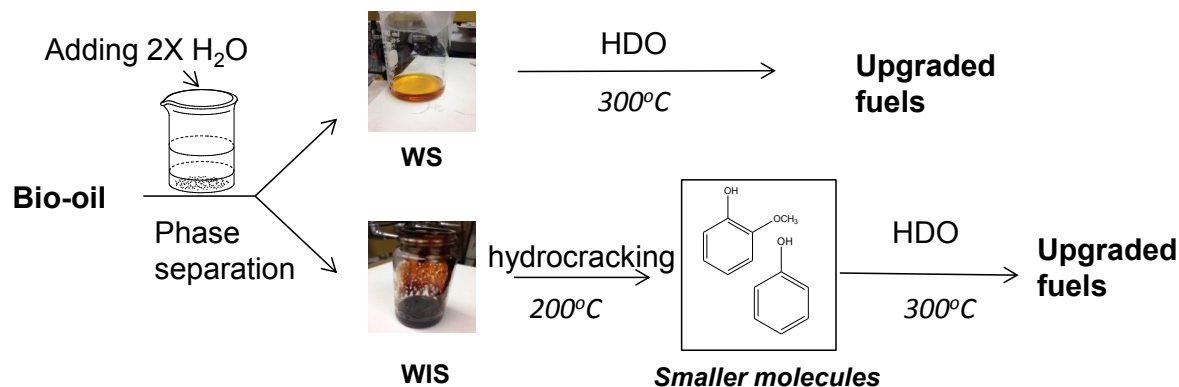
3.3.2 Bio-oil hydrotreatment

3.3.2.1 Hydrogenation on water soluble bio-oil

The top aqueous WS layer was then utilized for subsequent hydrogenation (HYD) using a commercial Ni/SiO$_2$-Al$_2$O$_3$ catalyst (65% Ni loading, Alfa Aesar). The hydrogenation reaction was performed with a stirred 300 mL batch reactor (Parr model 4564). The bio-oil WS fraction (30 g) and the catalyst (1.5 g) were introduced into the reactor, closed, flushed with H$_2$ and then pressurized with H$_2$ to 2.8 MPa (400 psi). The reaction mixture was heated to 300˚C and stirred at 500 rpm for 12 h (Figure 3.1). The reaction was then quenched by placing the reactor in an ice-water bath until it reached room temperature. The reaction mixer/products were characterized as described below.

3.3.2.2 Hydrocracking and hydrodeoxygenation on water insoluble bio-oil

The water-insoluble (WIS) bio-oil bottom layer (10 g) was dispersed in methanol (20 g) and hydrocracked at 200˚C using a Ni(65%)/ SiO$_2$-Al$_2$O$_3$ catalyst (Alfa Aesar) with 600 psi of H$_2$ pressure for 10 h. The catalyst to WIS bio-oil weight ratio was 1:20. The hydro-cracked WIS oil fraction was concentrated using a rotary evaporator to remove methanol. The WIS cracked oil was then mixed with n-hexane as solvent for HDO by using Ni/SiO$_2$-Al$_2$O$_3$ catalyst at 250˚C and 4.1 MPa (600 psi) of H$_2$ pressure for 10 h. The reaction mixer/products were characterized as described below.

Figure 3.1 The flow diagram of overall bio-oil hydrotreatment.

3.3.3. Bio-oil and its upgrading products characterization

GC-MS (FOCUS-ISQ, Thermoscientific) was used to characterize the volatile components in the bio-oil, WS and WIS fractions (1.0 mg of bio-oil sample was solubilized in 1 mL of CH_2Cl_2 containing anthrancene (0.05 mg mL^{-1}) as internal standard), where separation was achieved using a RTx-5MS capillary column (30 m × 0.25 mm Ø, Restek) using a temperature program of 40°C (hold for 2 min) to 250°C (10min) at 5°C min^{-1}. Compounds were identified using known standards, mass spectral library matching (National Institute of Standards and Technology (NIST) 2008), and by their mass spectra. The WS layer of bio-oil was characterized by high-performance liquid chromatography (HPLC), in duplicate, using a Rezex ROA organic acid column (7.8 × 30 cm, Phenomenex) and a Waters HPLC (Waters, Milford, MA) equipped with a differential refractive index detector (ERC-5710, ERMA), on elution with 0.005 N aqueous sulfuric acid (0.5 mL min^{-1}) at 65°C. In addition, the non-volatile compounds in the bio-oil were analyzed by ESI-MS. Bio-oil samples (1 mg) were dissolved in methanol containing 1% acetic acid (1 mL) and directly analyzed in both positive and negative ion electrospray ionization-mass spectrometry (ESI-MS, m/z 90-2000)

on a Finnigan LCQ-Deca instrument (Thermoquest, San Jose, CA) at a flow rate of 10 μL min^{-1}. Data analysis was based on the calculation of number average molar mass (M_n) as $M_n = \Sigma M_i N_i / \Sigma N_i$ and weight average molar mass (M_w) as $M_w = \Sigma M_i^2 N_i / \Sigma M_i N_i$ with M_i as m/z and N_i as intensity of ions [19].

3.4 Result and discussion

3.4.1 Bio-oil characterization

3.4.1.1 Compositions of bio-oil identified by GC-MS

Bio-oils are very complex mixtures of different chemical species derived from depolymerization and fragmentation of biomass main components, covering a wide range of molecular weights [5]. The bio-oil obtained from Douglas-fir fast pyrolysis in this study was characterized by GC-MS as shown in Figure 3.2 and products listed in Table 3.1. Oxygenated cyclic compounds were also detected in the bio-oil in the retention time range between 32 and 45 min, such as 13-isopropyl-podocarpa-8,11,13-trien-15-oic acid (41.07 min). It should be noted that there is a high proportion of oxygenated compounds and only minor oxygen-free hydrocarbon produced in the pyrolysis oil. These oxygen-containing groups were mainly composed by carboxylic acid, ester, aldehydes and ketones, aliphatic and aromatic alcohols, phenols, and methoxylated phenols, which have been also identified in other studies [5]. Hydroxyl and aldehyde groups are chemically unstable and thus need to be further deoxygenated to hydrocarbons. In addition, carbon double bonds were also identified, such as vinyl-guaiacol and propenyl-guaiacols, that are reactive and can easily polymerize at room temperature [20]. In terms of the amount of compounds in the bio-oil, acetic acid (2.4%), furfural (4.7%), cresol (3.4%), phenols (6.4%), guaiacols (19%) and oxygenated acids

(7.6%) represented the major components of the pyrolysis bio-oil. The phenolic compounds were derived from lignin pyrolysis [21]. Furan derivatives were derived from hemicellulose and cellulose pyrolysis [22, 23]. However, no levoglucosan was detected in the bio-oil by GC-MS, which is generated from cellulose pyrolysis [24]. In view of these identified compounds, those with carbon numbers ranging from C_4 to C_{12} can be theoretically transformed to gasoline or jet fuels hydrocarbons if effective deoxygenation is performed.
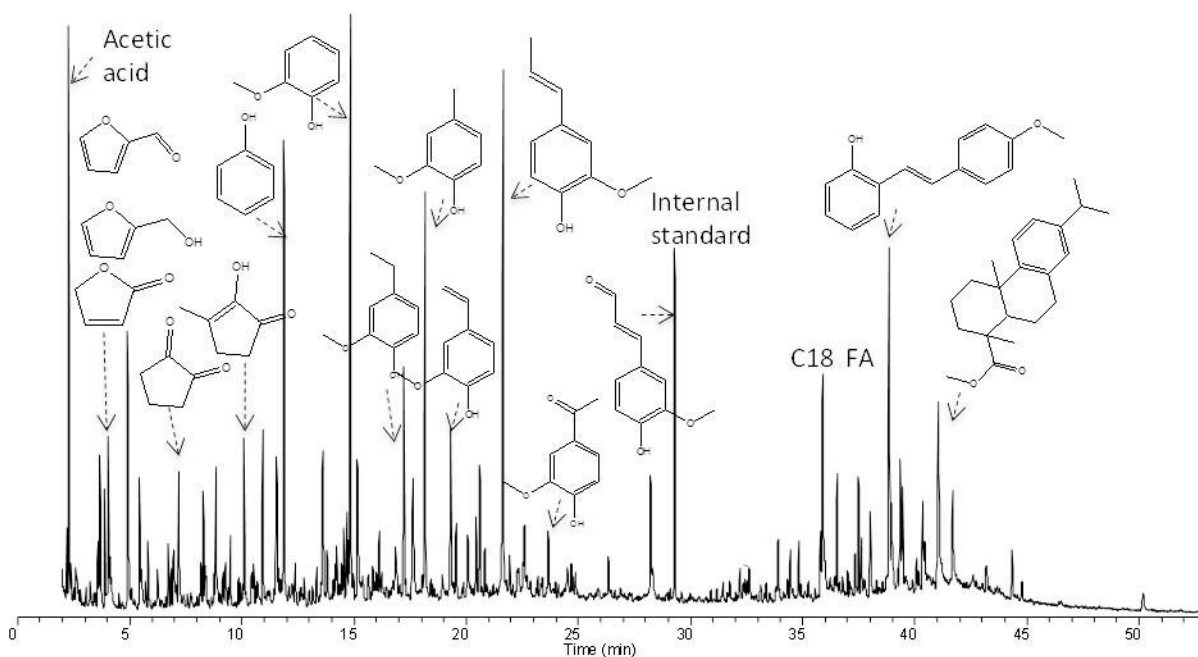
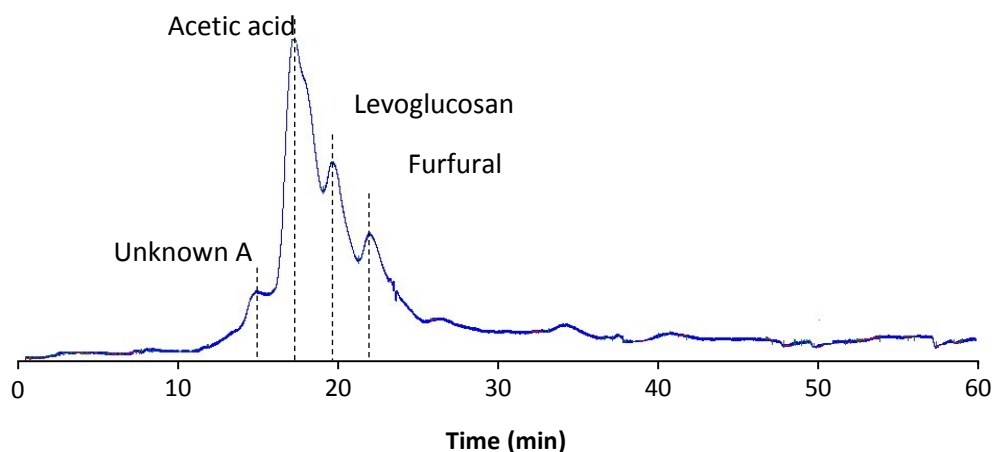**Figure 3.2** GC-MS on bio-oil from Douglas-fir fast pyrolysis.

Table 3.1 Products in Douglas-fir pyrolysis bio-oil identified by GC-MS

Retention time (min)	Identified compounds	Conc. (mg/g)	M^+ (m/z)
2.29	acetic acid	24.3	84
3.68	ethylene glycol monoacetate	10.6	104
3.87	butanedial	6.7	86
4.05	2-ethylbutyl acetate	18.5	144
4.92	furfural	19.7	96
5.45	furfural alcohol	12.6	98
5.81	2-propanone,1-hydroxy-acetate	4.9	116
6.25	styrene	3.8	104
6.71	2-methyl-2-cyclopentenone	4.2	96
6.97	2(5H)-furanone	8.5	84
7.19	1,2-cyclopentanedione	9.6	98
8.29	5-methyl-2-furaldehyde	6.6	110
8.86	phenol	12.7	94
10.10	2-hydroxy-3-methyl-2-cyclopenten-1-one	13.7	112
10.94	m-cresol	11.4	108
11.56	p-cresol	17.4	108
11.89	guaiacol	31.9	124
13.61	2,3-dimethyl-phenol	14.3	122
14.85	4-methyl-guaiacol	39.4	138
15.16	1,2-benzenediol	15.7	110
16.14	5-ethyl-m-cresol	5.1	136
17.23	4-ethyl-guaiacol	17.4	152
17.64	4-methyl-1,2-benzenediol	15.7	124
18.18	4-vinyl-guaiacol	27.6	150
19.31	4-(2-propenyl)-guaiacol	14.9	164
19.56	4-propyl-guaiacol	5.9	166
20.45	vanillin	6.4	152
20.62	4-(1-propenyl)-(E)-guaiacol	10.8	164
21.66	4-(1-propenyl)-(Z)-guaiacol	41.2	164
22.61	4-hydroxy-3-methoxy-acetophenone	8.3	166
23.66	guaiacylacetone	6.8	180
26.35	4-(ethoxymethyl)-2-methoxyphenol	5.9	182

28.22	3-(4-hydroxy-3-methoxyphenyl)-propenal	12.9	178
35.90	cis-vaccenic acid	27.8	282
36.54	13a-methyl-13-vinyl-podocarp-8-(14)-en-15-al	9.1	286
37.50	pimara-7,15-dien-3-one	7.6	286
38.86	4-methoxy-2-hydroxystilbene	25.9	226
e	Ethyl pimarate	13.9	330
41.07	13-isopropyl-podocarpa-8,11,13-trien-15-oic acid	23.8	300
41.69	abietic acid	10.6	302

3.4.1.2 High-performance liquid chromatography (HPLC)

Figure 3.3 shows the HPLC chromatogram of the WS of bio-oil from Douglas fir fast pyrolysis. Distinctive peaks of unknown A, acetic acid, levoglucosan and furfural are observed at 14.7, 17.0, 19.4 and 21.8 min, respectively. This interpretation on the HPLC was conducted by a combination of standard solution and related references [25, 26]. Both acetic acid and furfural have been identified by GC-MS. Moreover, the expected levoglucosan was also detected, which is the main product derived from pyrolysis of cellulose.
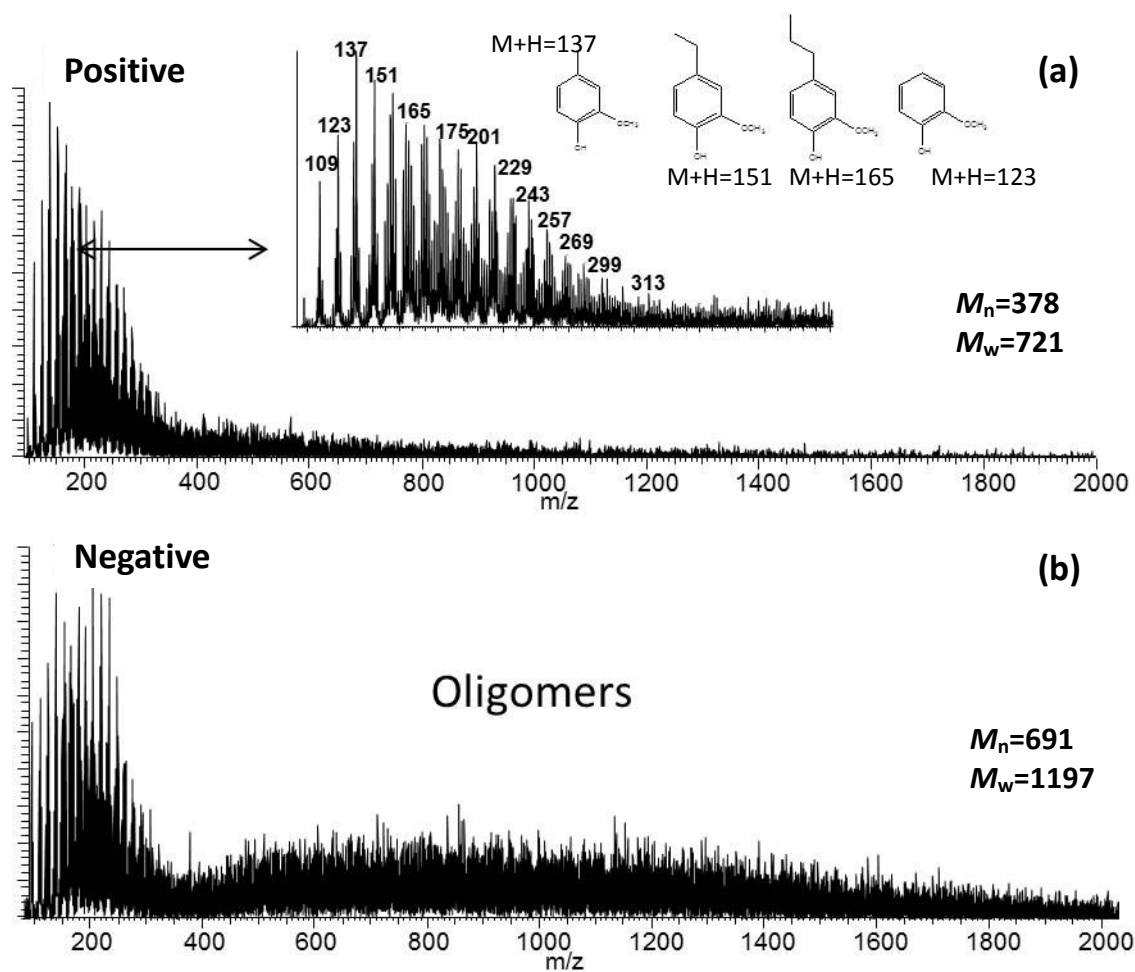

Figure 3.3 HPLC on WS of bio-oil from Douglas-fir fast pyrolysis.

Nevertheless, high molecular weight oxygenated compounds (oligomers) were also present in the bio-oils but could not be detected by GC-MS and HPLC [27]. However, these oligomers could be precursors to coke formation, since they participate in polymerization reactions during their catalytic upgrading processes [28]. Therefore, it was extremely important to characterize these oligomers to better understand the coke formation mechanisms.

3.4.1.3 ESI-MS of the bio-oil

ESI-MS has been successfully used to characterize the oligomers in bio-oil. Positive and negative ion ESI-MS spectrums for the pyrolysis bio-oil are shown in Figure 3.4. However, positive ion spectrum only shows part of the compounds in bio-oil while most oligomers were characterized by the negative ion MS. Nonetheless, the peak clusters in positive ion spectrum confirmed the existence of most of those compounds already identified by GC-MS, such as cresol ($[M+H]^+$ = 109 m/z), guaiacol ($[M+H]^+$ = 123 m/z), methyl-guaiacol ($[M+H]^+$ = 137 m/z), ethyl-guaiacol ($[M+H]^+$ = 151 m/z), propenyl-guaiacol ($[M+H]^+$ = 165 m/z) (Figure 3.4 a). In the negative ion ESI-MS, oligomers with molecular weight ranging from 400 to 2000 g/mol were identified which cannot be detected by GC-MS. The M_n and M_w calculated from negative ion ESI-MS were 691 and 1197 g/mol, respectively.

Figure 3.4 Positive and negative ion ESI-MS on bio-oil from Douglas-fir fast pyrolysis.

3.4.2 Bio-oil HDO results

Direct hydrogenation (HYD) on raw bio-oil easily led to coke formation which deactivated the catalyst. Therefore, in the present study the bio-oil from Douglas-fir fast pyrolysis was first separated into WS and WIS fractions. The reason for this process is that the WIS oil was recognized as the main component for coke formation and has to be separated for further cracking before HYD. Consequently, two kinds of HYD on bio-oil was

carried out: 1) bio-oil WS fraction HYD, and 2) pyrolytic lignin WIS fraction hydrocracking and HYD.

3.4.2.1 Hydrogenation on water soluble bio-oil

The liquid products from the HYD of bio-oil WS fraction are shown in Figure 3.5. The HYD products were separated by centrifugation resulting in a top organic layer (17% yield) and an aqueous bottom layer (Figure 3.5-b). Other organics were possibly decomposed into gas products. The composition of the organic layer was then characterized by GC-MS, which shows many volatile alkane products produced after hydrogenation with a Ni(65%)/SiO_2-Al_2O_3 catalyst at 300˚C and 2.8 MPa of H_2, which could explain this phase separation after the HYD reaction.

Direct comparison of the identified compounds before and after HYD were conducted and given in Table 3.2. Results indicate the main products in organic layer after HYD were phenol (7.4%), cyclohexane (4.8%), pentanol (4.0%), hexanol (4.0%), and methyl cyclohexane (2.1%). Except for phenol, these compounds had not been identified in the crude bio-oil before, which implies that effective HYD and HDO occurred over the Ni/SiO_2-Al_2O_3 catalyst. Alkanes including cyclohexane and methyl-cyclohexane were derived from phenol and methoxylated phenols after hydrogenation followed by dehydration. However, no direct HDO for bio-oil was detected for this catalyst. This result agrees with the conclusions that HDO of phenols over Ni catalyst was suppressed by water. The products ranged from C_6 to C_9 and are partially in the range of gasoline and jet fuels.
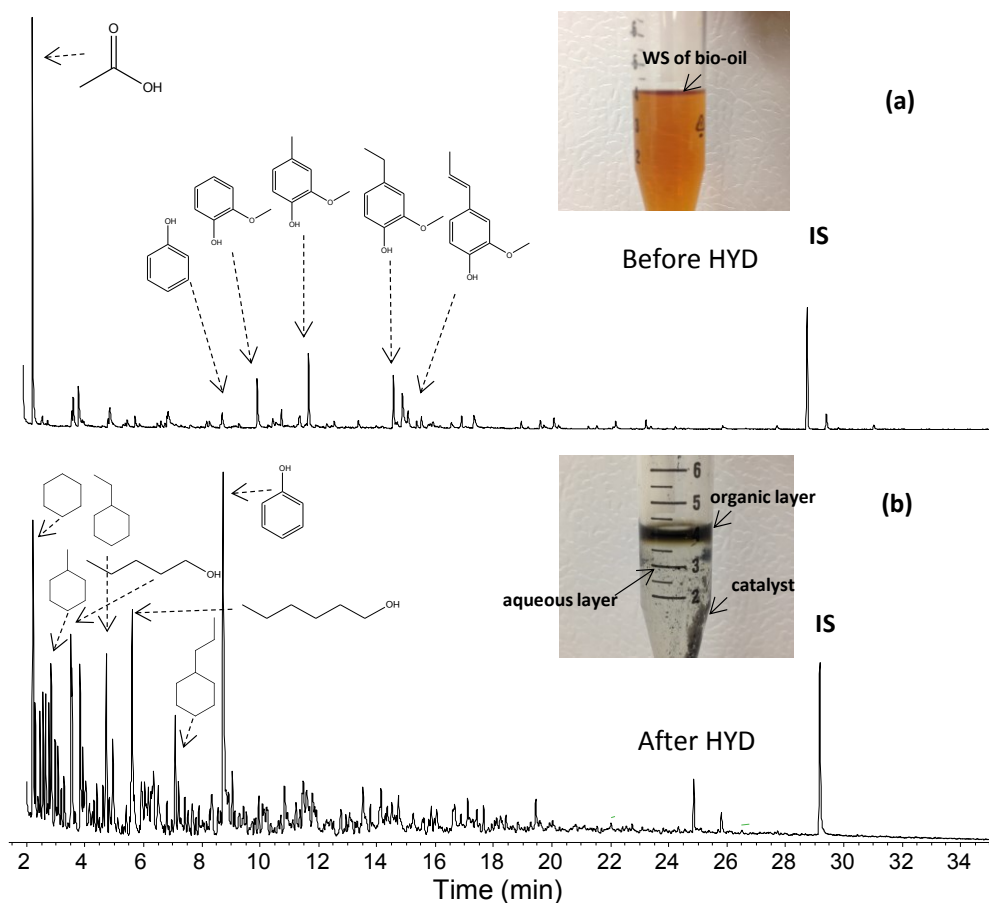
Figure 3.5 GC-MS chromatograms of the Douglas-fir (a) WS of bio-oil and (b) hydrogenated products in organic layer.

In addition, pentanol and hexanol are likely derived from furans and sugars in the WS bio-oil, respectively. Although no sugars were detected by GC-MS in the WS bio-oil fraction, they were detected by HPLC. In fact, the pentanol and hexanol were more energy dense than ethanol or even butanol and can thus be used for fuel as well. Nevertheless, there were still unreacted phenolics and minor amounts of ketones, furans, and esters remaining in the top organic layer (Table 3.2). These oxygen-containing compounds are unstable and have to be reduced or removed before converting to fuel. Further work will target on increasing the energy density of the top organic layer

Table 3.2 Identified compounds from Douglas-fir bio-oil WS fraction before and after hydrogenation (HYD).

Retention time (min)	Identified compounds	Area % of peaks in GC-MS		M^+ (m/z)
		Before HYD	After HYD	
2.22	cyclohexane		4.81	84
2.29	tetrahydro-2-metylfuran		2.10	86
2.30	acetic acid	11.68		60
2.46	2- pentanone		1.06	86
2.55	3-pentanone		1.46	86
2.65	tetrahydropyran		1.28	86
2.84	methyl-cyclohexane		2.11	98
2.98	ethyl-cyclopentane		1.02	98
3.07	2-methyl-butanol		1.01	88
3.51	1-pentanol		4.02	88
3.66	1-hydroxy-2-butanone	1.2		88
3.72	1,2-ethanediol-momacetate	2.74		104
3.83	2-methyl-3-pentanone		1.9	100
3.90	butanedial	2.74		86
3.91	2-hexanone		0.83	100
4.40	n-butyl acetate		0.7	116
4.73	ethylcyclohexane		2.59	112
4.95	2-methyl-cyclopentanone		1.51	98
4.98	2,5-dimethyl-furan	3.14		96
5.61	1-hexanol		3.97	102
5.93	1-methyl-2 propylcyclopetane		1.12	126
6.04	5-methyl-3-hexanone		1.11	114
7.01	2-(5H)-furanone	3.7		84
7.09	propylcyclohexane		1.61	126
7.20	butylcyclopentane		1.26	126
8.37	5-methyl-2-furaldehyde	1.55		110
8.72	phenol	1.35	7.42	94
9.95	n-butylcyclohexane		0.48	140
10.19	2-hydroxy-3-methyl-2-cyclopenten-1-one	4.24		112

10.83	o-cresol	1.23	1.47	108
11.48	p-cresol	1.39	1.11	108
11.97	guaiacol	5.09		124
13.51	3,4-xylenol		1.45	122
14.74	2-methoxy-p-cresol		0.86	138
14.94	4-methyl-guaiacol	4.22		138
15.24	1,2-benzenediol	4.94		110
17.11	p-ethyl-guaiacol	1.95	0.64	152
18.86	p-ethenyl-guaiacol	0.98		150
19.44	p-propylguaiacol		0.6	166
20.54	vanillin	1.26		152
22.40	propenyl-guaiacol	3.21		164
24.84	o-cyclohexyl-phenol		0.88	176
25.79	p-cyclohexyl-phenol		0.42	176

Figure 3.6 shows the difference between the organic components in bio-oil WS fraction before and after catalytic HYD. It can be noted that acids and aldehydes completely disappeared after HYD. Additionally, more alkanes (29.5%) and alcohols (17.7%) were produced over the Ni(65%)/SiO$_2$-Al$_2$O$_3$ catalyst. Therefore, this process is very promising for producing renewable transportation fuels from bio-oil WS phase. However, there were still unreacted phenolics and minor amounts of ketones, furans, and esters in the reaction product top organic layer (Table 3.2). These oxygen-containing compounds are unstable and must be reduced or removed before converting to fuel. Future work will target on increasing the energy density of the top organic layer. Figure 3.6 shows the difference between the organic components in bio-oil WS fraction before and after catalytic HYD. It can be easily noted that acid and aldehyde completely disappeared after HYD. More importantly, greater amounts of alkanes (29.5%) and alcohols (17.7%) were produced compared to the Ni(65%)/SiO$_2$-Al$_2$O$_3$ catalyst. Therefore, this process is very promising for producing renewable transportation fuels from the bio-oil WS phase.
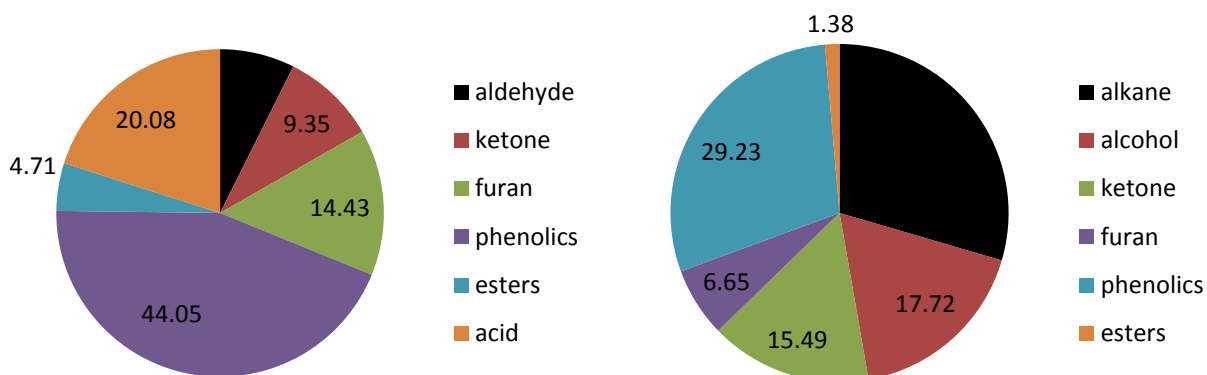
Figure 3.6 The identified organic components distribution in Douglas-fir bio-oil WS phase (left) before and (right) after hydrogenation over Ni(65%)/SiO$_2$-Al$_2$O$_3$.

3.4.2.2 Hydrocracking and hydrodeoxygenation on water insoluble bio-oil

It is known that pyrolysis bio-oil contains about 20% pyrolytic lignin (WIS fraction) [29, 30]. These oligomers can easily block catalyst active sites during high temperature HYD. As mentioned previously, 300°C is a suitable temperature for phenol HDO, however, the temperature was high enough for this pyrolytic lignin material to form coke. Fortunately, the pyrolytic lignin can be easily separated by centrifuging the bio-oil to WS and WIS fractions. The bio-oil WIS fraction is predominately pyrolytic lignin with minor amounts of monomeric phenolics and furans. The purpose of hydrocracking (HC) the bio-oil WIS fraction is to decrease the pyrolytic lignin molecular weight. To achieve this goal, a solvent such as methanol in the presence of a catalyst is suitable for HC reactions to occur [11]. Preliminary tests using Ni(65%)/SiO$_2$-Al$_2$O$_3$ catalyst for HC pyrolytic lignin into small phenolics was shown to work successfully. ESI-MS was employed to characterize the oligomeric material in the
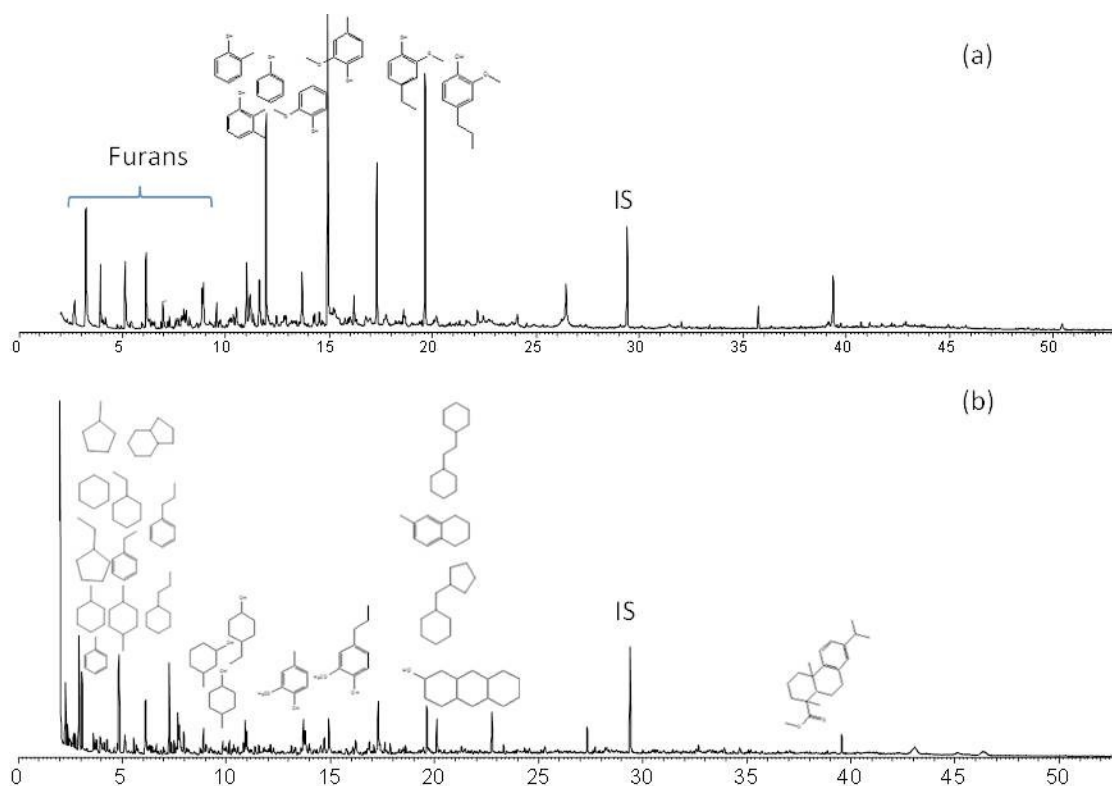
bio-oil WIS fraction before and after HC. Figure 3.7-a is a ESI-MS of the WIS fraction revealing the presence of oligomers between 400 and 2000 g mol^{-1}. More specifically, the ESI-MS showed peak clusters between 90 and 400 g mol^{-1} (monomers and dimers) and >400 g mol^{-1} (>trimers). After hydrocracking, the bio-oil HC-WIS fraction (Figure 3.7-b) showed the peaks >400 g mol^{-1} disappeared showing the presence of monomers and dimers. These results clearly show that hydrocracking of the bio-oil WIS fraction was successfully achieved. To note the thermally cracked bio-oil still contained some methanol and needs to be removed before HDO processing.
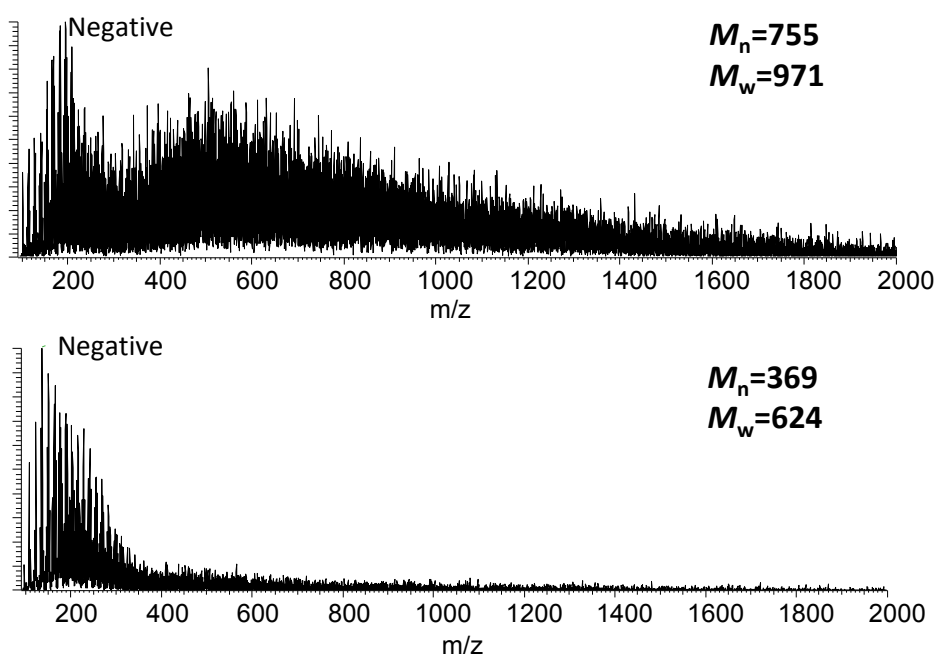
Figure 3.7 Negative ion ESI-MS characterization on Douglas-fir bio-oil (a) WIS fraction before and (b) after hydrocracking (HC-WIS).

The hydrocracked Douglas-fir bio-oil WIS fraction (HC-WIS) was then subjected to HDO treatment over Ni(65%)/SiO$_2$-Al$_2$O$_3$. Figure 3.8 shows the GC-MS chromatograms of Douglas-fir bio-oil HC-WIS fraction before and after HDO. More phenolics and furans were

detected in the HC-WIS but these almost completely disappeared after the HDO reaction. As shown in Figure 3.8-b, the main HC-WIS-HDO products were cycloalkanes and cyclohexanols. These alkanes can be directly employed as green gasoline. Most interestingly, there were di-cycloalkanes produced as well. These compounds are likely derived from aromatic ring condensation as observed in the products from HDO of phenol. These compounds have higher boiling points. In summary, it can be concluded that the water insoluble bio-oil can also be a promising feedstock for diesel or jet fuel production.

Figure 3.8 GC-MS chromatograms of Douglas-fir bio-oil HC-WIS (a) before and (b) after HDO over Ni(65%)/SiO$_2$-Al$_2$O$_3$.
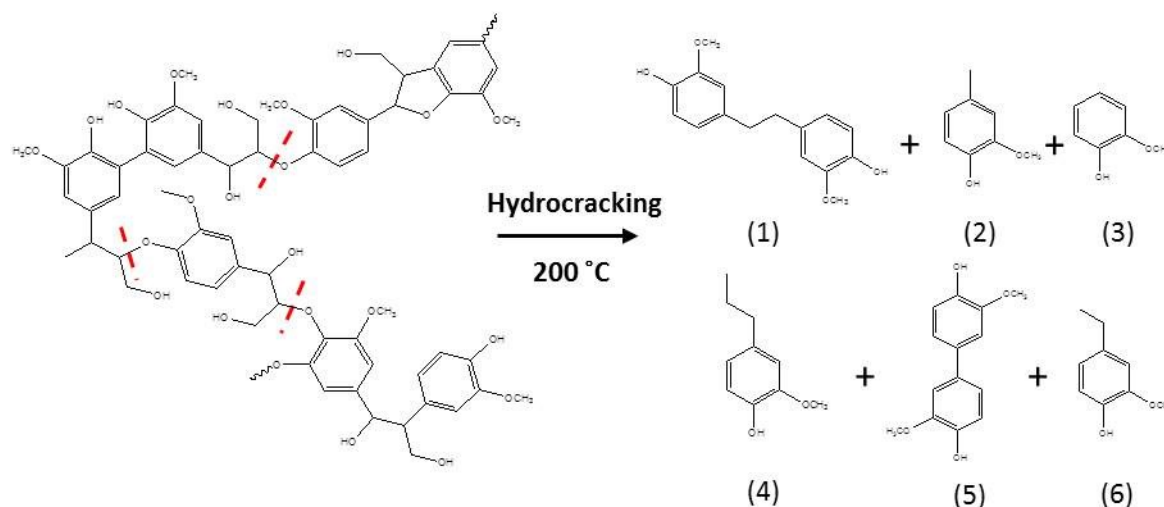
Figure 3.9 Proposed catalytic hydrocracking mechanisms in pyrolytic lignin.

Oligomeric pyrolytic lignin (WIS fraction) is an important constituent of bio-oils but it has detrimental effects on bio-oil properties such as viscosity, reactivity, and stability [31]. More importantly, it is considered as the main component for coke formation during hydrotreatment of bio-oil as reported in many studies [11, 32]. The results from this study indicate that the WIS fraction can be further processed in a methanol solvent for hydrocracking reactions. A possible mechanism for pyrolytic lignin HC was proposed in Figure 3.9. The cleavage of linkage β-O-4 in PL was the desirable reactions for the production of phenolics with small molecular weight. As evidenced by the ESI-MS results, there were also dimers detected besides monomers. Moreover, those alkyl double bonds (propenyl-guaiacol, etc) were completely saturated by HYD over Ni catalyst. The pyrolytic lignin (WIS) and its cracked products (HC-WIS) will thus be stabilized as well.

3.5 Conclusions

In this study, fast pyrolysis of Douglas-fir feedstock was conducted to obtain pyrolysis bio-oil. The produced bio-oil then was characterized by gas chromatography-mass spectrometry (GC-MS) and electron spray ionization mass spectrometry (ESI-MS). Phenols, furans, acetic acid, fatty acids and other oxygenates were identified by GC-MS. Pyrolytic lignin oligomers were identified by the negative ion ESI-MS. The calculated M_n and M_w for the Douglas–fir bio-oil were respectively 691 and 1197 g mol^{-1}.

Bio-oil hydrogenation on both water soluble (WS) and water insoluble (WIS) fractions was successfully carried out. Ni(65%)/SiO$_2$-Al$_2$O$_3$ was selected as the catalyst for bio-oil hydrogenation due to its good performance on phenol HDO. Liquid products from bio-oil WS hydrogenation were composed of alkanes in the top layer comprising of cycloalkanes (30%) and alcohols (18%). The pyrolytic lignin rich bio-oil WIS fraction can effectively be hydrocracked in methanol over a Ni(65%)/SiO$_2$-Al$_2$O$_3$ catalyst to monomeric and dimeric compounds (HC-WIS). A further HDO treatment on the HC-WIS fraction had successfully deoxygenated the phenolics into cycloalkanes. All the produced alkanes and alcohols can be directly used as drop-in transportation fuels.

3.6 References

1.   Rafael Luque, J.C.a.J.C., *Handbook of biofuels production: processes and technologies*. Woodhead Publishing Series. 2011: Woodhead. 659.

2.   Brown, R.C., ed. *Thermochemical Processing of Biomass: Conversion into Fuels, Chemicals, and Power*. ed. C.V. Stevens. 2011, John Wiley & Sons.

3.   Dickerson, T. and J. Soria, *Catalytic Fast Pyrolysis: A Review.* Energies, 2013. **6**(1): p. 514-538.

4.   Bridgwater, A.V., *Review of fast pyrolysis of biomass and product upgrading.* Biomass and Bioenergy, 2012. **38**: p. 68-94.

5.   Bertero, M., G. de la Puente, and U. Sedran, *Fuels from bio-oils: Bio-oil production from different residual sources, characterization and thermal conditioning.* Fuel, 2012. **95**: p. 263-271.

6.   Zhang, X., et al., *Hydrotreatment of bio-oil over Ni-based catalyst.* Bioresource Technology, 2013. **127**: p. 306-311.

7.   Elliott, D.C., G.G. Neuenschwander, and T.R. Hart, *Hydroprocessing Bio-Oil and Products Separation for Coke Production.* ACS Sustainable Chemistry & Engineering, 2013. **1**(4): p. 389-392.

8.   Zhang, H., et al., *Characterization of Coke Deposition in the Catalytic Fast Pyrolysis of Biomass Derivates.* Energy & Fuels, 2014. **28**(1): p. 52-57.

9.   Xu, X., et al., *Two-step catalytic hydrodeoxygenation of fast pyrolysis oil to hydrocarbon liquid fuels.* Chemosphere, 2013. **93**(4): p. 652-660.

10.   DC. Elliot, S.-J.L., and T.R. Hart, *Stabilization of Fast Pyrolysis Oil: Post Processing*. 2012, PNNL.

11.   Zhe Tang, Y.Z., and Qingxiang Guo, *Catalytic Hydrocracking of Pyrolytic Lignin to Liquid Fuel in Supercritical Ethanol.* Industrial & Engineering Chemistry Research, 2010. **46**: p. 6.

12.   Bi, P., et al., *Production of aromatics through current-enhanced catalytic conversion of bio-oil tar.* Bioresource Technology, 2013. **136**: p. 222-229.

13.   Fele Žilnik, L. and A. Jazbinšek, *Recovery of renewable phenolic fraction from pyrolysis oil.* Separation and Purification Technology, 2012. **86**: p. 157-170.

14.   Zhao, C., et al., *Highly Selective Catalytic Conversion of Phenolic Bio-Oil to Alkanes.* Angewandte Chemie International Edition, 2009. **48**(22): p. 3987-3990.

15.   Vispute, T.P. and G.W. Huber, *Production of hydrogen, alkanes and polyols by aqueous phase processing of wood-derived pyrolysis oils.* Green Chemistry, 2009. **11**(9): p. 1433.

16.   Graça, I., et al., *Catalytic cracking of mixtures of model bio-oil compounds and gasoil.* Applied Catalysis B: Environmental, 2009. **90**(3-4): p. 556-563.

17.   Wang, S., et al., *Biogasoline Production from the Co-cracking of the Distilled Fraction of Bio-oil and Ethanol.* Energy & Fuels, 2014. **28**(1): p. 115-122.

18.   Ferrini, P. and R. Rinaldi, *Catalytic Biorefining of Plant Biomass to Non-Pyrolytic Lignin Bio-Oil and Carbohydrates through Hydrogen Transfer Reactions.* Angewandte Chemie International Edition, 2014. **53**(33): p. 8634-8639.

19.   Osman, N.B., A.G. McDonald, and M.-P.G. Laborie, *Analysis of DCM extractable components from hot-pressed hybrid poplar.* Holzforschung, 2012. **66**(8).

20.   Ortega, J.V., et al., *Physical and chemical characteristics of aging pyrolysis oils produced from hardwood and softwood feedstocks.* Journal of Analytical and Applied Pyrolysis, 2011. **91**(1): p. 190-198.

21.   Ben, H., et al., *Production of renewable gasoline from aqueous phase hydrogenation of lignin pyrolysis oil.* Fuel, 2013. **103**: p. 1148-1153.

22.   Shen, D.K., S. Gu, and A.V. Bridgwater, *Study on the pyrolytic behaviour of xylan-based hemicellulose using TG–FTIR and Py–GC–FTIR.* Journal of Analytical and Applied Pyrolysis, 2010. **87**(2): p. 199-206.

23.   Qu, T., et al., *Experimental Study of Biomass Pyrolysis Based on Three Major Components: Hemicellulose, Cellulose, and Lignin.* Industrial & Engineering Chemistry Research, 2011. **50**(18): p. 10424-10433.

24.   Venkatakrishnan, V.K., et al., *High-pressure fast-pyrolysis, fast-hydropyrolysis and catalytic hydrodeoxygenation of cellulose: production of liquid fuel from biomass.* Green Chemistry, 2014. **16**(2): p. 792.

25.   Kawamoto, H., W. Hatanaka, and S. Saka, *Thermochemical conversion of cellulose in polar solvent (sulfolane) into levoglucosan and other low molecular-weight substances.* Journal of Analytical and Applied Pyrolysis, 2003. **70**(2): p. 303-313.

26.   Kawamoto, H., M. Murayama, and S. Saka, *Pyrolysis behavior of levoglucosan as an intermediate in cellulose pyrolysis: polymerization into polysaccharide as a key reaction to carbonized product formation.* Journal of Wood Science, 2003. **49**(5): p. 469-473.

27.   Zhou, S., et al., *Effect of sulfuric acid concentration on the yield and properties of the bio-oils obtained from the auger and fast pyrolysis of Douglas Fir.* Fuel, 2013. **104**: p. 536-546.

28.   Srinivas.S, D.A., Bakhshi. N, *Thermal and catalytic upgrading of a biomass derived oil in a dual reaction system.* The Canadian Journal of Chemical Engineering, 2000. **78**: p. 343-354.

29. Mullen, C.A. and A.A. Boateng, *Characterization of water insoluble solids isolated from various biomass fast pyrolysis oils.* Journal of Analytical and Applied Pyrolysis, 2011. **90**(2): p. 197-203.

30. Bayerbach, R. and D. Meier, *Characterization of the water-insoluble fraction from fast pyrolysis liquids (pyrolytic lignin). Part IV: Structure elucidation of oligomeric molecules.* Journal of Analytical and Applied Pyrolysis, 2009. **85**(1-2): p. 98-107.

31. Bayerbach, R., et al., *Characterization of the water-insoluble fraction from fast pyrolysis liquids (pyrolytic lignin).* Journal of Analytical and Applied Pyrolysis, 2006. **77**(2): p. 95-101.

32. Ibáñez, M., et al., *Effect of operating conditions on the coke nature and HZSM-5 catalysts deactivation in the transformation of crude bio-oil into hydrocarbons.* Catalysis Today, 2012. **195**(1): p. 106-113.

Chapter 4: Conclusion

4.1 Conclusion

Utilization of lignocellulosic biomass for renewable biofuels production is highly desirable for meeting transportation fuel needs. Among several conversion technologies, fast pyrolysis is considered the most promising due to a high yield liquid bio-oil readily produced from this process at a relatively low cost. However, the pyrolysis bio-oils are acidic, chemically unstable liquids with low energy density. This is because bio-oils contain many active oxygen containing compounds, high molecular weight oligomers and 15-60 % or more, of water, which thus has to be upgraded before used as transportation fuels. Catalytic hydrodeoxygenation (HDO) of bio-oil was proven to be an effective method to deoxygenate pyrolysis bio-oil to green hydrocarbon fuels. Therefore, novel active catalysts for HDO process are needed.

In this work, a series of Ni, and Ru-based catalysts on different supports were prepared and tested for the hydrodeoxygenation (HDO) of phenol. All the catalysts maintained a broad range of physicochemical properties as evidenced by TEM and XRD. Besides the helical structure, mesoporous channels were also observed from silica nanosprings based catalysts. The best metal dispersity was achieved on the surface of silica nanosprings which performed better than other supports in term of phenol conversion and degree of deoxygenation (DOD).

Both Ni and Ru based catalysts effectively deoxygenate phenol into hydrocarbons, which were mainly composed of cyclohexane, cyclohexene and bicyclohexyl. Moreover, minor amounts of oxygenated intermediates including cyclohexanol, cyclohexanone, and

cyclohexyl-phenol were also detected after the HDO of phenol. These results revealed that phenol aromatic ring hydrogenation and a subsequent dehydration are the main reactions that occurred for all Ni and Ru catalysts. However, the different support for one metal (Ni or Ru) may lead to distinctive catalyst activity due to their different physicochemical properties. For instance, silica based Ni catalysts performed better than alumina based, especially in the presence of water. The Ni(20%)-NS was the best performing Ni catalyst based on having the highest conversion and DOD. Of the Ru based catalysts the Ru-NS were the best performing exhibiting nearly complete phenol conversion and DOD. The Ru-NS showed good catalytic ability (stability) after 5 several treatments. These results clearly show that these NS were excellent supports for HDO reactions especially with Ru. Therefore, NS are a suitable support for HDO of pyrolysis bio-oil.

In term of the pyrolysis oil hydrotreatment, fast pyrolysis on Douglas-fir feedstock was first conducted to obtain pyrolysis bio-oil. The major products identified from the produced bio-oil were phenols, furans, acetic acid, fatty acids, sugar and other oxygenates. Pyrolytic lignin oligomers were identified by the negative ion ESI-MS. The calculated number and weight average molar mass for the bio-oil were 691 and 1197, respectively.

Renewable hydrocarbons were successfully produced by hydrogenation on both water soluble and water insoluble bio-oil. Ni(65%)/SiO$_2$-Al$_2$O$_3$ were selected as the catalyst for bio-oil hydrogenation due to its good performance on phenol HDO. Liquid products from water soluble bio-oil hydrogenation were composed of a top organic layer and bottom aqueous layer. According to GC-MS, the main compounds in the top organic layer were 30% cycloalkanes and 18% alcohols. Conversely, pyrolytic lignin in water insoluble bio-oil has been effectively cracked in methanol over Ni(65%)/SiO$_2$-Al$_2$O$_3$ catalyst, which was shown by ESI-MS. A further step of HDO on the cracked oil had successfully deoxygenated the

phenolics into cycloalkanes. All the produced alkanes and alcohols can be directly used as drop-in transportation fuels.

4.2 Limitations

There were challenges experienced during this study. One of the great limitations is that a possible interference from solvents including methanol and hexane for hydrodeoxygenation of pyrolysis bio-oil. The solvents not only increase the cost of the process but also may react with hydrogen gas to an unknown extent. Therefore, it is difficult to conduct the mass balance accurately after the bio-oil HDO reactions.

4.3 Future work

Future research will focus on hydrodeoxygenation of pyrolysis oil by NS based catalysts. In addition, other catalyst characterization techniques including H_2- and NH_3-TPD and BET-surface will be also conducted to characterize the acidity and surface area of Ni-NS and Ru-NS catalysts. In this study, only monometallic Ni or Ru was employed on the silica nanosprings to study the HDO of phenol. But bimetallic catalysts are the mostly applied catalysts for hydrodeoxygenation reaction. Previous studies claimed that Co (cobalt), Cu (copper), and Mo (molybdenum) can be the promoters for Ni catalysts. Thus, Ni-Co, Ni-Cu, and Ni-Mo based nanosprings catalysts will be synthesized in the future to study the effects on the activity and selectivity of catalysts. Additionally, Ni-P (phosphide) will be another interesting modification on Ni catalyst because metal phosphide catalysts favor the hydrodeoxygenation of furans.
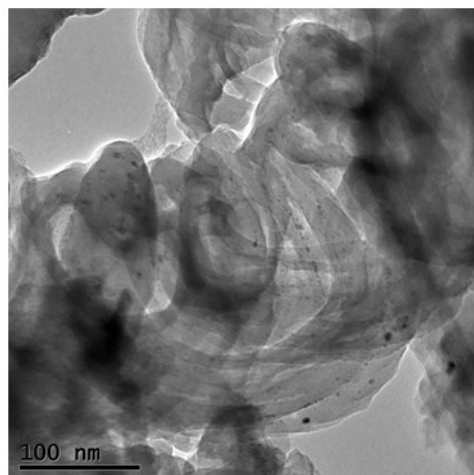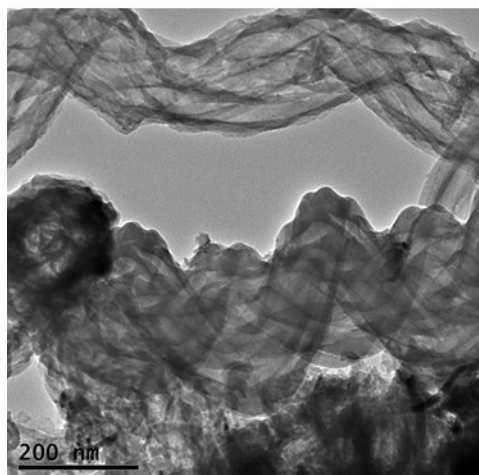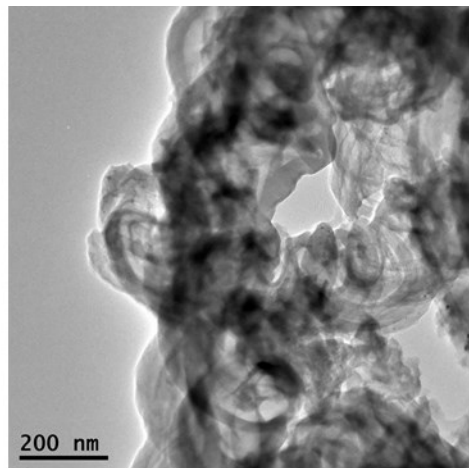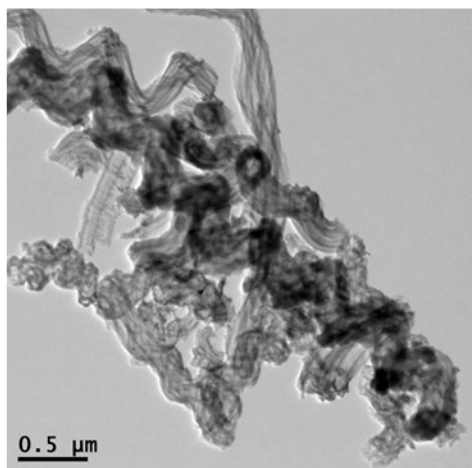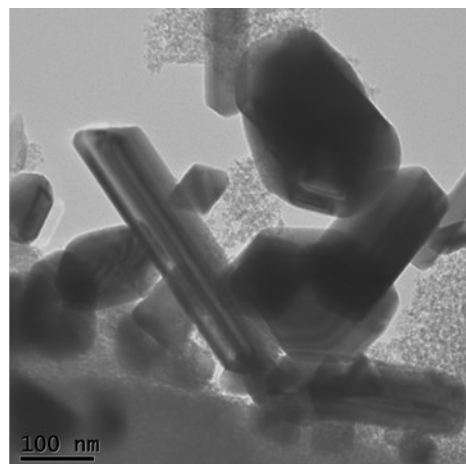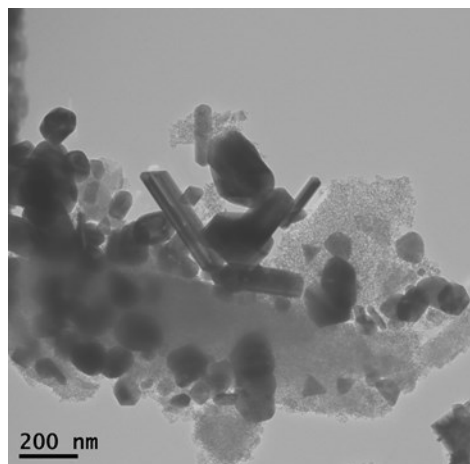
Appendix

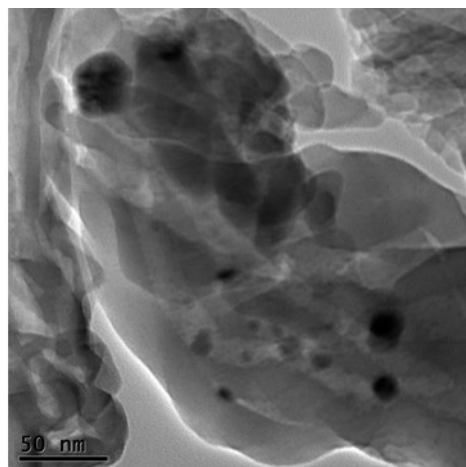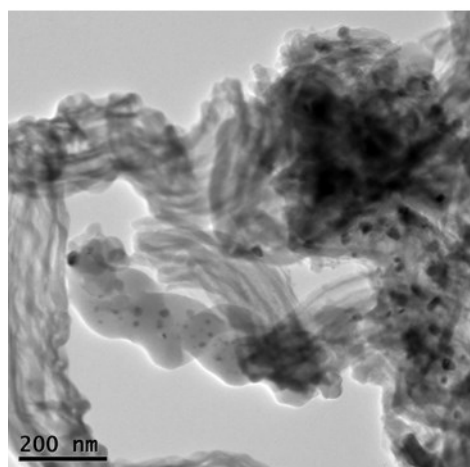Supplementary TEM data

1. Ru(20%)-NS
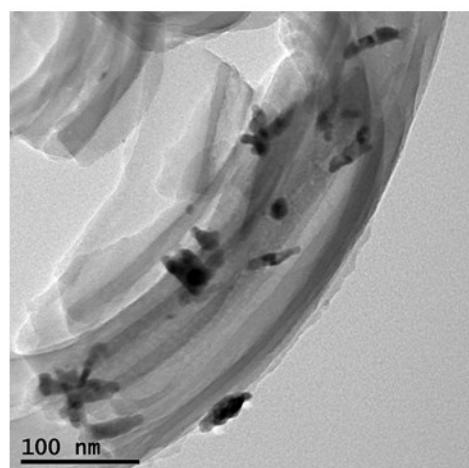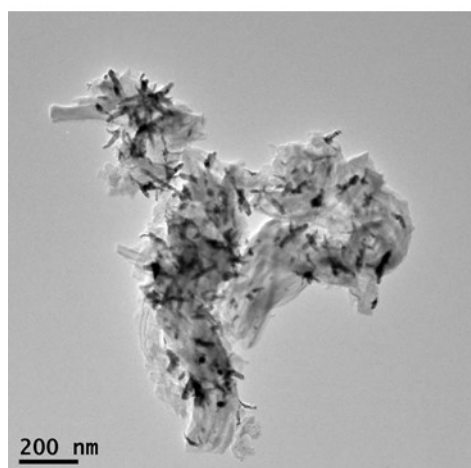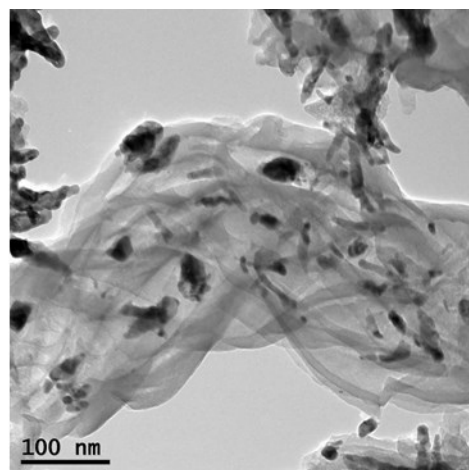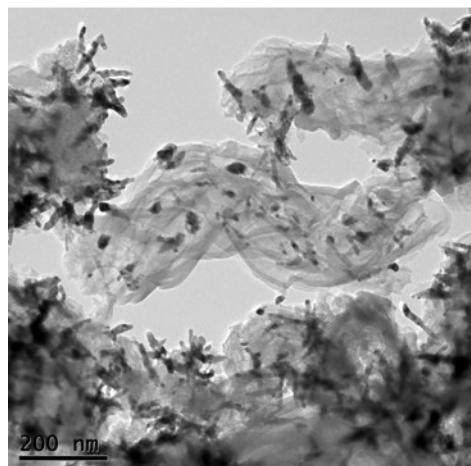
2. Ru (5%)-NS

3. Ni(20%)-silica gel (#2)

4. Ni(20%)-NS

Supplementary GC-MS on HDO products from Bio-oil-WIS-HC over Ni(20%)-NS catalyst